FERMI-GBM: Brief history of Simulations and Calibrations (after >15 years!)

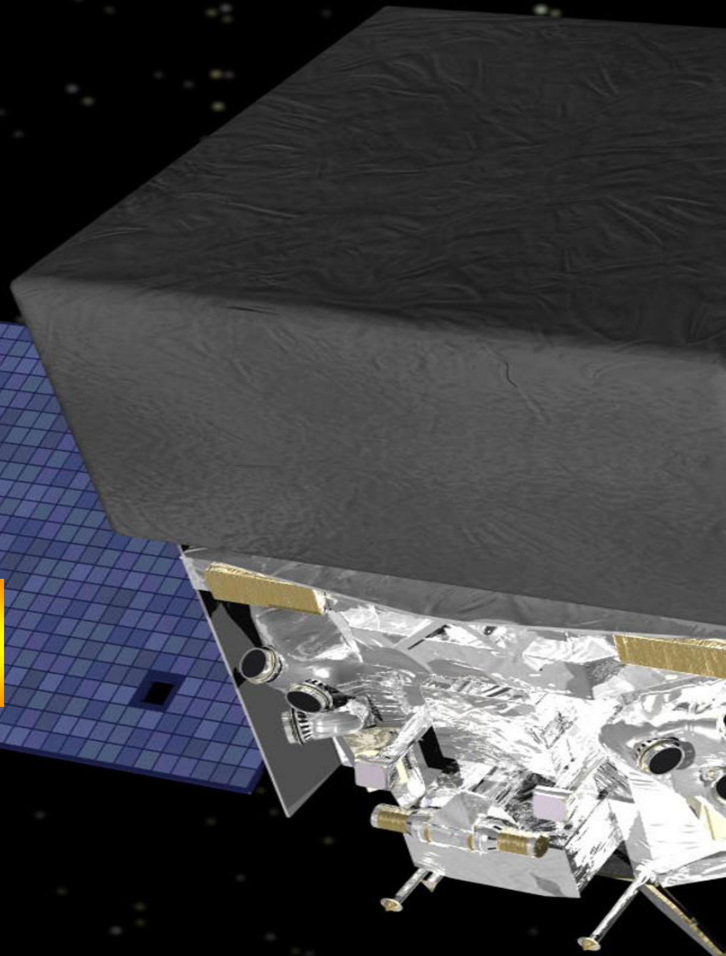

Dr. Elisabetta Bissaldi*

Associate Professor
Member of the Fermi and CTA Consortium
Affiliate member of the H.E.S.S. Collaboration

Input from M. Kippen, A. Hoover, H. Steinle, A. von Kienlin, M. S. Briggs, etc… Thanks!!!

IUCAA GEANT4 tifr

1st National Workshop on GEANT4 and its Application to High-Energy Physics and Astrophysics

*Dipartimento Interateneo di Fisica "M.Merlin" – Politecnico & INFN Bari
elisabetta.bissaldi@ba.infn.it

The Fermi mission

Launched 2008

Key features
huge **FoV**
&
large **energy range**

Large Area Telescope (LAT)
Pair conversion telescope
20 MeV → 300 GeV

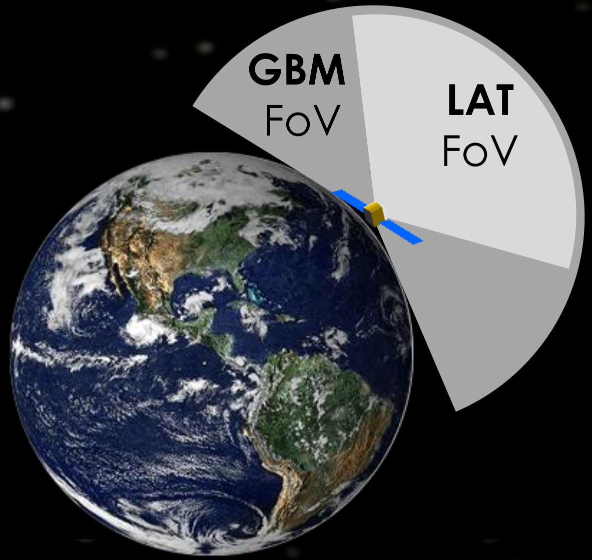

Gamma-ray Burst Monitor (GBM)
14 Plastic scintillator detectors
8 keV – 40 MeV

The (HE) gamma-ray sky

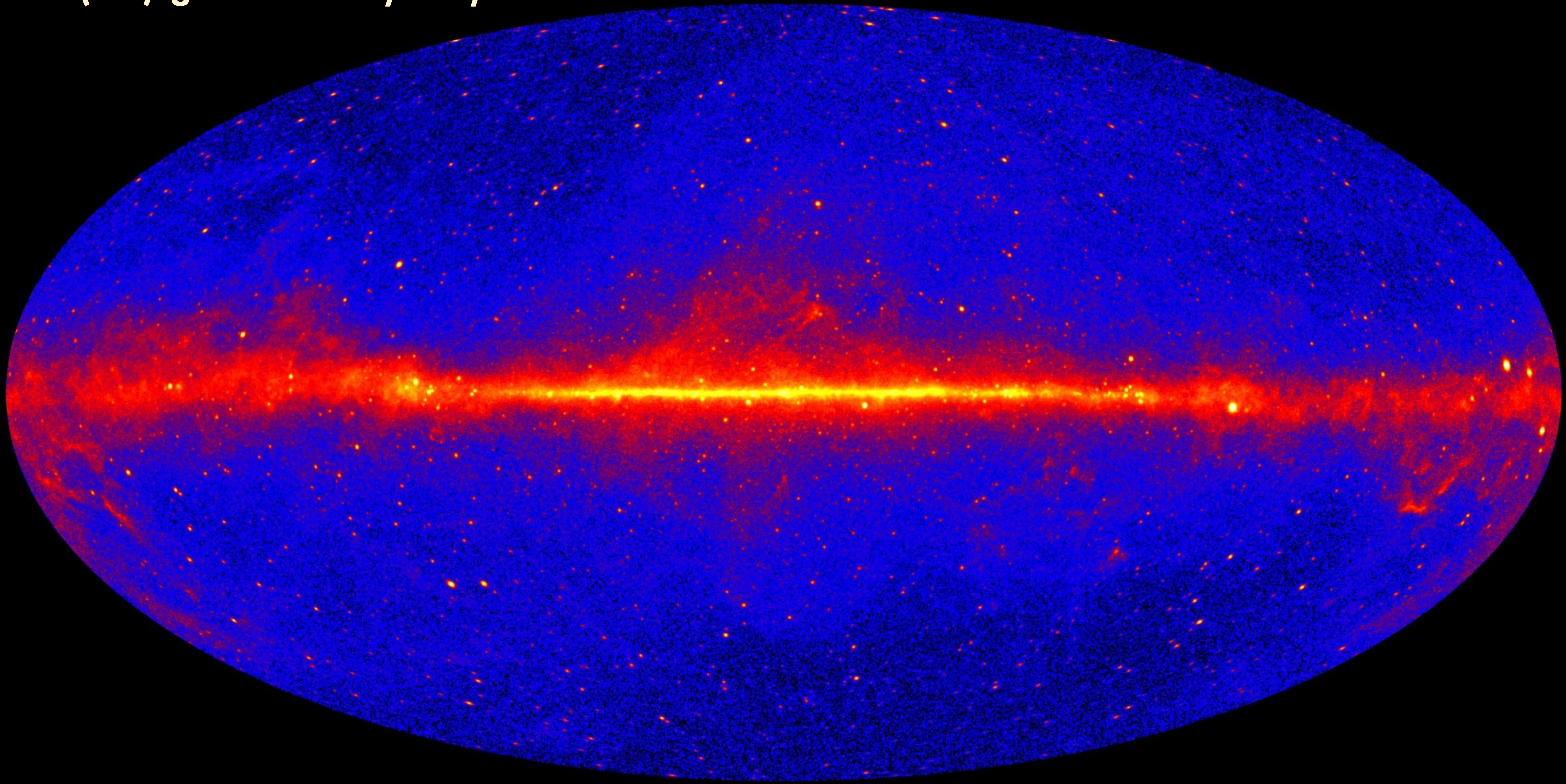

Credit: NASA/DOE/Fermi LAT Collaboration

Gamma-Ray Bursts (GRBs)

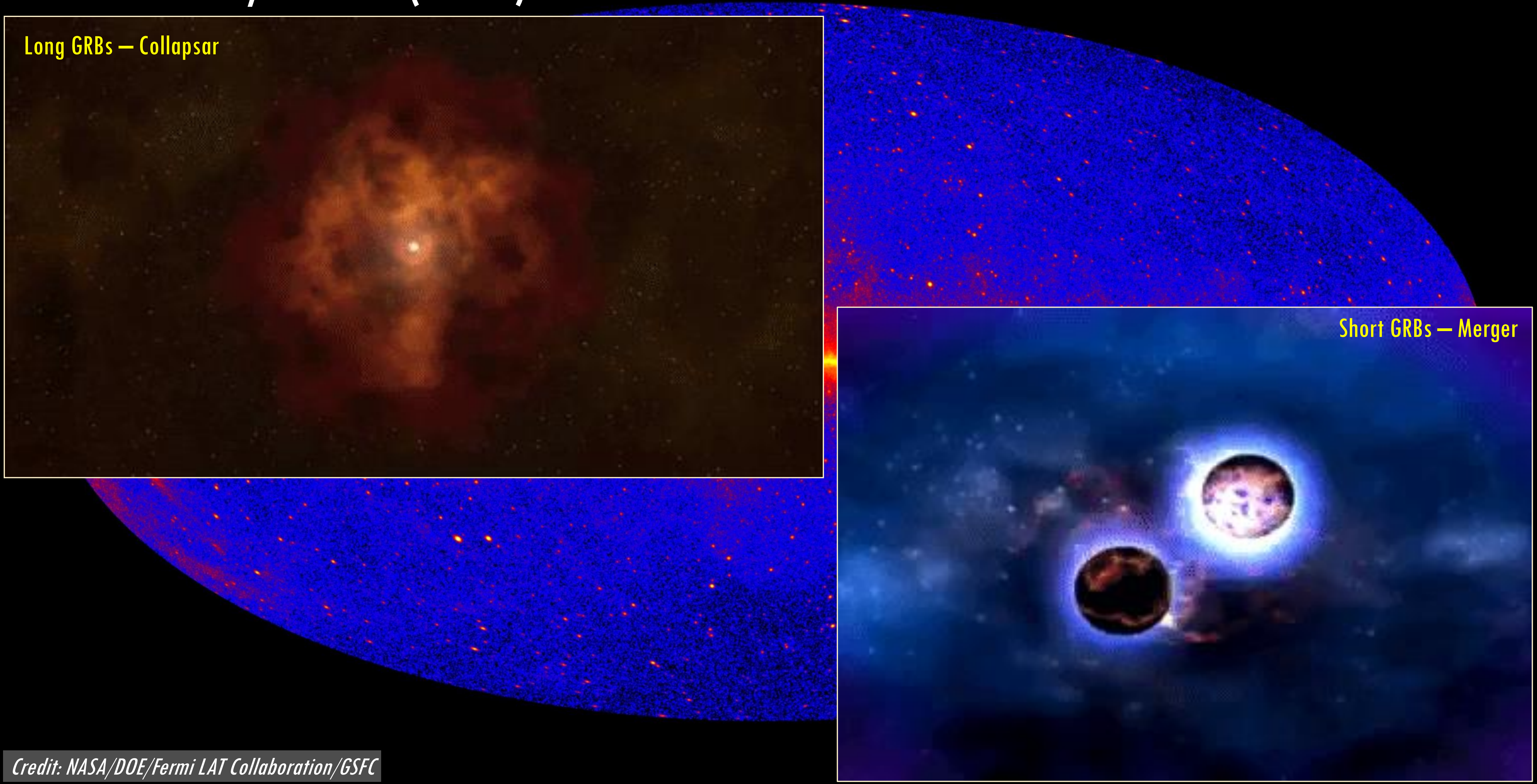

Credit: NASA/DOE/Fermi LAT Collaboration/GSFC

The Fermi mission

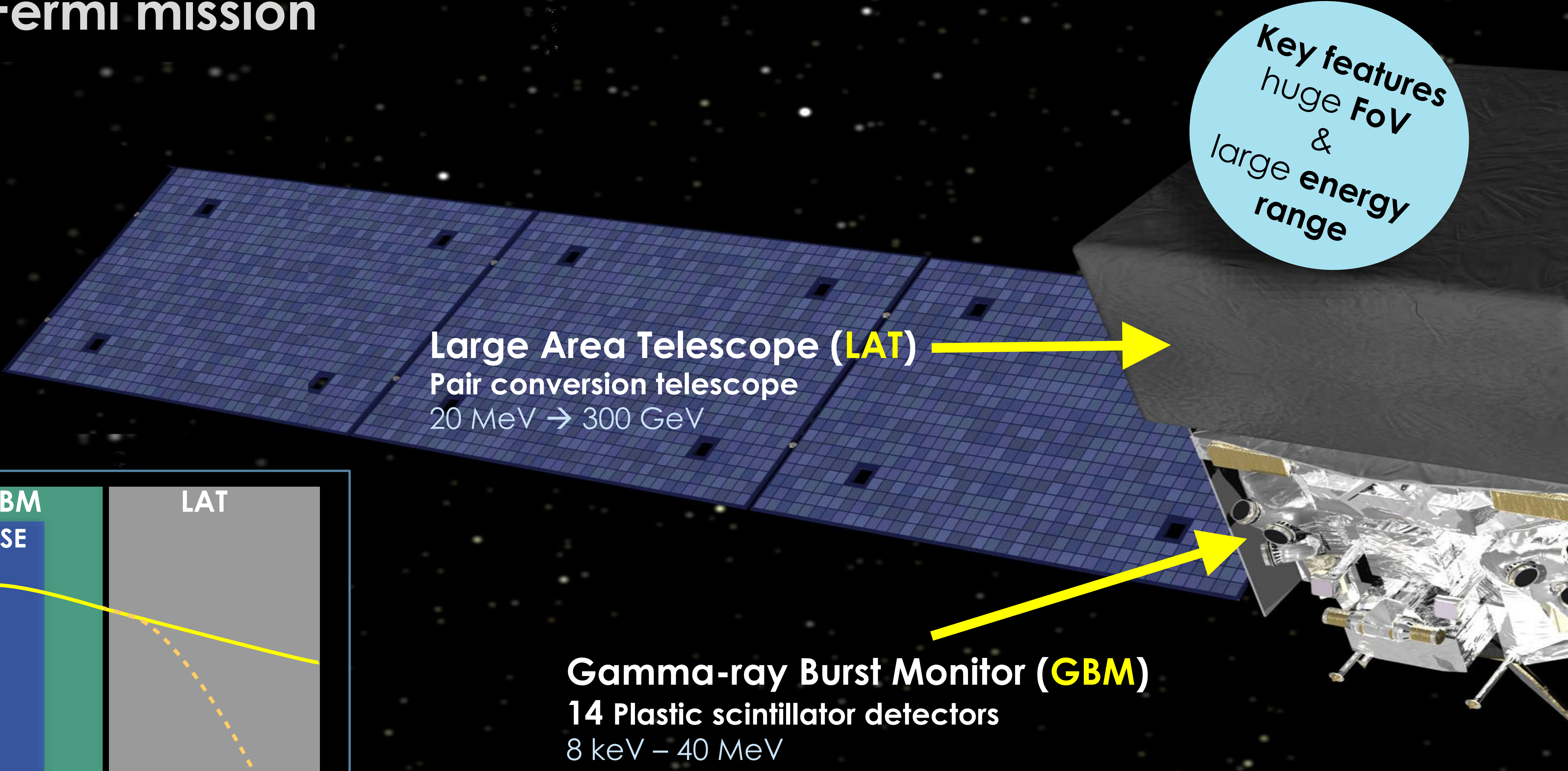

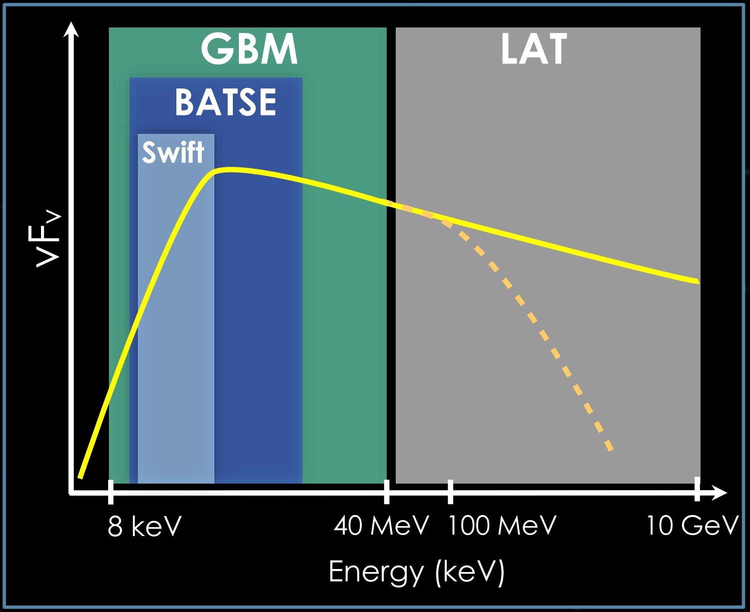

>8300 onboard triggers

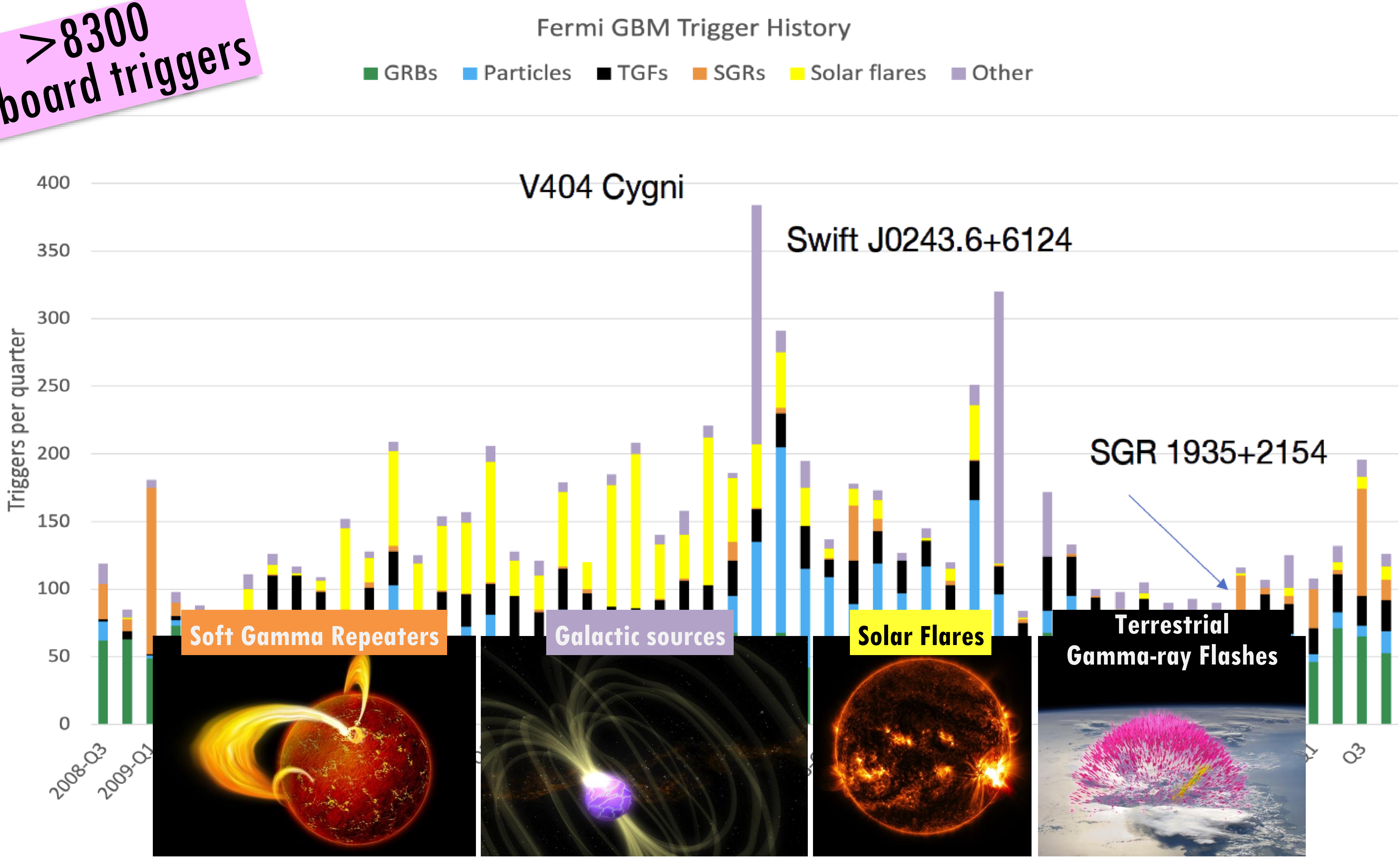

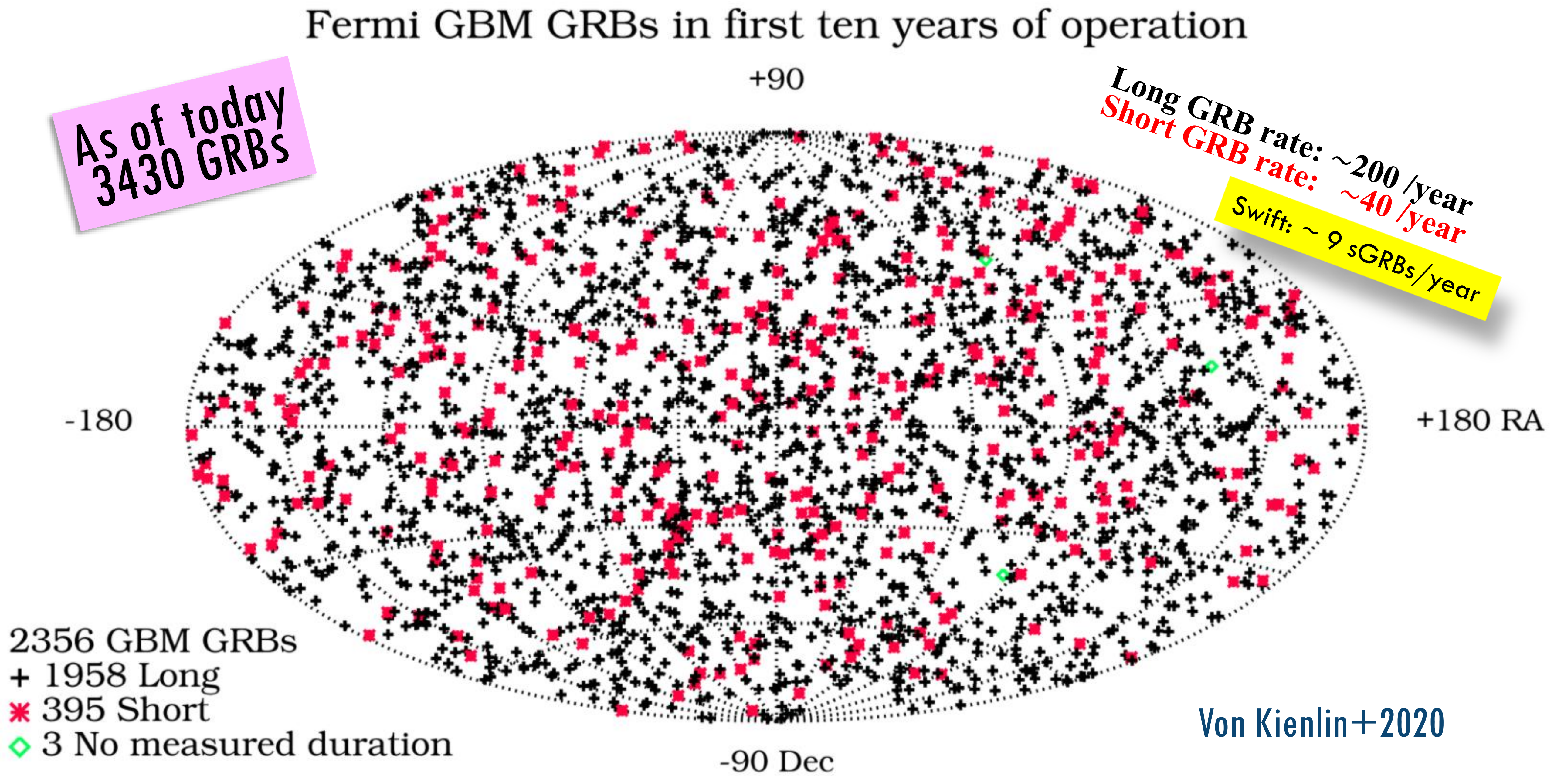
Fermi GBM GRBs in first ten years of operation
+90
-180
+180 RA
-90 Dec
2356 GBM GRBs
+ 1958 Long
395 Short
3 No measured duration
As of today
3430 GRBs
Long GRB rate: ~200 /year
Short GRB rate: ~40 /year
Swift: ~ 9 sGRBs/year
Von Kienlin+2020

GLAST Observatory: quick overview

Orbit
565km, circular

Inclination
28.5°

Spacecraft Integration
2006-2007

TV Test
2007/2008

Launch Date
June 2008

GLAST Lifetime
5 years (min)

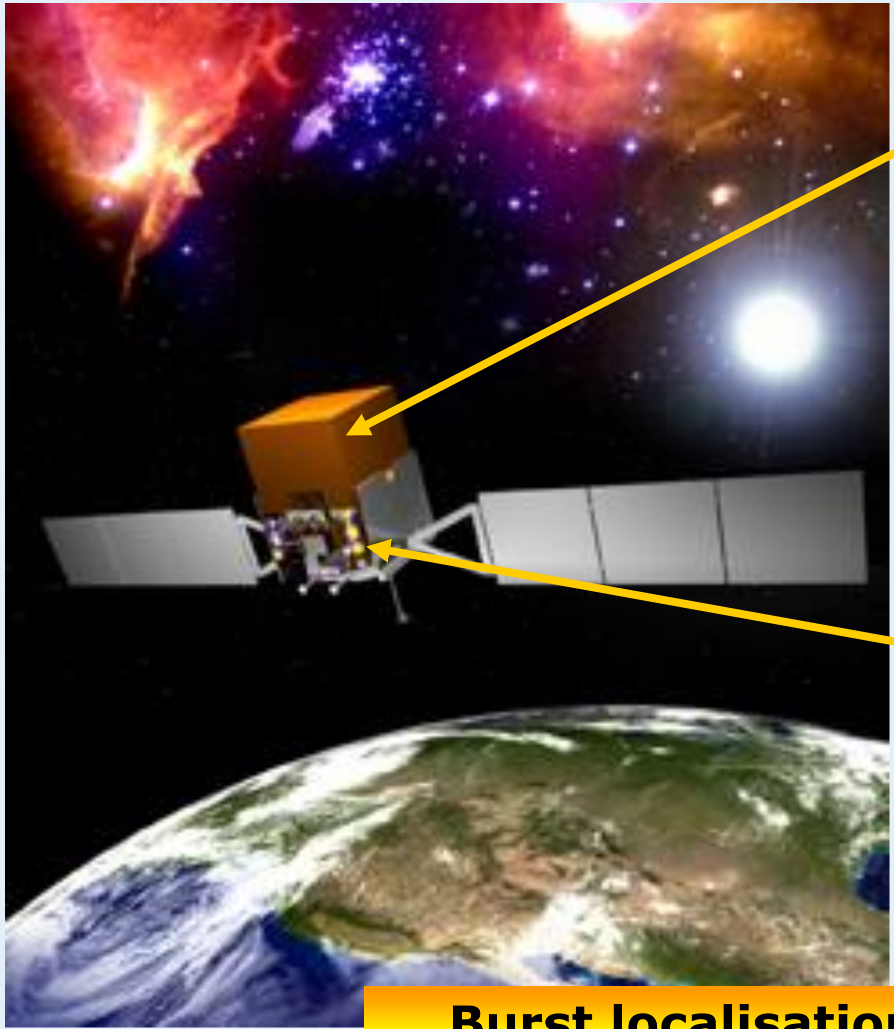

LAT
Large Area Telescope

- **Record gamma-rays in the energy range ~ 20 MeV – 300 GeV**

GBM
GLAST Burst Monitor

- **Provide correlative observations of transient events in the energy range ~ 10 keV – 25 MeV**

Burst localisation via count-rate comparison of different NaI-detectors (BATSE–principle)

The Fermi–GBM instruments

- GBM = 14 scintillation detectors

(12) Sodium Iodide (NaI) Scintillation Detectors

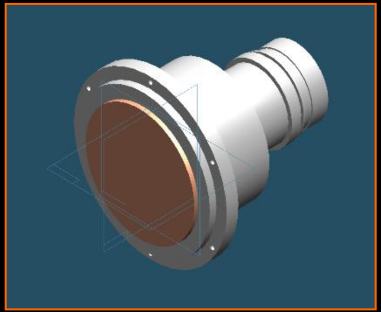

(2) Bismuth Germanate (BGO) Scintillation Detectors

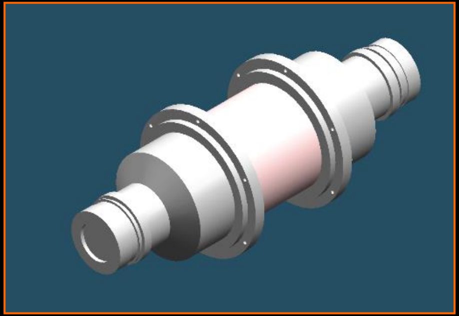

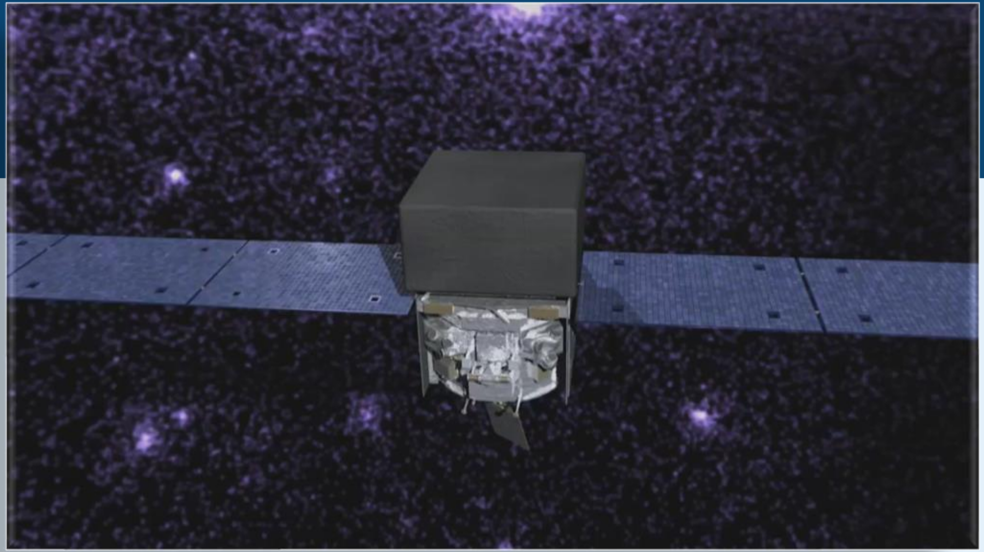

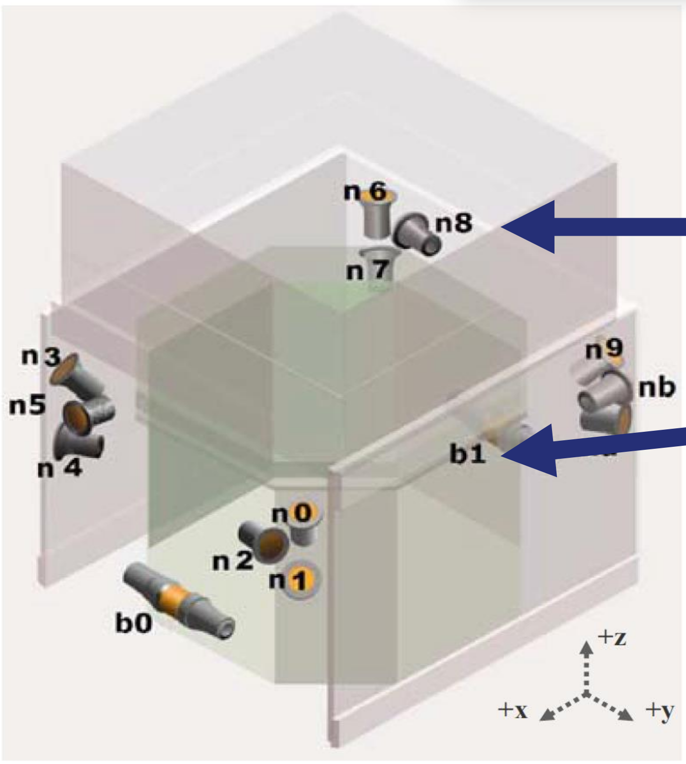

12 NaI(Tl)

2 BGO

Fermi–GBM Hardware Components

2 BGO detectors (MPE)

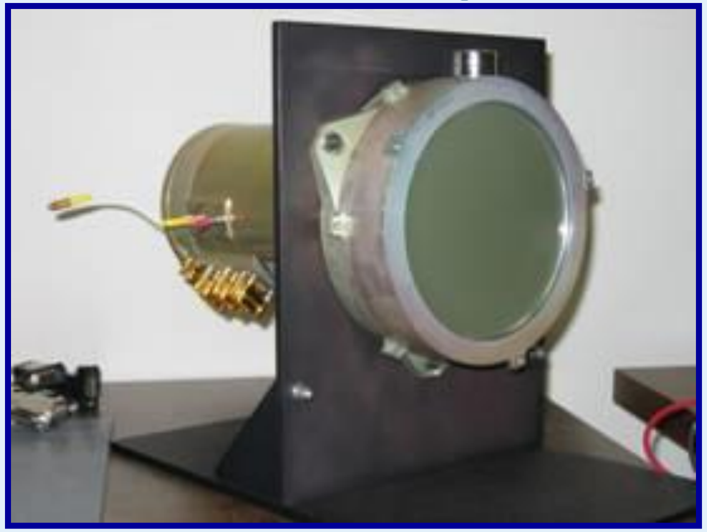

12 NaI detectors (MPE)

Power box
- **provides regulated power to:**
  - **DPU and detectors**
  - **HV for the PMTs**

(MPE)

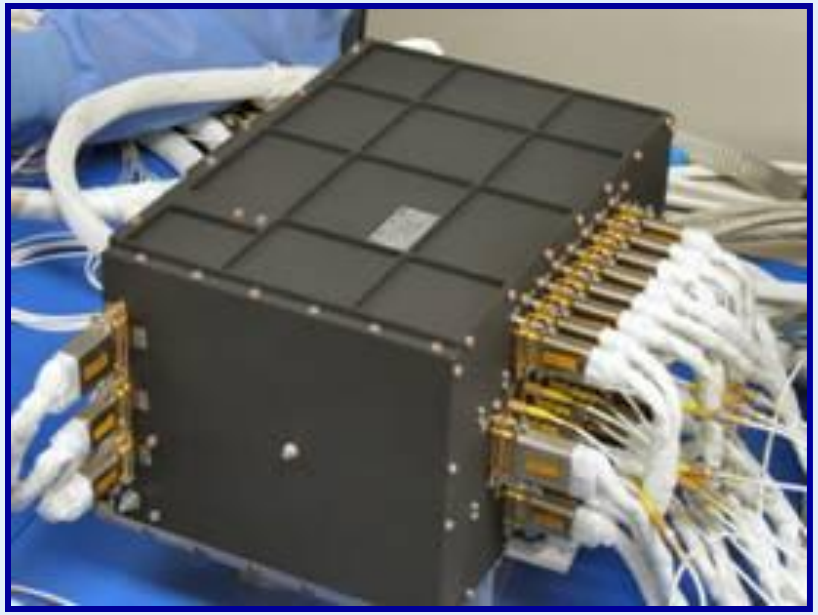

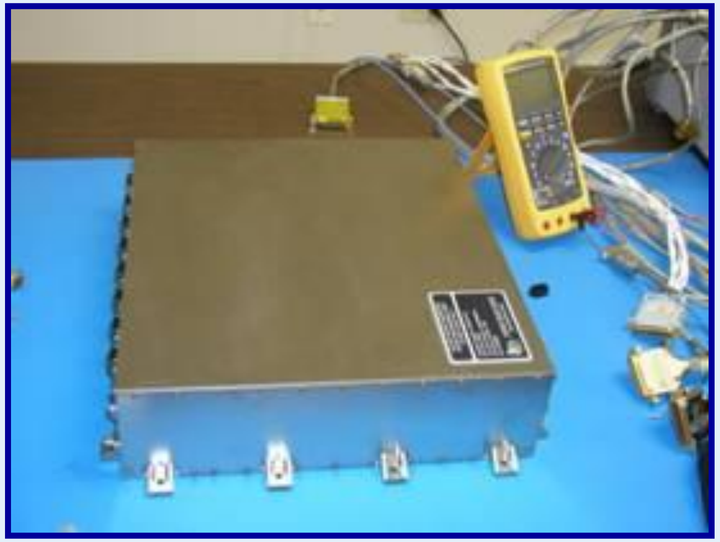

Data Processing Unit (DPU)
- **digitizes detector inputs**
- **controls high and low voltage to detectors**
- **provides control and S/C interface (MSFC)**

The Gamma-Ray Burst Monitor

- GBM single detectors calibration and tests campaigns (2004-2006) at the Max-Planck Institut for Extraterrestrial Physics (MPE, Germany)

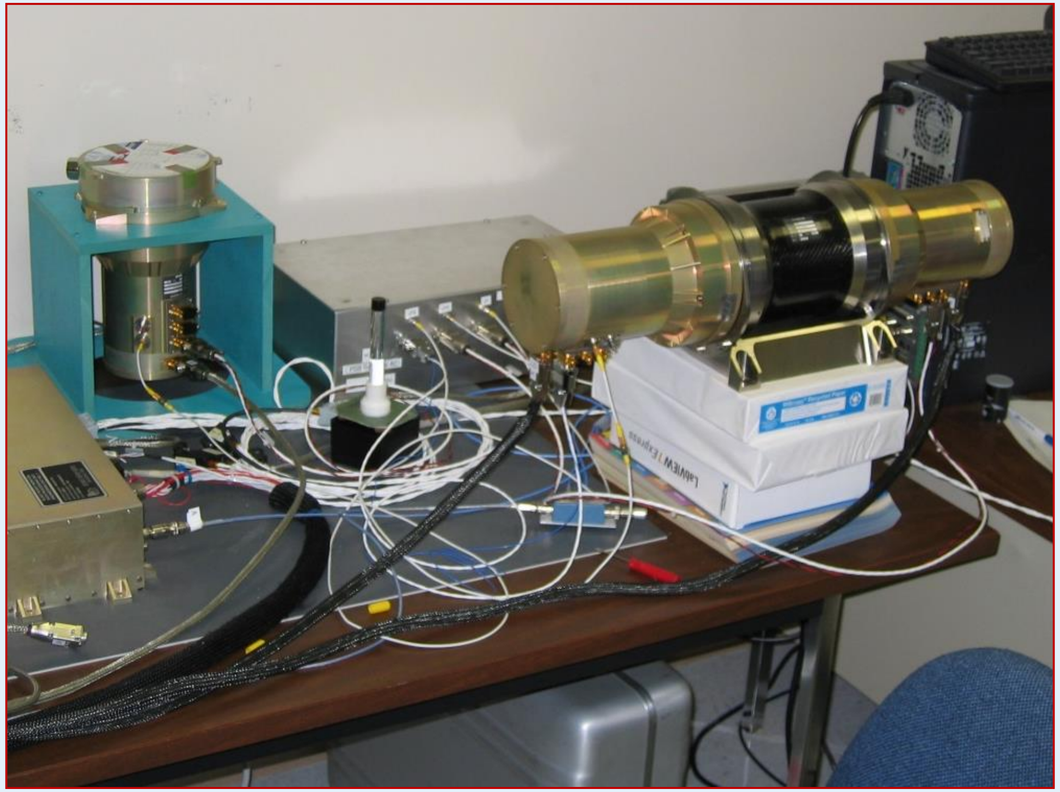

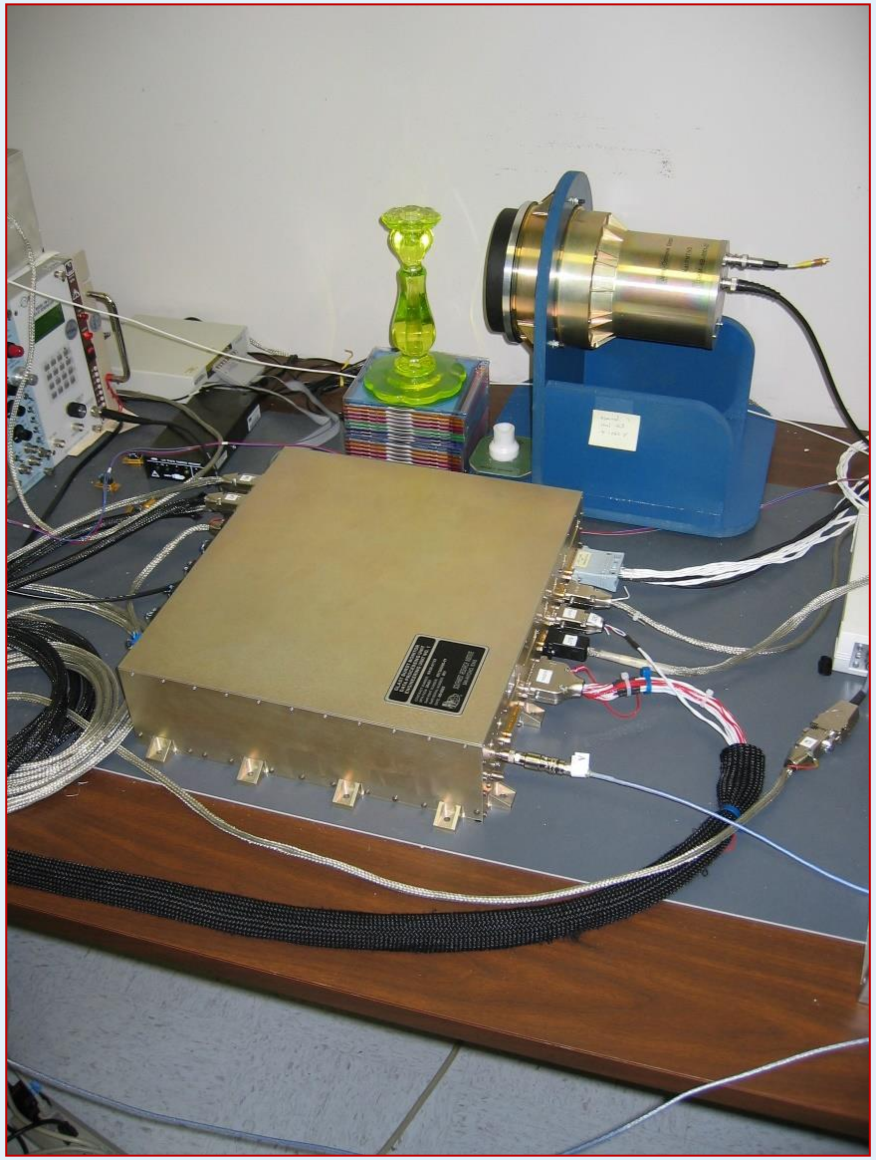

The Gamma-Ray Burst Monitor

- GBM full instrument calibration and tests campaigns (2006) at the Marshall Space Flight Center (Alabama, USA)

The Gamma-Ray Burst Monitor

- GBM integration onto the Fermi spacecraft (2007) at Phoenix, USA

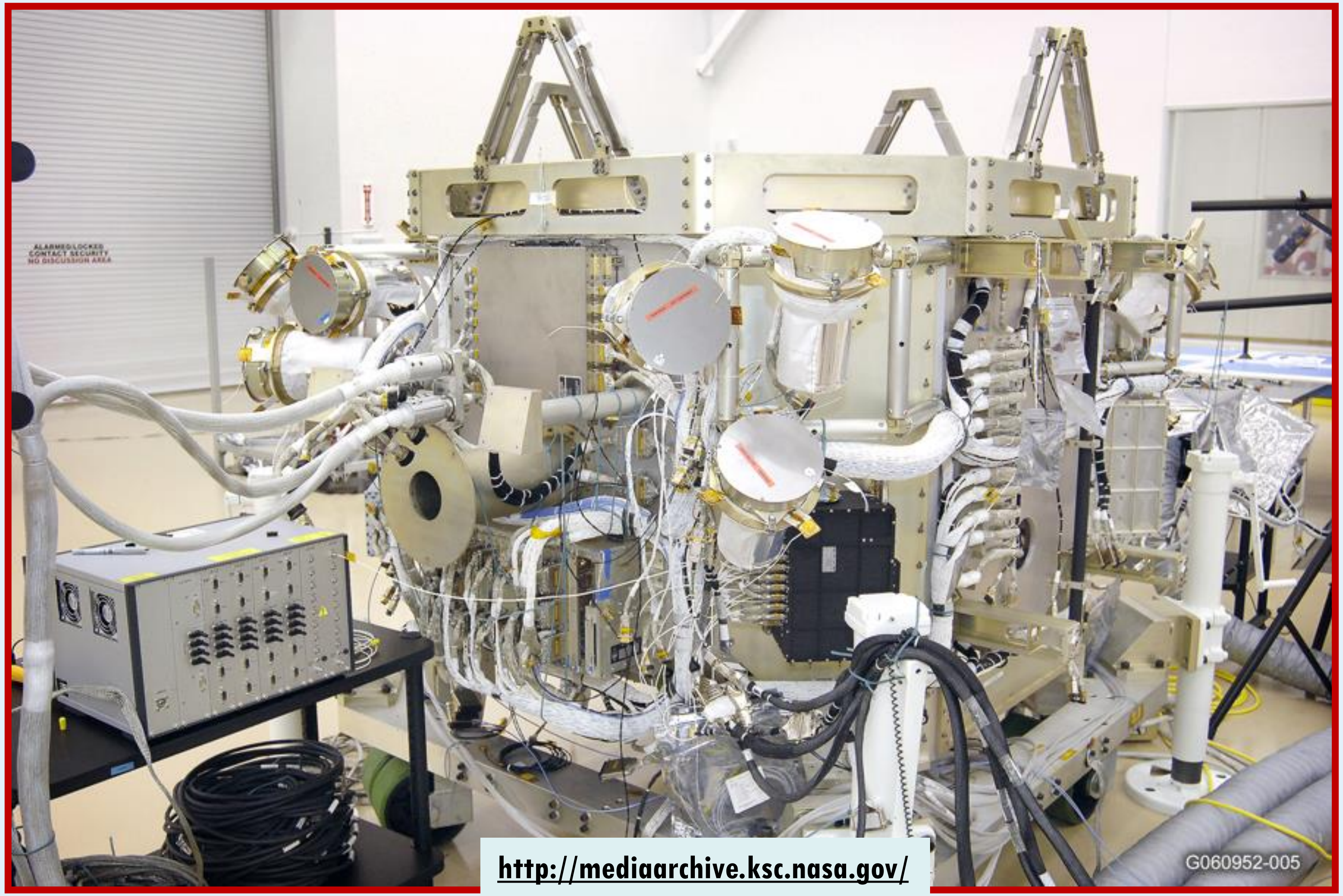

http://mediaarchive.ksc.nasa.gov/

The launch of the Fermi Mission

- Final phases in Spring 2008 at the Kennedy Space Center (Florida, USA)

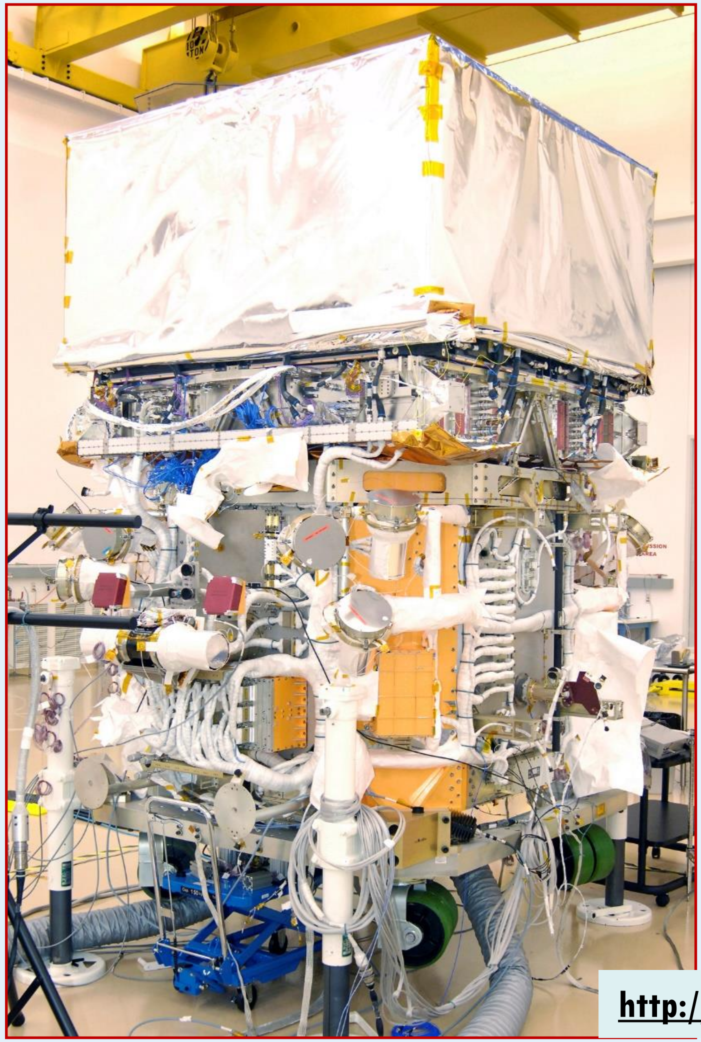

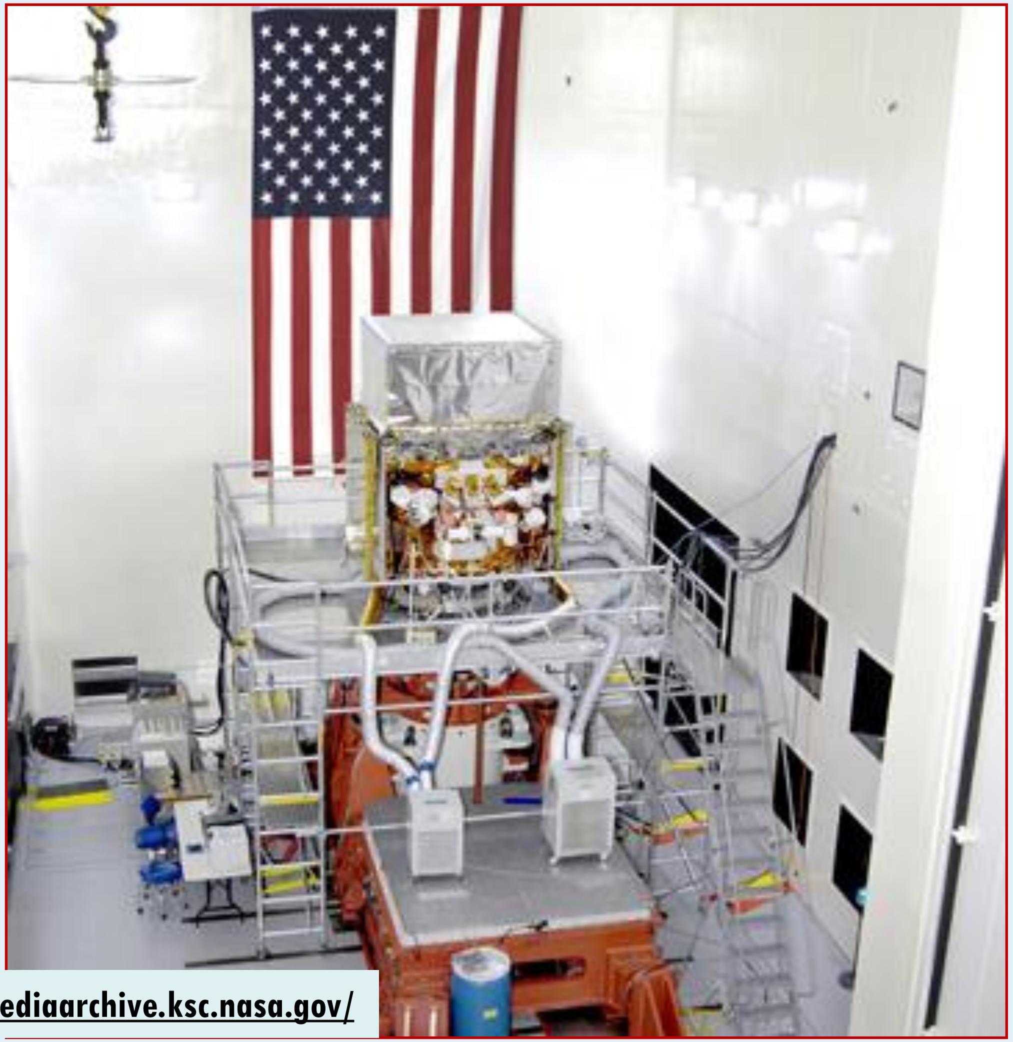

http://mediaarchive.ksc.nasa.gov/

The launch of the Fermi Mission

- Preparation to launch in May 2008 at the Kennedy Space Center (Florida, USA)

The launch of the Fermi Mission

- Preparation to launch in May 2008 at the Kennedy Space Center (Florida, USA)

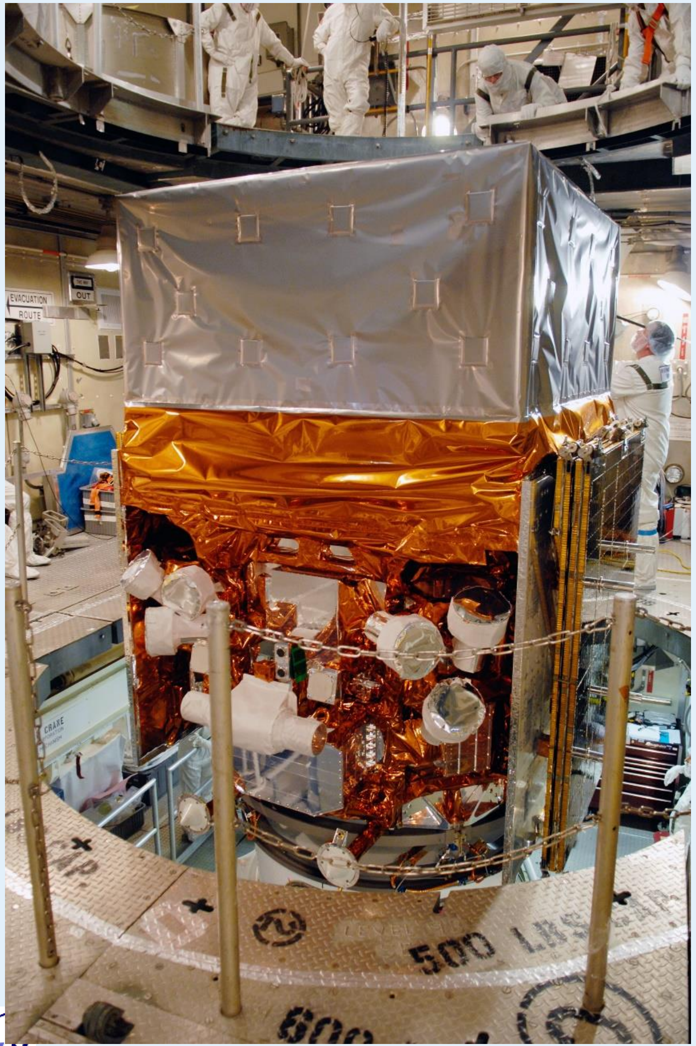

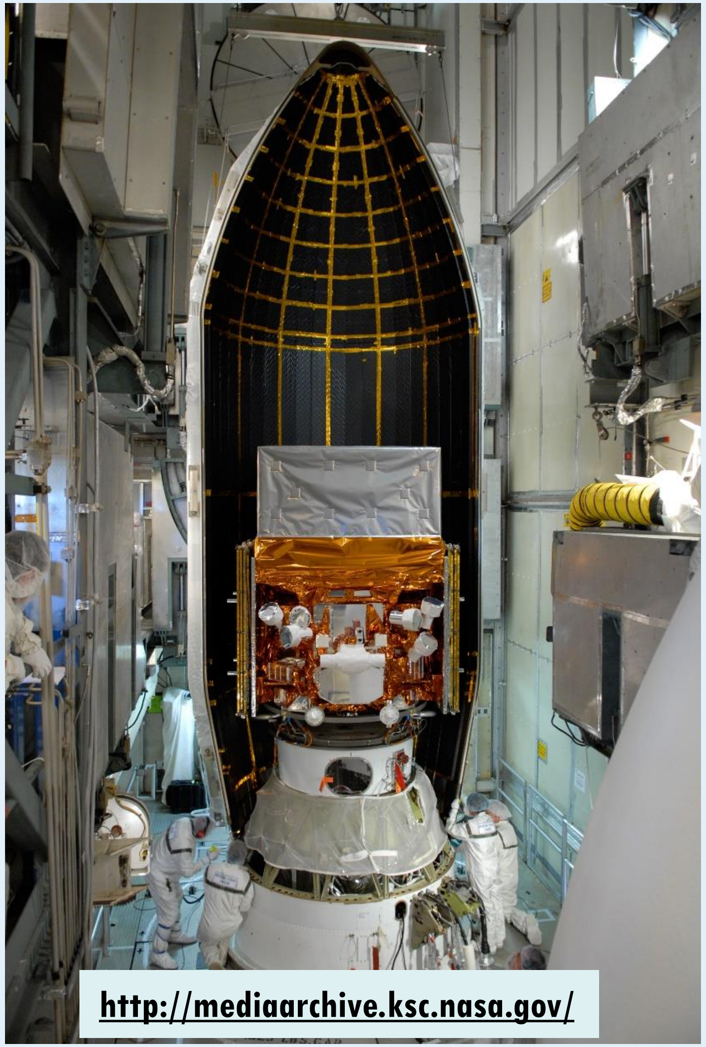

The launch of the Fermi Mission

http://mediaarchive.ksc.nasa.gov/

The launch of the Fermi Mission

https://www.youtube.com/watch?v=Znopi27RFY0

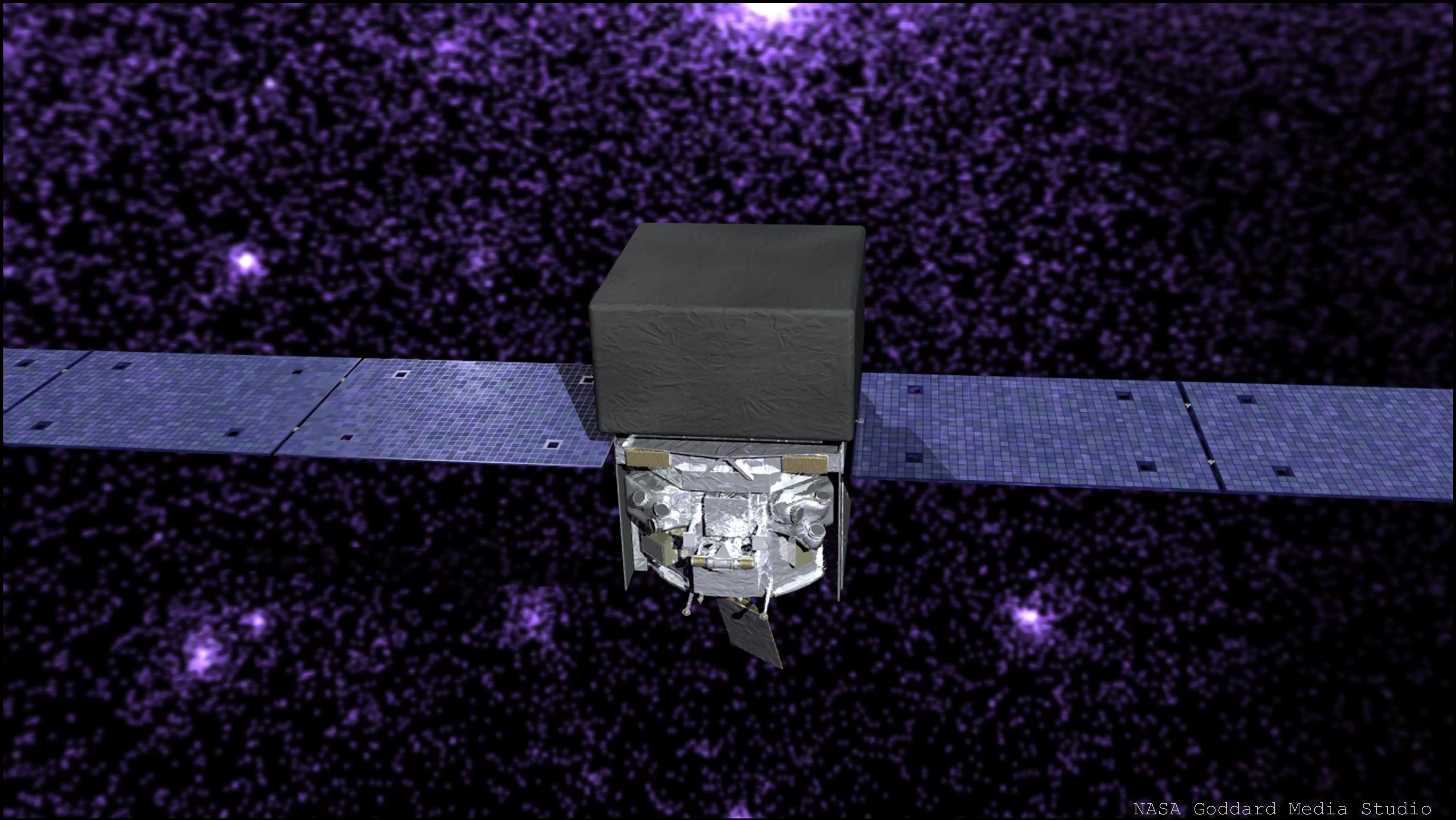

Credit: NASA's Goddard Space Flight Center/CI Lab

Fermi spacecraft orbit

- Circular «Low-Earth» orbit (LEO)
  - 565 km altitude (96 min period), 25.6 deg inclination

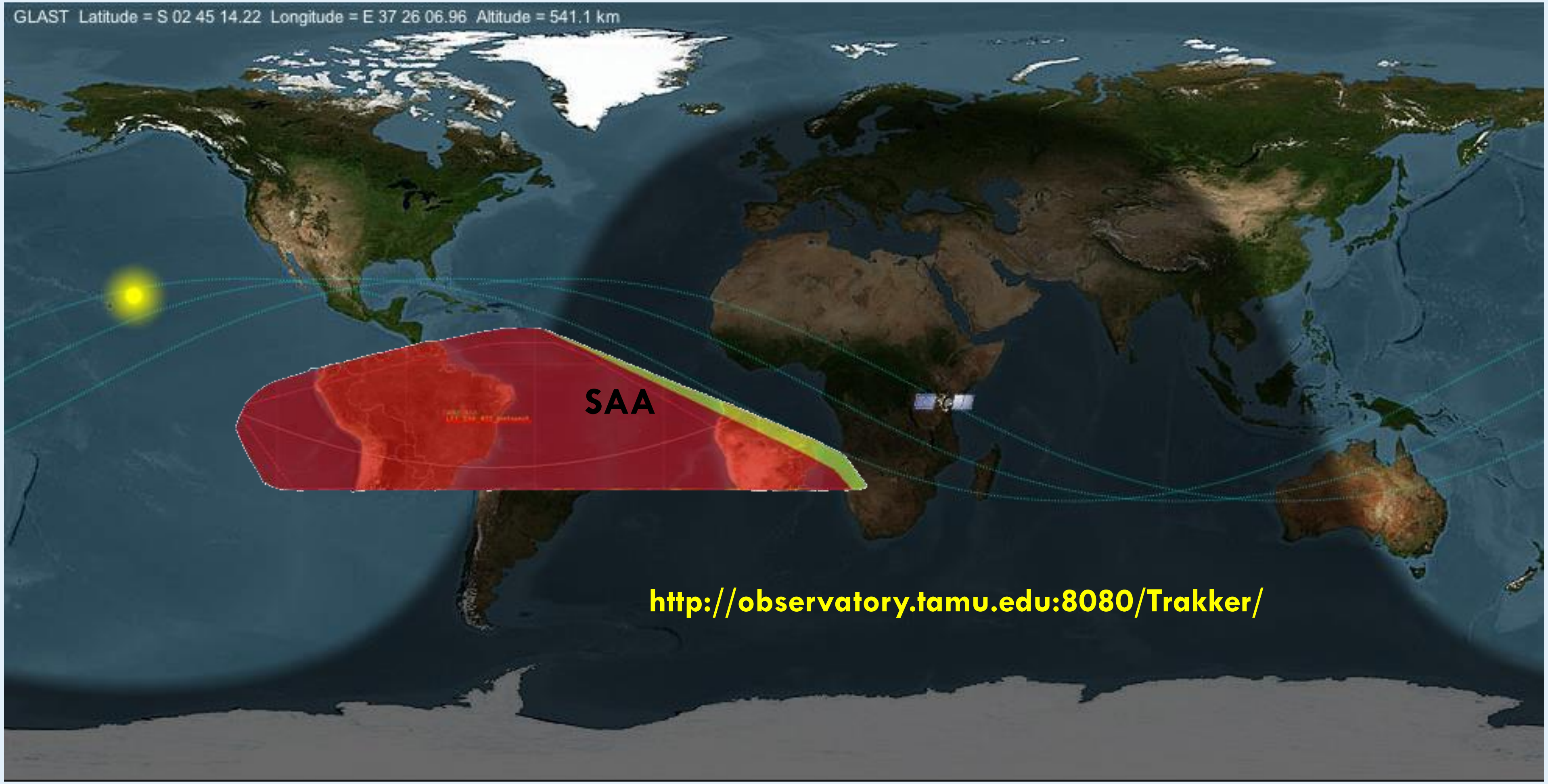

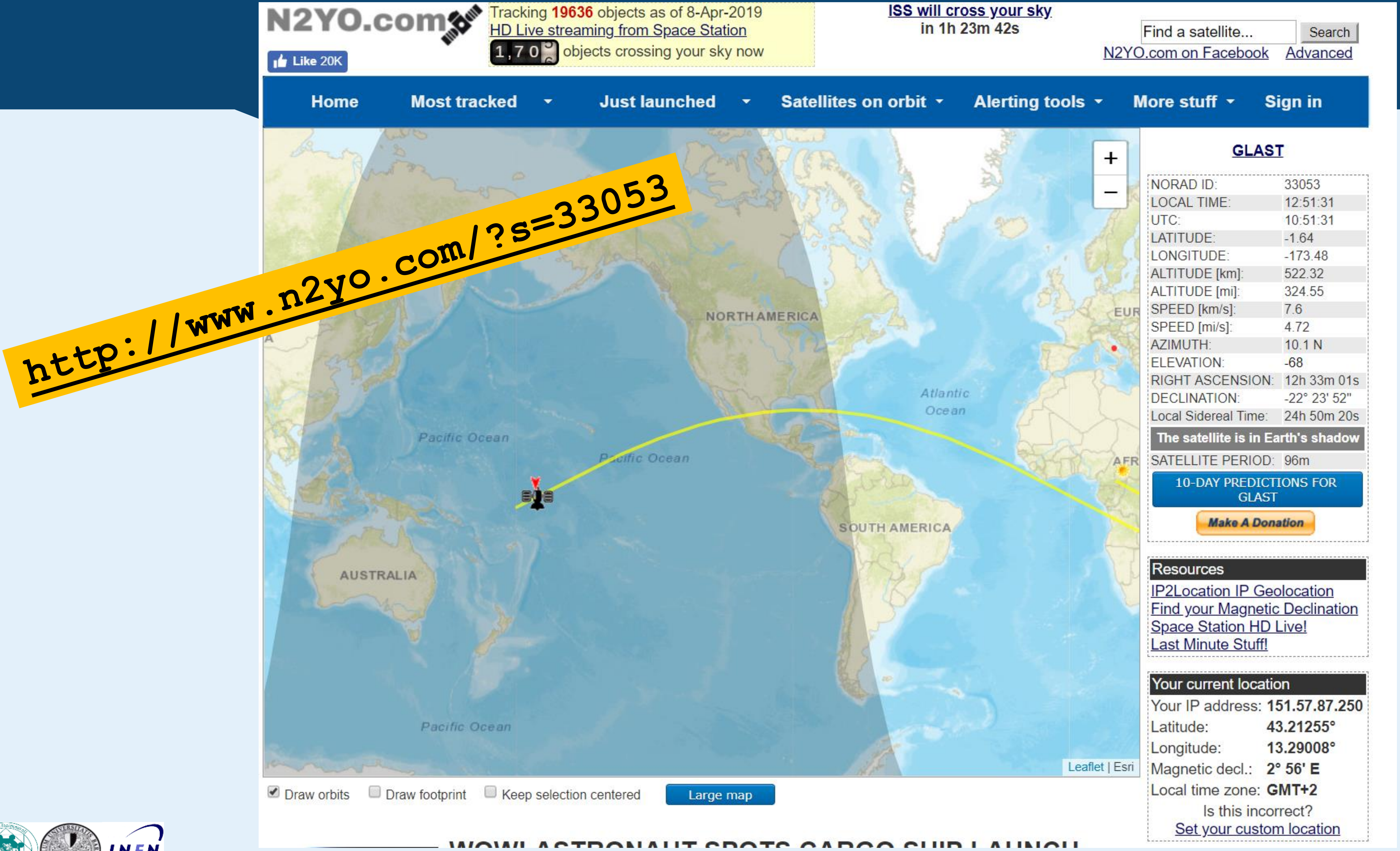
N2YO.com
Like 20K
Tracking 19636 objects as of 8-Apr-2019
HD Live streaming from Space Station
1,70 objects crossing your sky now
ISS will cross your sky
in 1h 23m 42s
Find a satellite...
Search
N2YO.com on Facebook
Advanced
Home
Most tracked
Just launched
Satellites on orbit
Alerting tools
More stuff
Sign in
http://www.n2yo.com/?s=33053
NORTH AMERICA
SOUTH AMERICA
AUSTRALIA
Pacific Ocean
Atlantic Ocean
GLAST
NORAD ID: 33053
LOCAL TIME: 12:51:31
UTC: 10:51:31
LATITUDE: -1.64
LONGITUDE: -173.48
ALTITUDE [km]: 522.32
ALTITUDE [mi]: 324.55
SPEED [km/s]: 7.6
SPEED [mi/s]: 4.72
AZIMUTH: 10.1 N
ELEVATION: -68
RIGHT ASCENSION: 12h 33m 01s
DECLINATION: -22° 23' 52"
Local Sidereal Time: 24h 50m 20s
The satellite is in Earth's shadow
SATELLITE PERIOD: 96m
10-DAY PREDICTIONS FOR GLAST
Make A Donation
Resources
IP2Location IP Geolocation
Find your Magnetic Declination
Space Station HD Live!
Last Minute Stuff!
Your current location
Your IP address: 151.57.87.250
Latitude: 43.21255°
Longitude: 13.29008°
Magnetic decl.: 2° 56' E
Local time zone: GMT+2
Is this incorrect?
Set your custom location
Leaflet | Esri
Draw orbits
Draw footprint
Keep selection centered
Large map

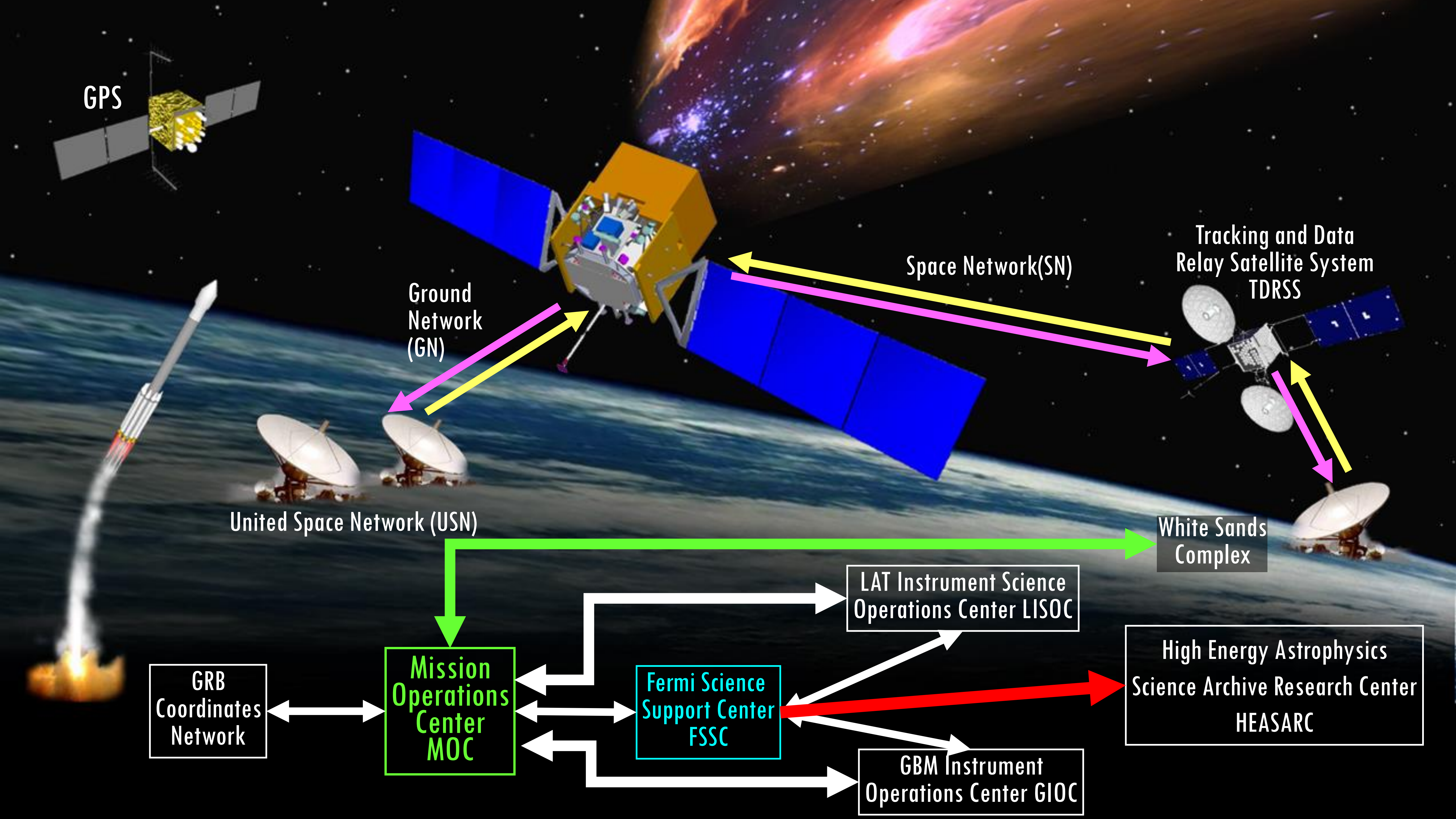
GPS
Ground Network (GN)
Space Network(SN)
Tracking and Data Relay Satellite System TDRSS
United Space Network (USN)
White Sands Complex
LAT Instrument Science Operations Center LISOC
High Energy Astrophysics Science Archive Research Center HEASARC
GRB Coordinates Network
Mission Operations Center MOC
Fermi Science Support Center FSSC
GBM Instrument Operations Center GIOC

Fermi–GBM NaI(Tl) Scintillators

- **12 NaI(Tl) detectors:**
  - Diameter: 12.7 cm (5")
  - Thickness: 1.27 cm (0.5")
  - Energy range: 10 keV – 1 MeV

NaI(Tl) detector FM04 @MPE 2005

Giselher Lichti @MPE 2005

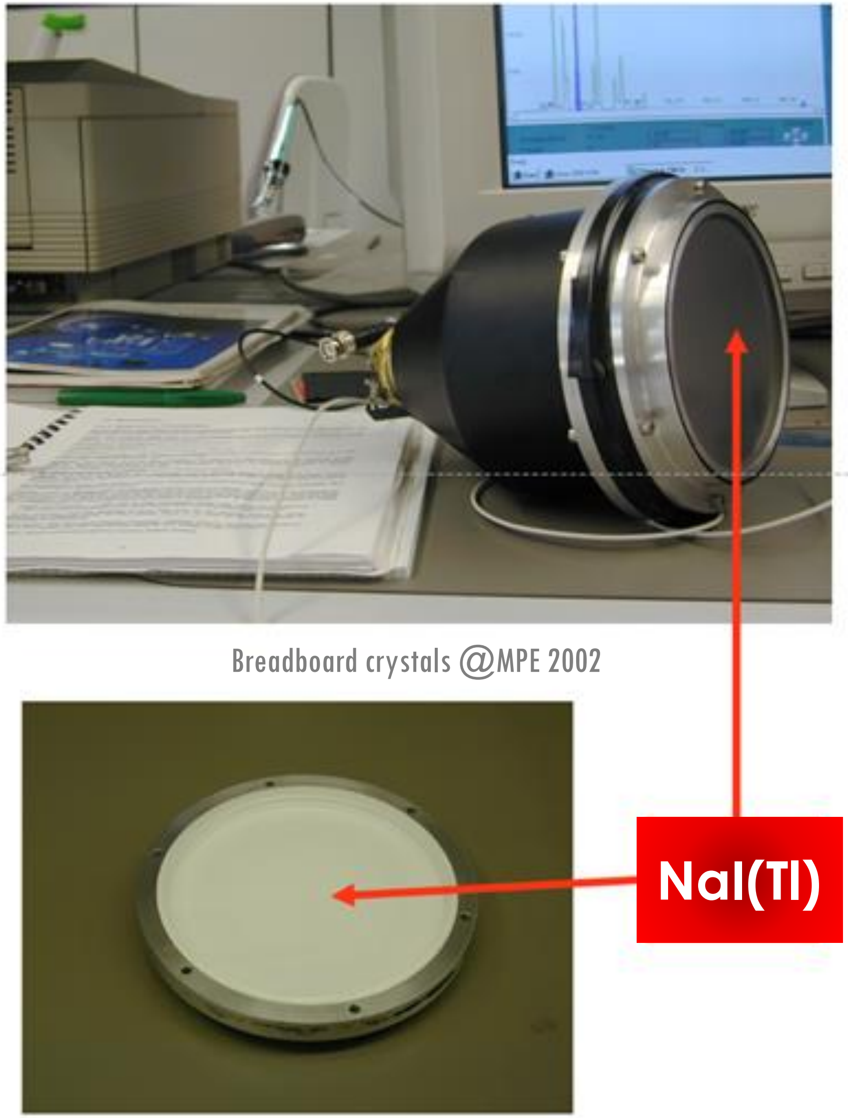

Breadboard crystals @MPE 2002

Fermi–GBM NaI(Tl) Scintillators

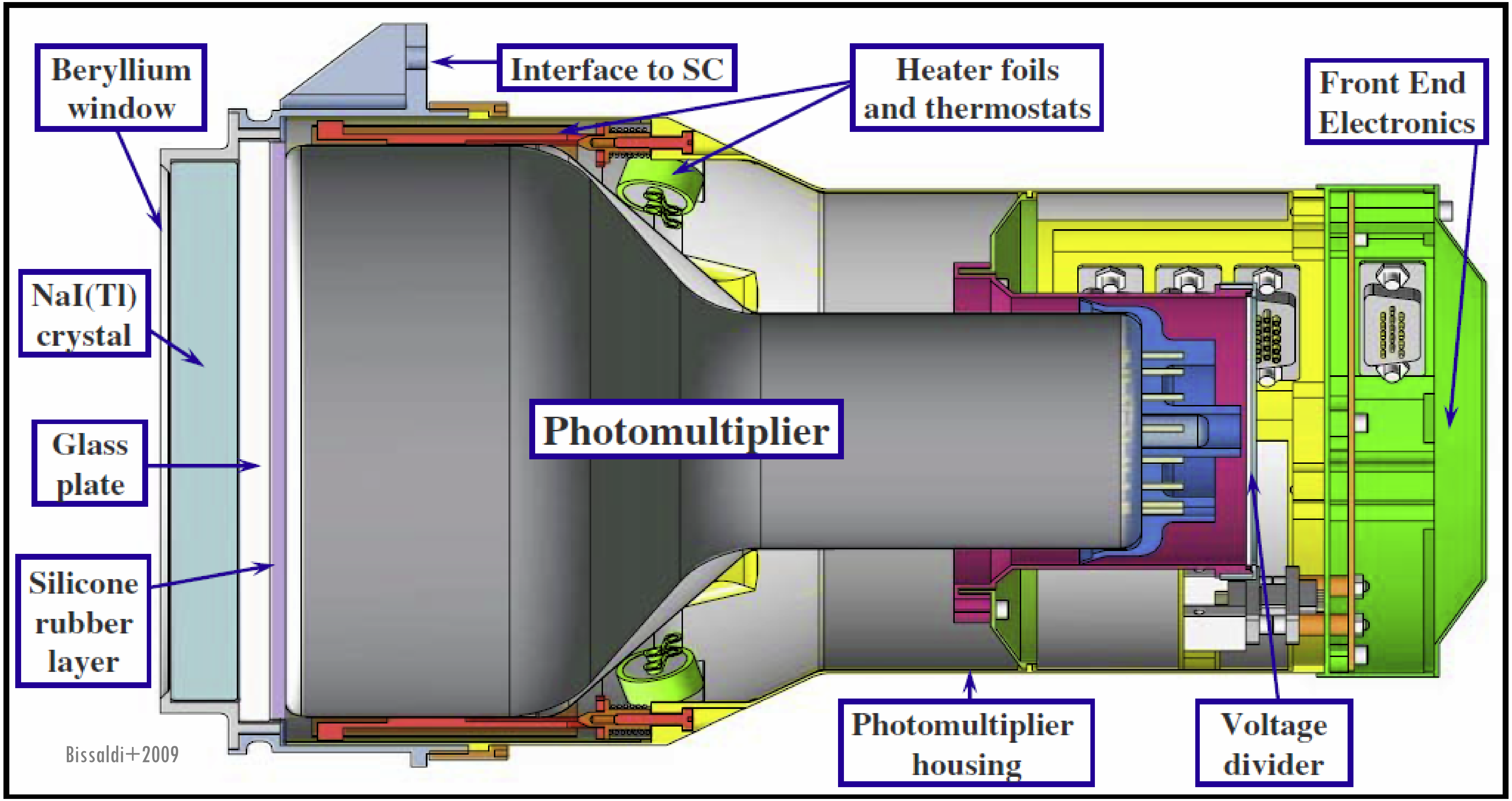

Fermi–GBM BGO Scintillators

- **2 BGO detectors:**
  - Diameter: 12.7 cm (5")
  - Thickness: 12.7 cm (5")
  - Energy range: 250 keV – 40 MeV

BGO detector FM01 @MPE 2005

Andreas von Kienlin @MPE 2005

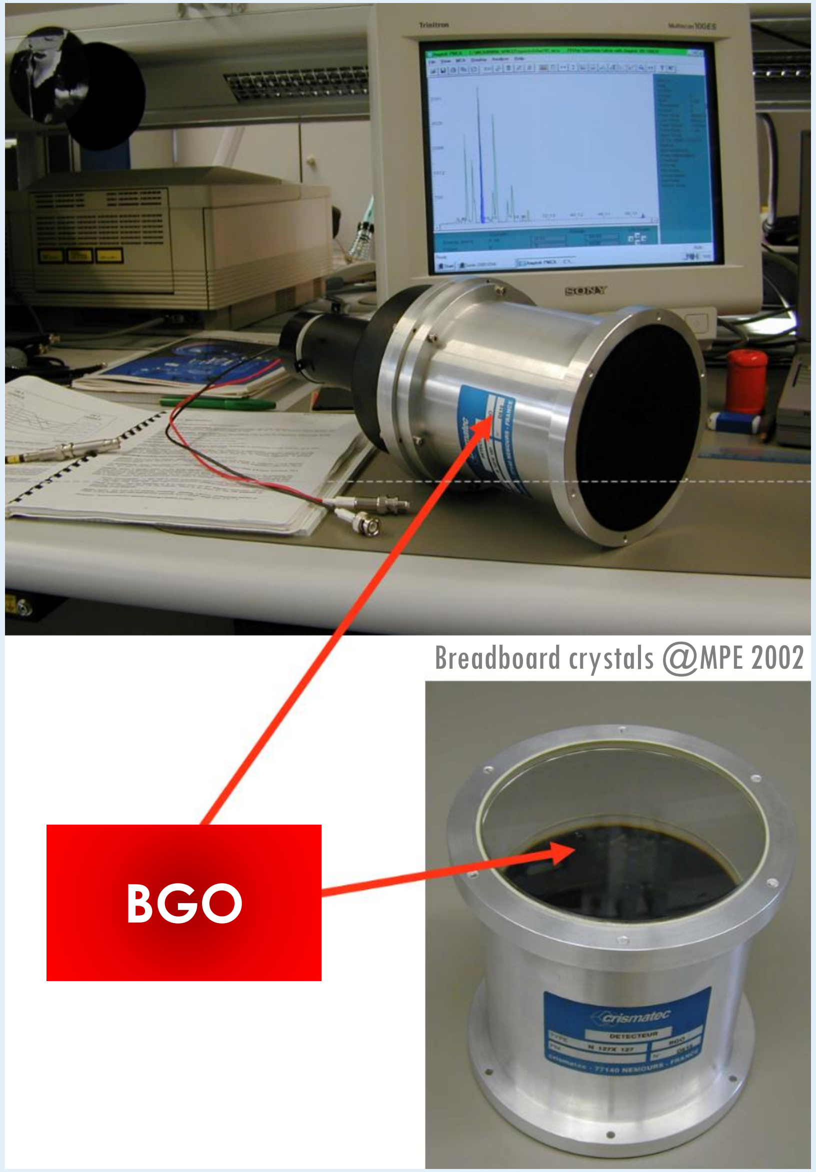

Breadboard crystals @MPE 2002

Fermi–GBM BGO Scintillators

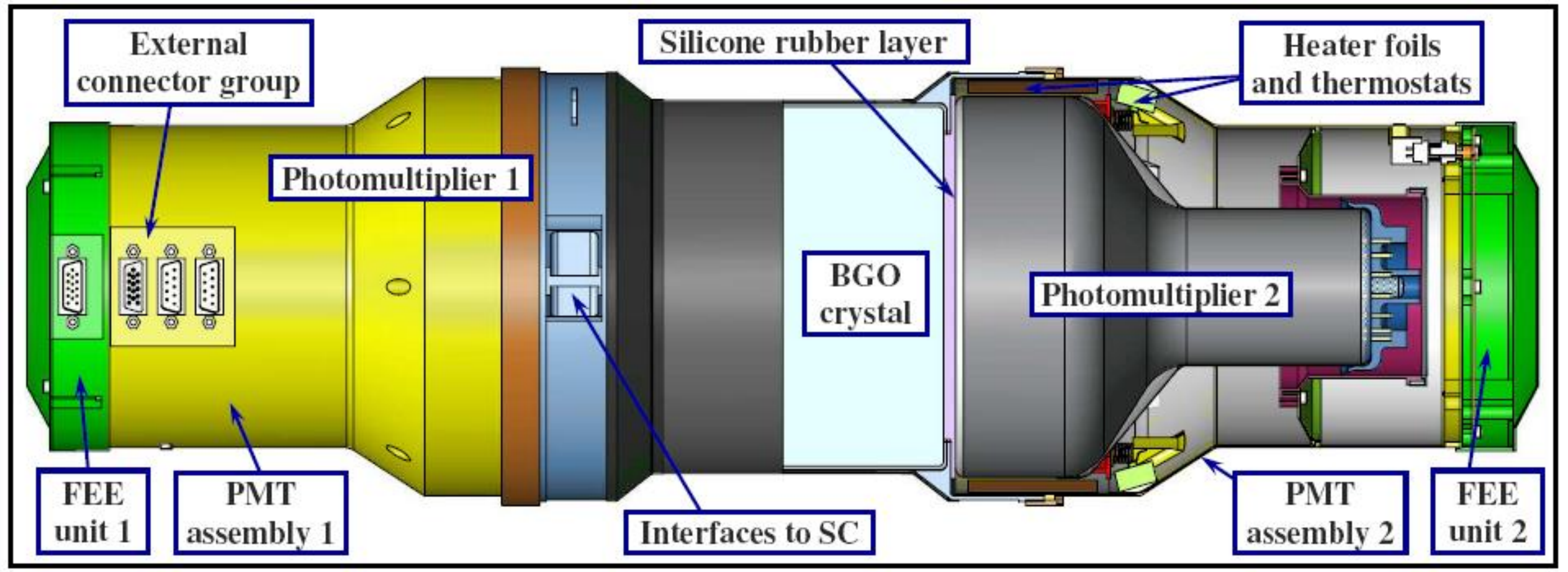

Bissaldi+2009

GBM Simulation: Purpose

The GBM simulation will characterize the instrument response to direct source photons, photons scattering from the spacecraft body, and photons scattering from the earth's atmosphere, for arbitrary source/earth geometry. GBM is a distributed system embedded in a complex environment, accurate simulation is the key to make GBM a useful instrument.

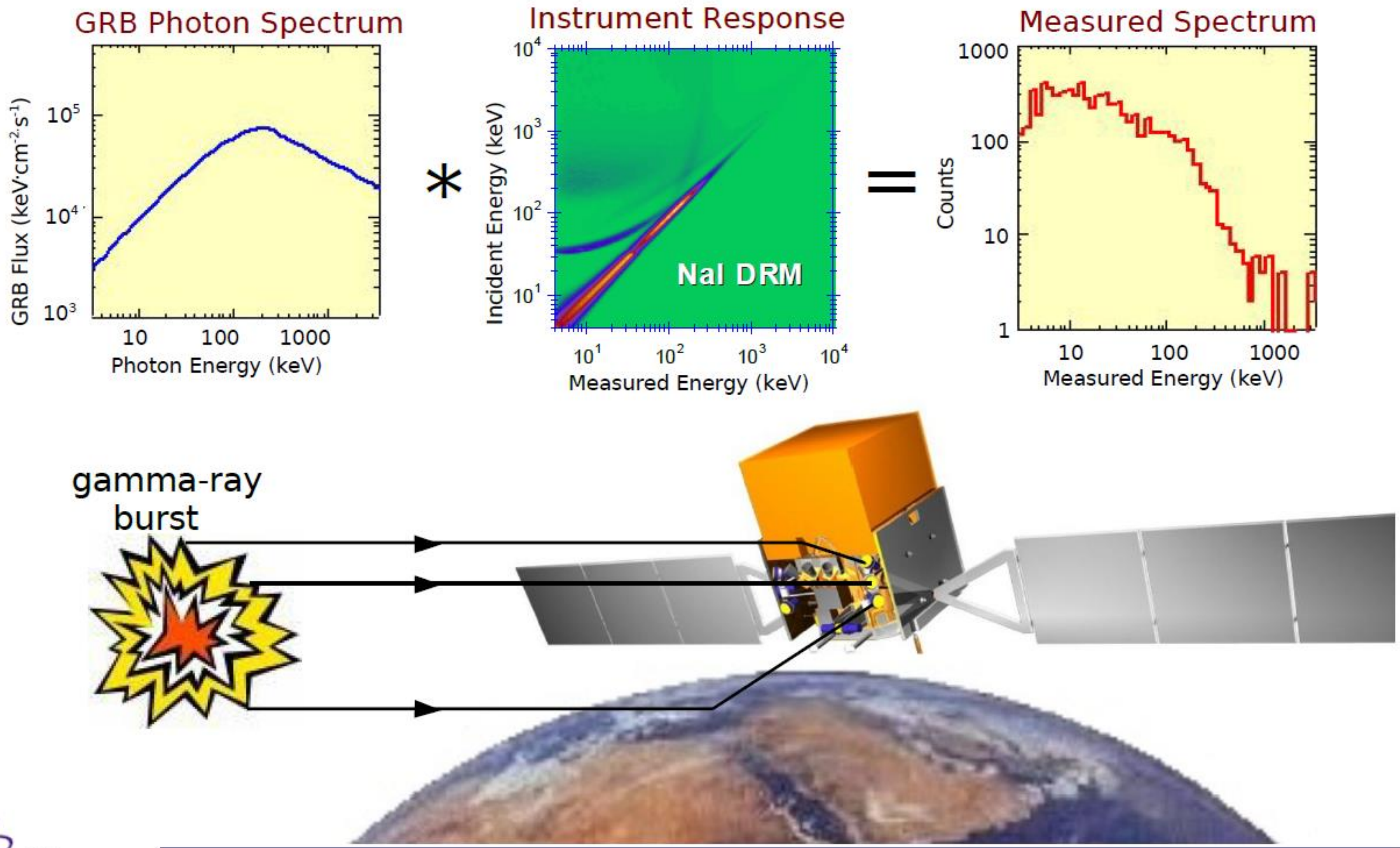

Hoover & Kippen 2004

GBM response to GRBs

GRB Photon Spectrum

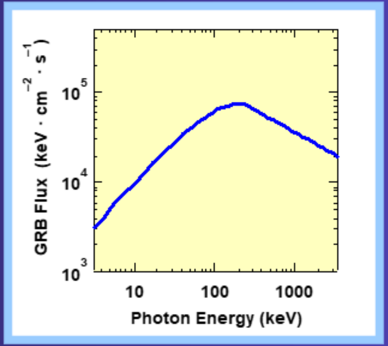

*

Instrument Response

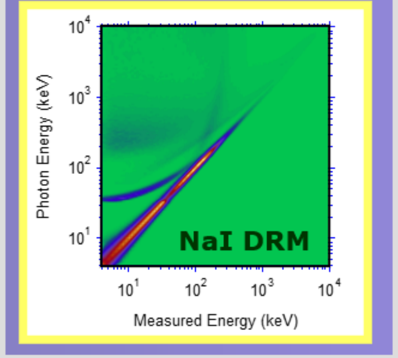

+

Instrument Background

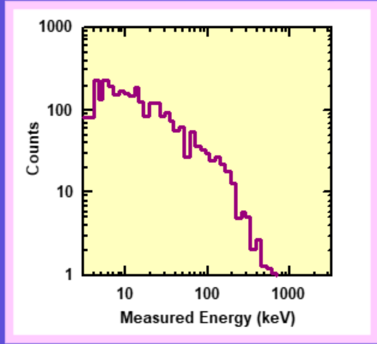

=

Observed Data

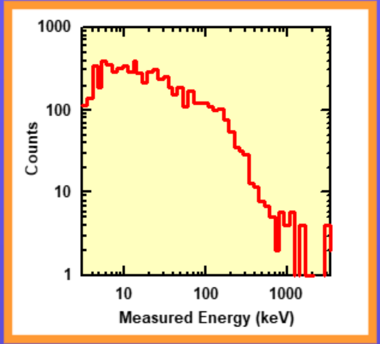

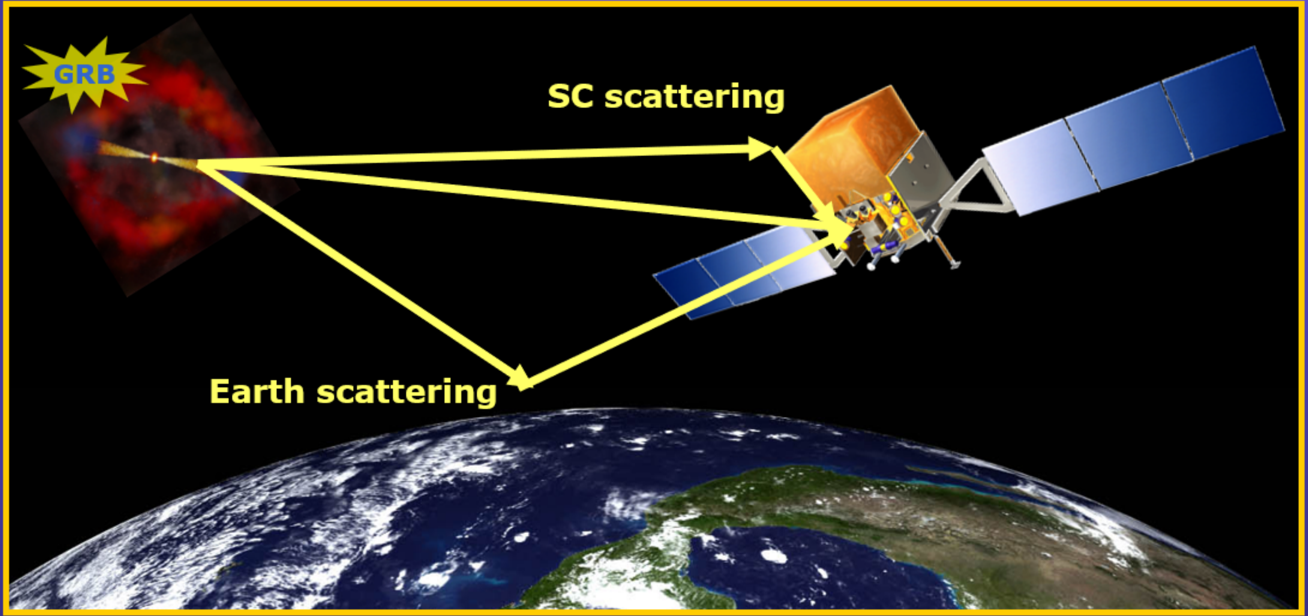

The simulation software must determine the response of the GBM detectors from several possible sources: 1) source photons which hit the detector directly and may scatter inside the detector itself, 2) source photons which scatter off the spacecraft before entering the detector, 3) source photons which scatter off the earth's atmosphere (and possibly the spacecraft also) before entering the detector. The simulation uses full-scale, detailed models of the NaI and BGO detectors, the spacecraft (currently in preparation), and the earth's atmosphere. When full-scale simulation production begins, we will simulate the detector, spacecraft, and atmospheric response for a range of energies and incident directions.

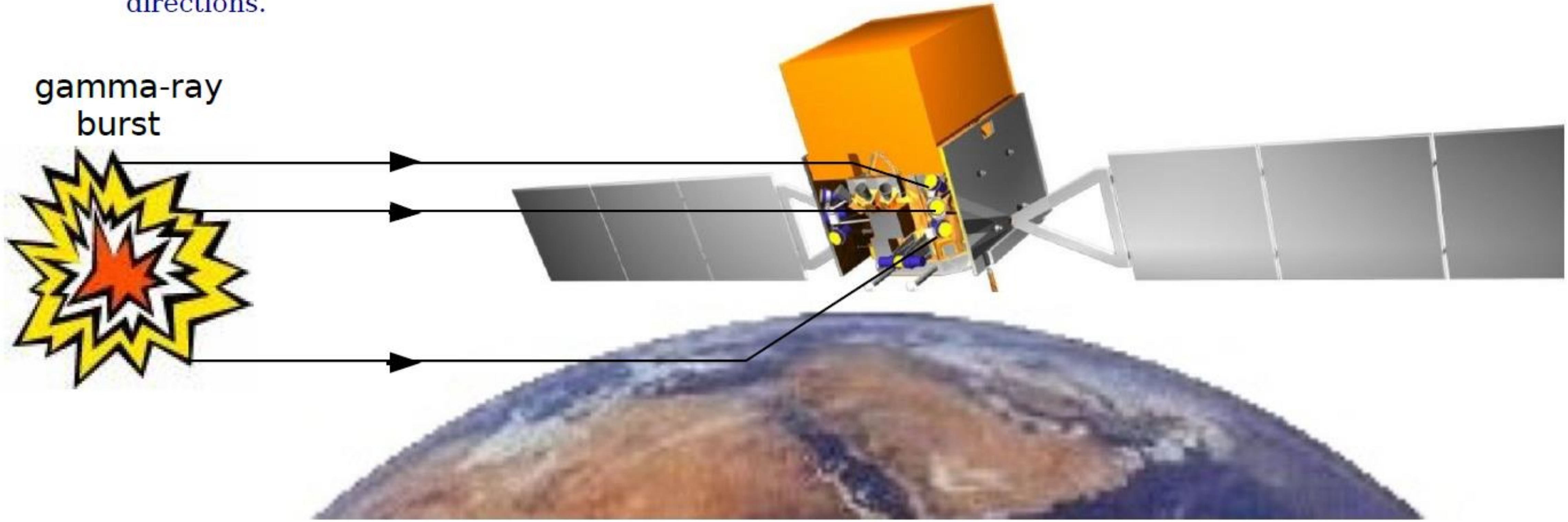

Hoover & Kippen 2004

Working Towards a GEANT4-based Solution

- *GRESS* = General Response Simulation System
- Original purpose: GLAST burst monitor detailed source response function generation
  - Prompt response only (no activation)
  - Extensive γ-ray validation library
    - Radioactive sources 6 keV to 4 MeV
    - Low-energy BESSY synchrotron data (2–20 keV)
    - High-energy van deGraf data (4, 6, 11 MeV)
    - Detailed angular/surface response scans
  - Full-spacecraft/instrument + separate Earth scattering simulations
  - Interface to analysis via NASA FITS files
- Future: Extend GRESS for more general HEA use
  - Choices of different data types (e.g., spectroscopy vs. tracking instruments) for each volume linked via GDML interfaces
  - Space environment background models via *ACTtools*-like inputs (or other)
  - Possibly include radioactive decay capability
  - Further validation against space instrument data (e.g., GLAST on-orbit, COMPTEL, etc.)

Examples from Detector Validation Library

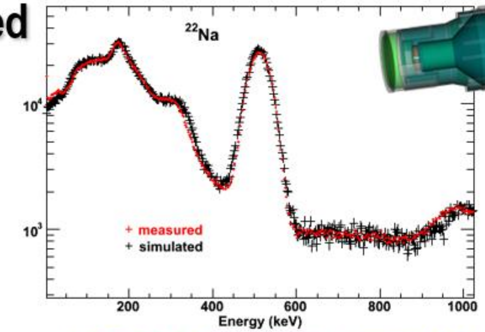

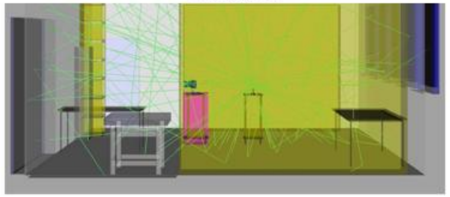

Two-stage Spacecraft Validation

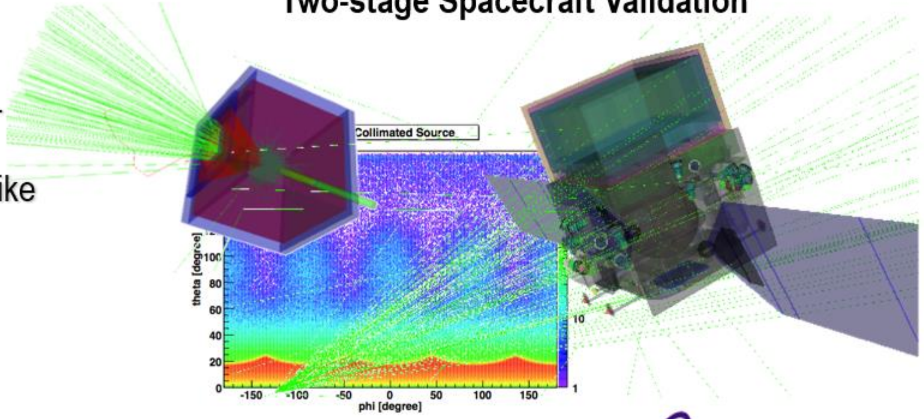

GRESS = General REsponse Simulation System

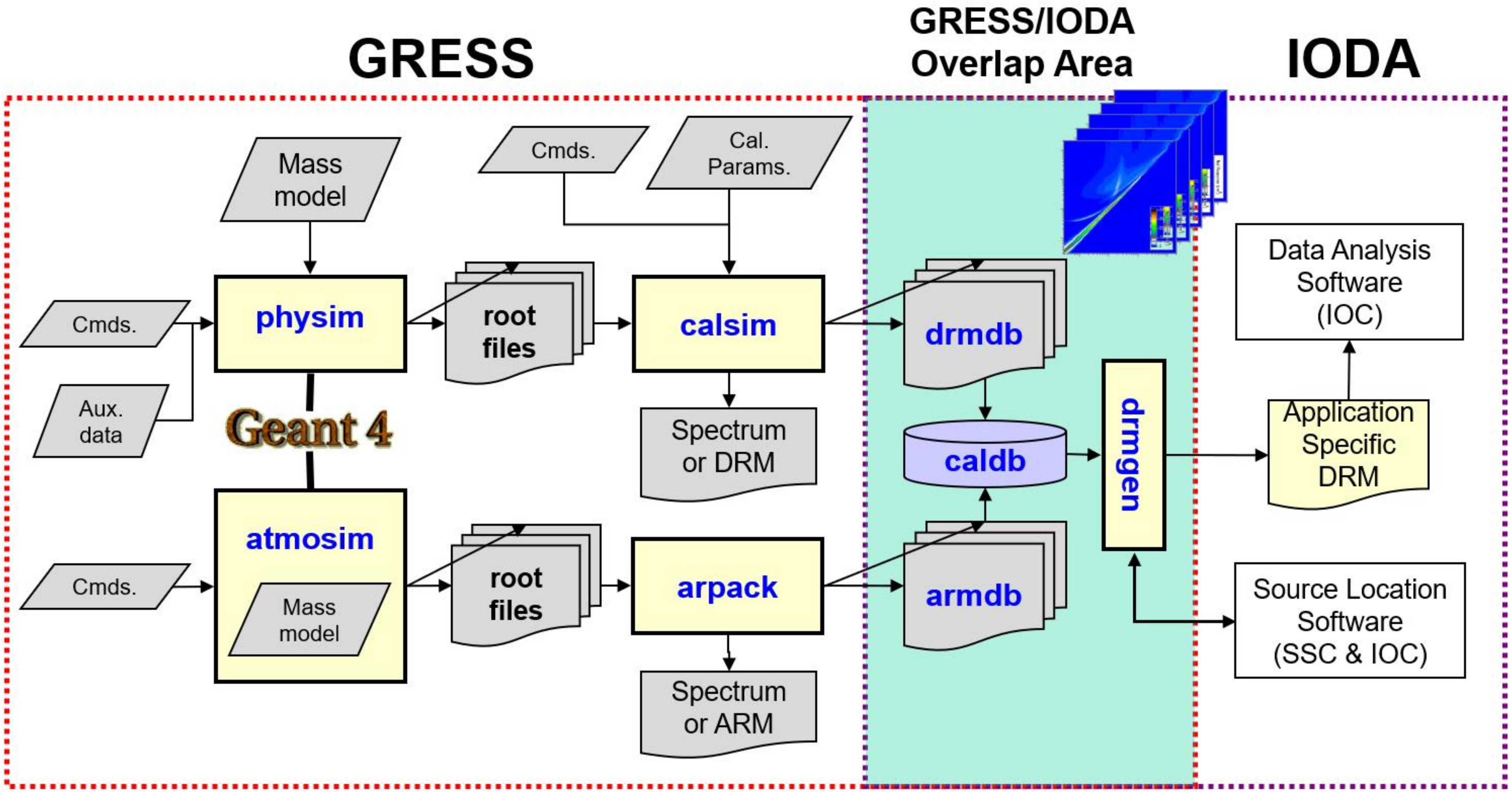

http://public.lanl.gov/mkippen/gress/

The GBM Response Simulation System (GRESS)

Comprehensive collection of **computer models, simulation software, and data packaging tools**, including facilities for (1) physical simulation through a modified GEANT4 toolkit architecture, (2) custom instrumental effects simulators, (3) custom data packages, and (4) interfaces to GBM data processing/analysis software

- Because of vastly differing scale size, GRESS separates total GBM instrument response into 2 components:
  - **"Direct" detector + spacecraft response**
    - Captures physical and instrumental response of the detectors + spacecraft combined system
    - Incorporates a detailed mass model of the GLAST observatory, including the GBM detectors, the Large Area Telescope, and all in-flight spacecraft components
  - **Atmospheric scattered response**
- Unlike many earlier space-borne gamma-ray instrument response simulation efforts (e.g., BATSE2, COMPTEL, etc.), **GRESS captures the combined response rather than separating detector simulations from passive spacecraft elements**
  - GLAST spacecraft is **highly non-uniform** in its scattering properties and the GBM detectors are embedded in this nonuniformity
- Direct response as a function of photon energy and direction captured in **a "Direct Response Matrix" (DRM) database**, including results from individual simulation runs at an array of incident source directions

GBM Simulation: Specifications

- **Definition:** Multi-purpose software suite that computes the physical and instrumental response of the GBM detectors
  - Primary purpose: generate detector response functions critical to analysis of flight science data
  - Other uses: instrument design, interpretation of calibrations, design of flight and ground analysis algorithms/software
- **Technique:** GEANT4 simulation
  - Verified through, and incorporating results from experimental calibration

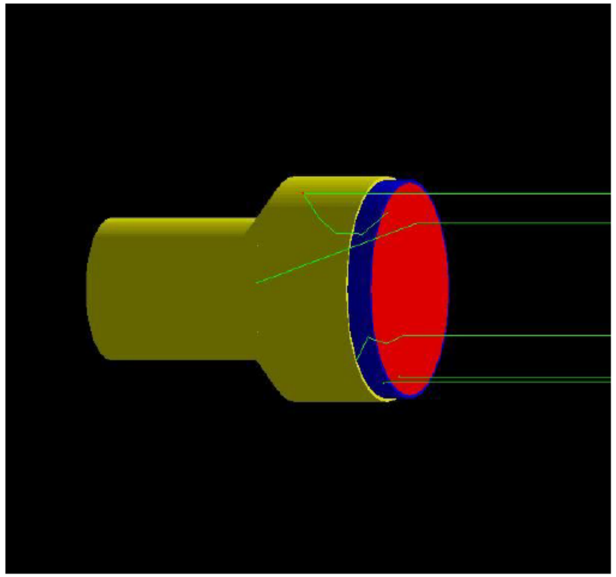

- **Major Components**
  - Mass model (geometry + composition)
  - Incident particle distributions
  - Radiation transport physics
  - Instrumental/calibration effects
  - DRM database
  - DRM synthesizer/generator

Hoover & Kippen 2004

GBM Simulation: Architecture

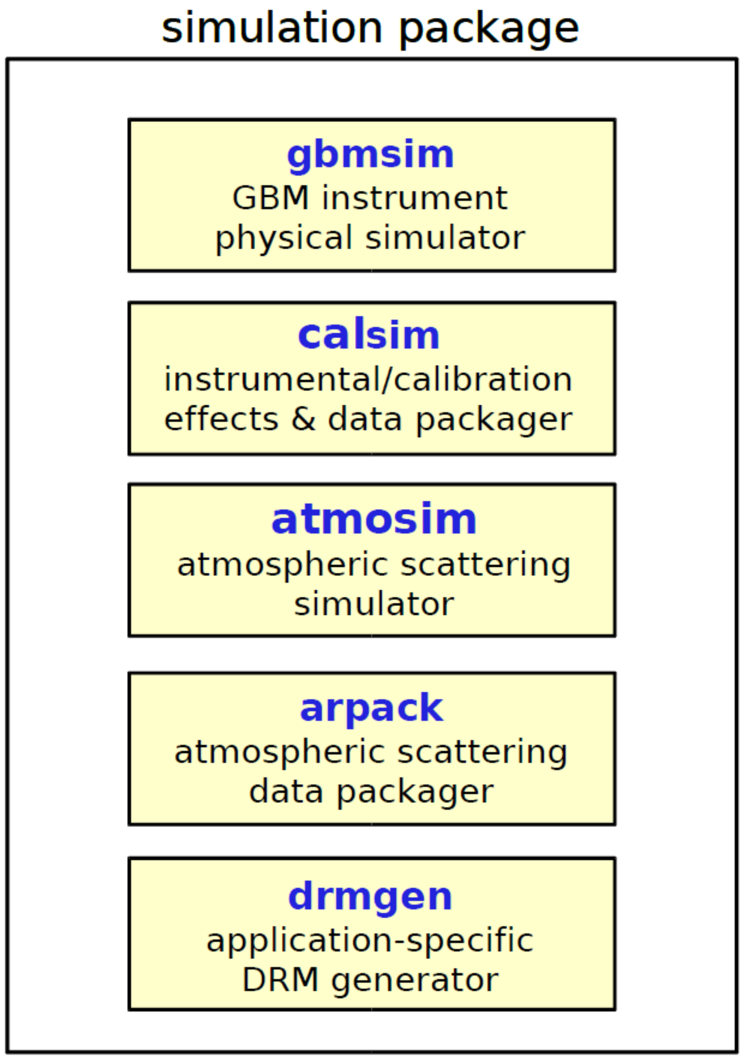

- Integrated package that will encompass all GBM instrument response software and data needs
- Configuration controlled (e.g. - CVS) as a single deliverable package with component software/data modules
- All packages (and their dependencies) will use GNU compilers — mainly g++
- All data files have headers with detailed job tracking data

Hoover & Kippen 2004

GBM Simulation Design (1)

gbmsim
GBM instrument
physical simulator

Inputs
- Instrument+environment mass model (custom GDML file format)
- Commands (interactive command line or command macro file[s])
- Auxilary data (spatial/spectral dists.)

Outputs
- Raw event file(s) (ROOT format)
- Interactive visualizations

External Dependencies
- GEANT4 — General MC Rad. Transport package from CERN
- ROOT — Data handling/analysis package from CERN
- XERCES — portable c++ XML parser from Apache.org

calsim
instrumental/calibration effects
simulator & data packager

Inputs
- Raw event files (root; from gbmsim or atmosim)
- Commands (interactive command line or command macro file[s])
- Calibration parameters file (ascii)

Outputs
- Processed data file(s) (FITS format)
  e.g., spectra, DRMs, etc.

External Dependencies
- ROOT — Data handling/analysis package from CERN
- CCFits — FITS data file I/O for c++ from NASA/GSFC

Hoover & Kippen 2004

GBM Simulation Design (2)

atmosim atmospheric scattering simulator	**arpack** atmospheric scattering data packager

atmosim

Inputs
- Earth atmosphere mass model (internally coded)
- Commands (interactive command line or command macro file[s])

Outputs
- Event files (ROOT format)
- Interactive visualizations

External Dependencies
- GEANT4 — General MC Rad. Transport package from CERN
- ROOT — Data handling/analysis package from CERN
- CCFits — FITS data file I/O for c++ from NASA/GSFC

arpack

Inputs
- Event files (ROOT; from atmosim)
- Commands (interactive command line or command macro file[s])

Outputs
- Atmospheric response matrices (ARM; FITS format)

External Dependencies
- ROOT — Data handling/analysis package from CERN
- CCFits — FITS data file I/O for c++ from NASA/GSFC

Hoover & Kippen 2004

NaI Detectors

- In general, the detail of the simulation mass model will be inversely proportional to the distance from the NaI and BGO detectors (NaI/BGO detectors and nearby spacecraft components will be modeled with high precision, internal workings of the LAT and distant spacecraft body with less precision)

- We await detailed drawings and materials specifications, in the meantime we are working with a simplified mass model

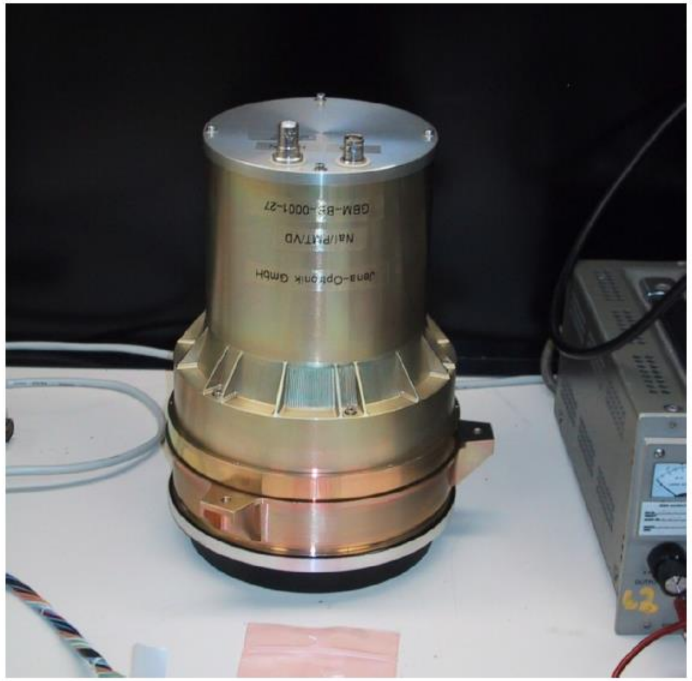

NaI detector (x12): 1.27 cm thick by 12.7 cm diameter; 5 keV to 1 MeV spectral coverage; 0.25 mm Beryllium window

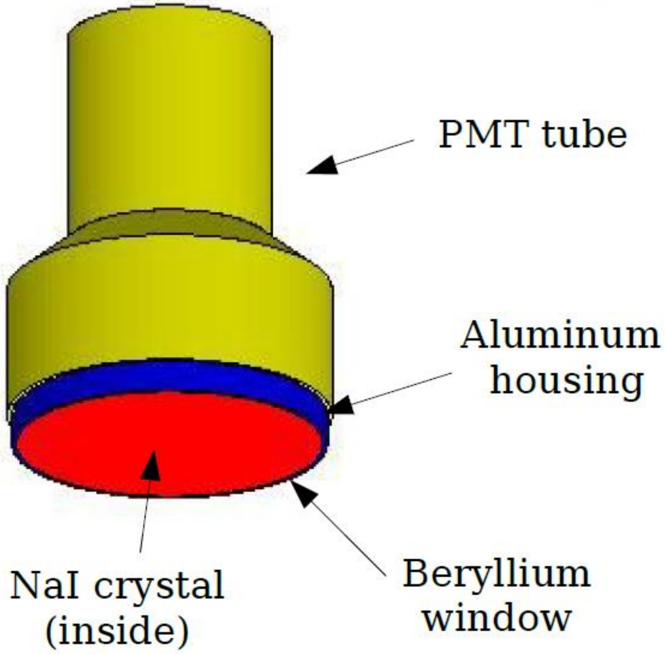

Hoover & Kippen 2004

NaI detectors

- To generate a proper DRM, a high degree of precision and accuracy is required in the simulation model of these detectors, particularly around the NaI crystal and its interface to the photomultiplier tube.

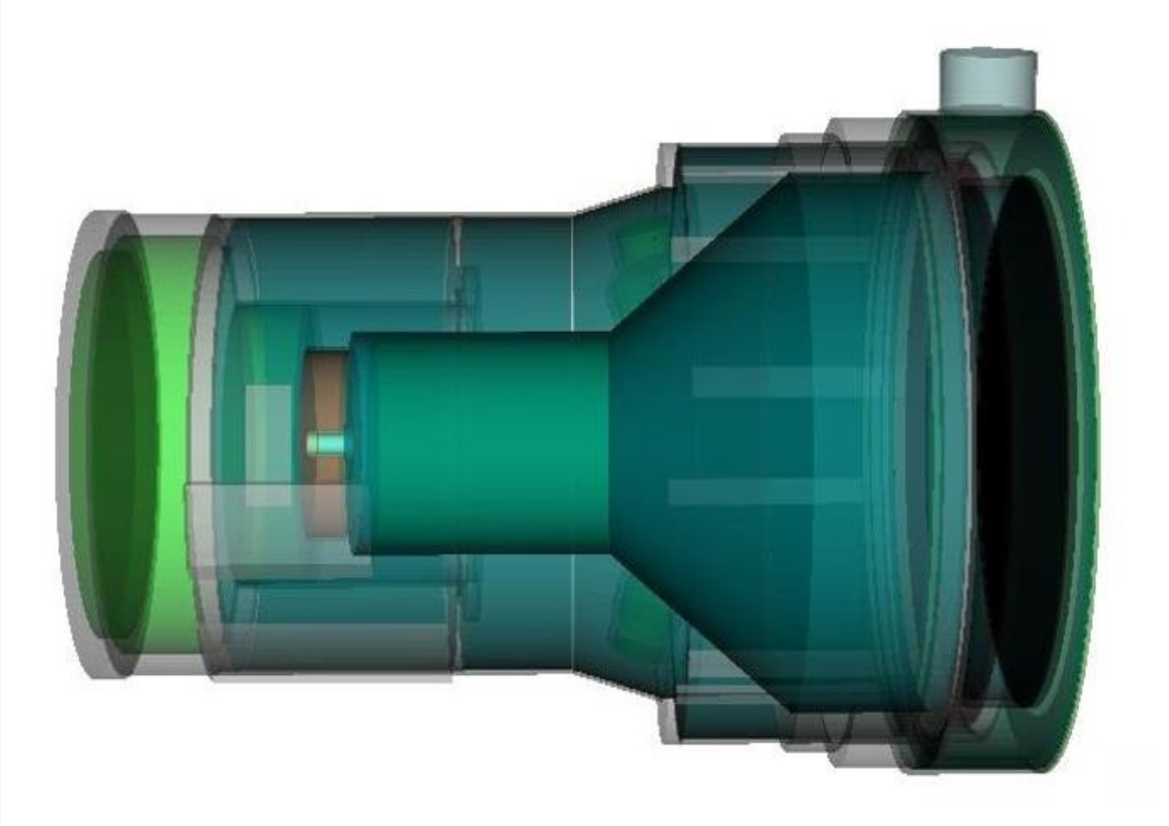

Cut-away view of the NaI detector simulation model.

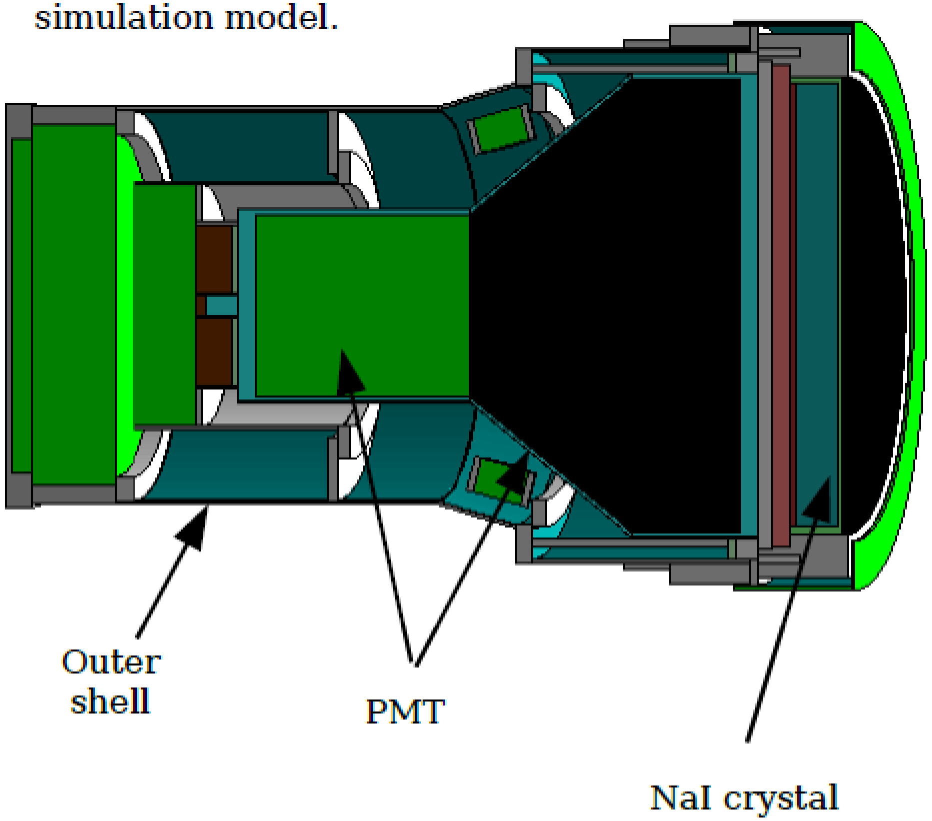

BGO Detectors

BGO detector (x2): 12.7 cm thick by 12.7 cm diameter; 150 keV to 30 MeV spectral coverage; viewed by 2 PMTs

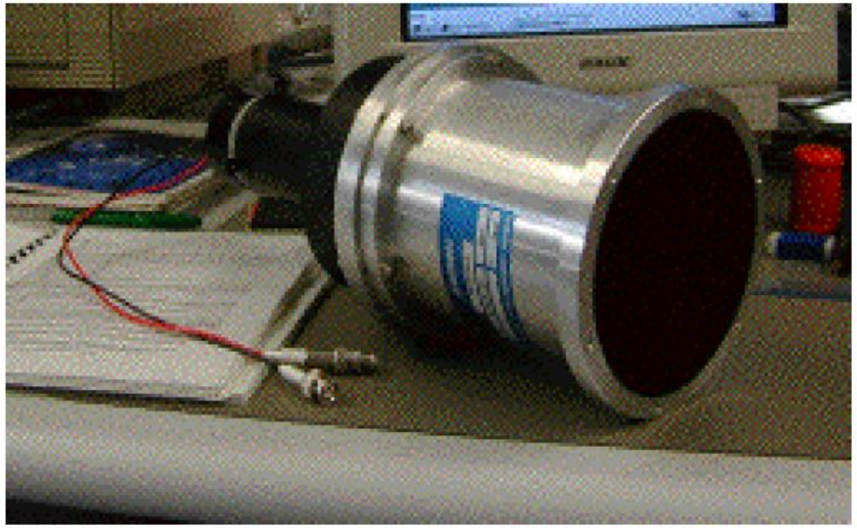

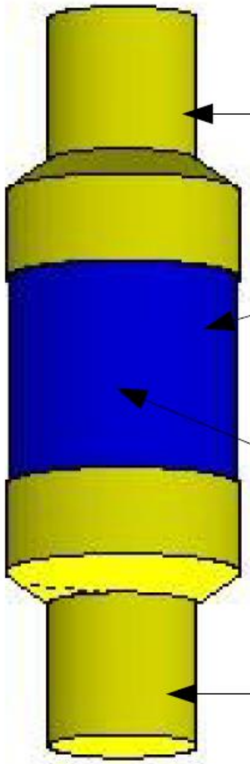

Hoover & Kippen 2004

BGO detectors

External view of the BGO detector simulation model.

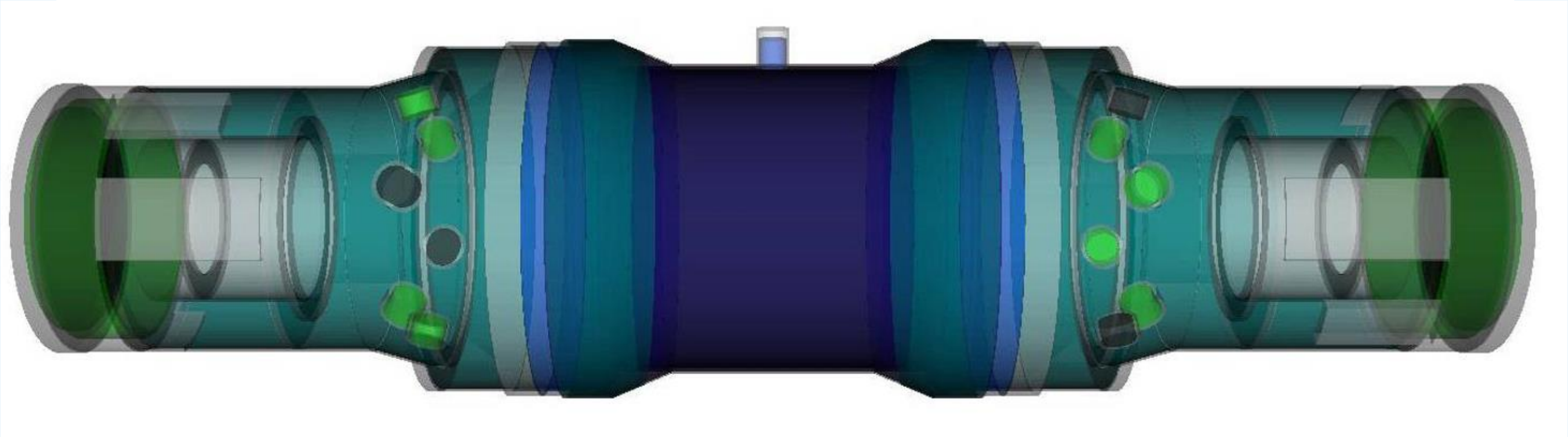

Cut-away view of the BGO detector simulation model.

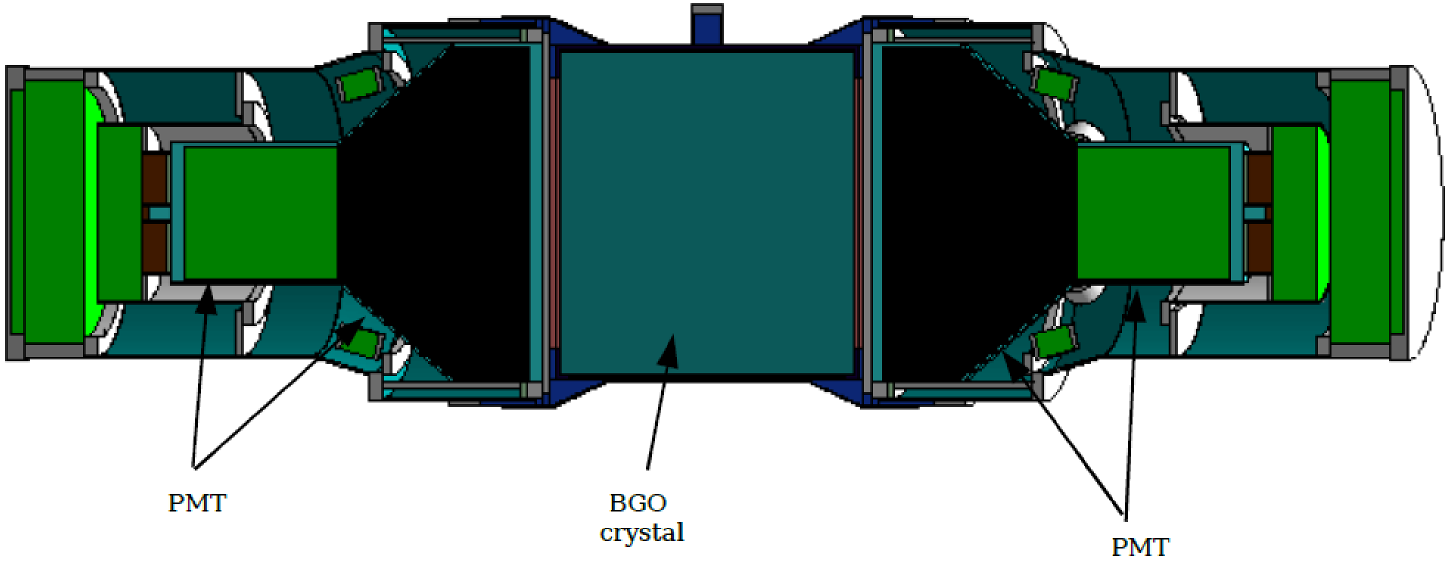

Low Energy Compton Scattering

GEANT does not properly handle low-energy Compton scattering, where atomic binding effects are important and cause Doppler broadening

A GEANT extension called G4LECS (GEANT4 low energy Compton scattering), developed by R.M. Kippen, is used to correct for this deficiency.

R.M. Kippen, *New Astronomy Reviews*, 48, 221-225 (2004)

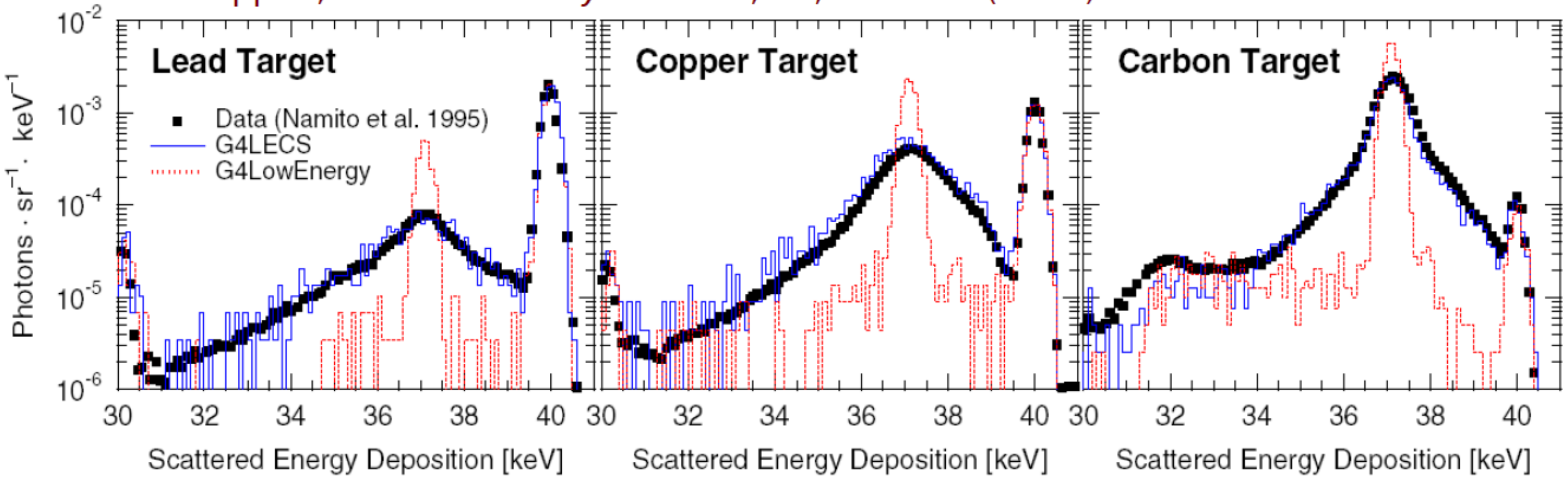

Hoover & Kippen 2004

Example: NaI Spectrum

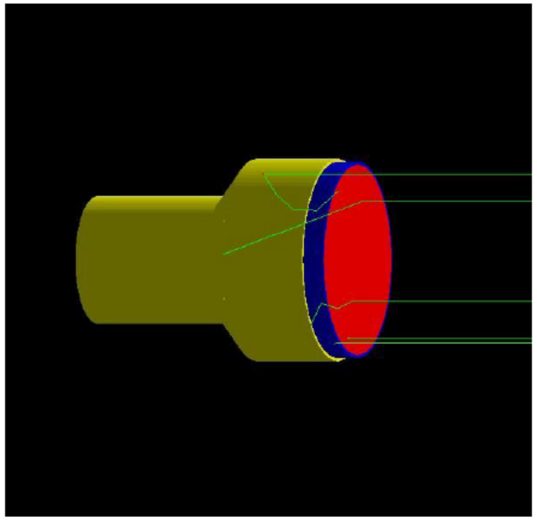

- Simple NaI detector mass model
- Normal incidence, 10^5 recorded events

gbmsim – raw physical data

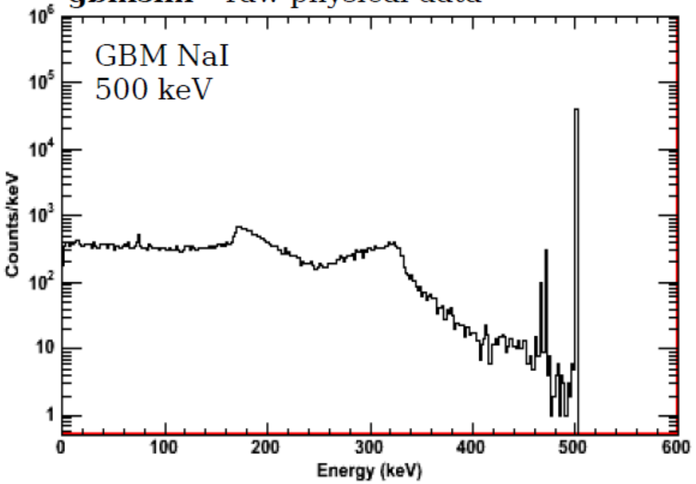

calsim – instrument-like data

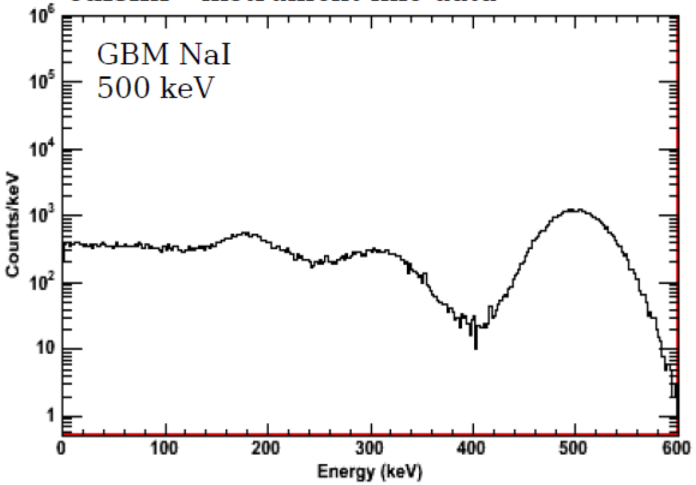

Hoover & Kippen 2004

GBM Simulation Design (3)

drmgen
application-specific
DRM generator

Inputs

- DRMdb/ARMdb databases (FITS; from calsim/atmosim)
- Commands (interactive command line, command macro file, or callable)

Outputs

- Application-specific DRM (FITS format or memory for callable mode) with or without atmospheric scattering

External Dependencies

- CCFits — FITS data file I/O for c++ from NASA/GSFC
- CALDB/CalTools from NASA/GSFC

Detector Response Matrix: Example

Example: development version (no atmospheric response), normal incidence, 100k events per 158 energies

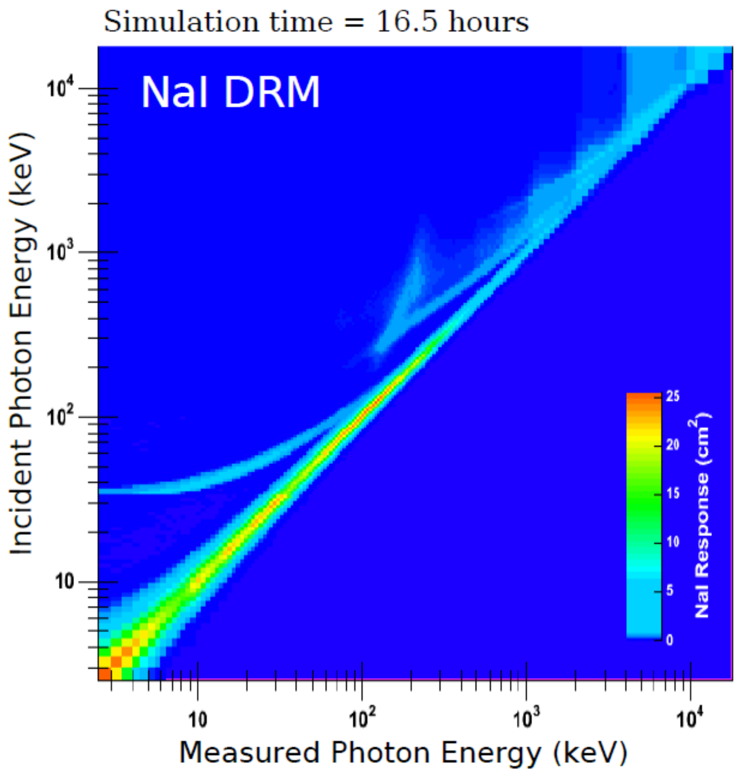

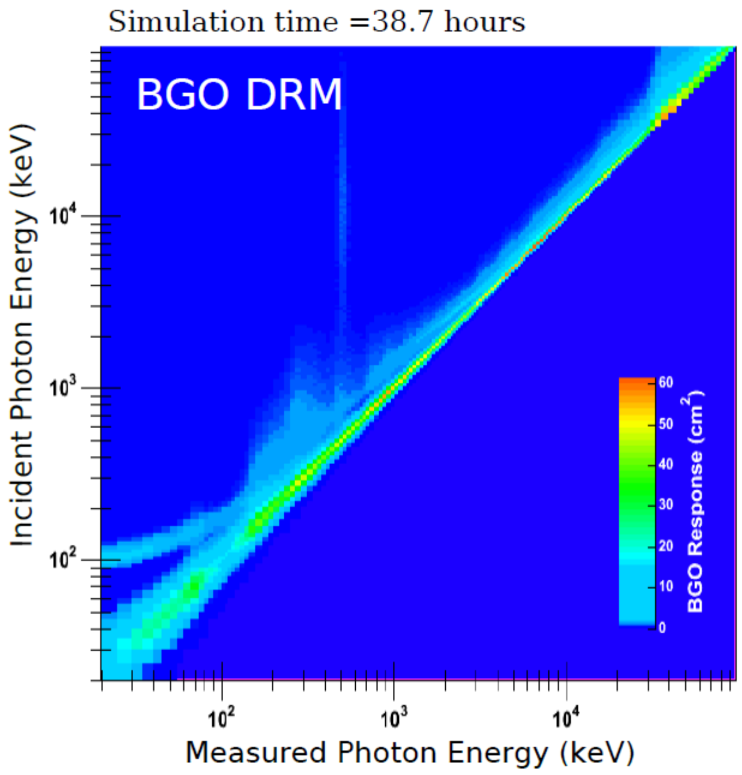

Hoover & Kippen 2004

Atmosphere Model (1)

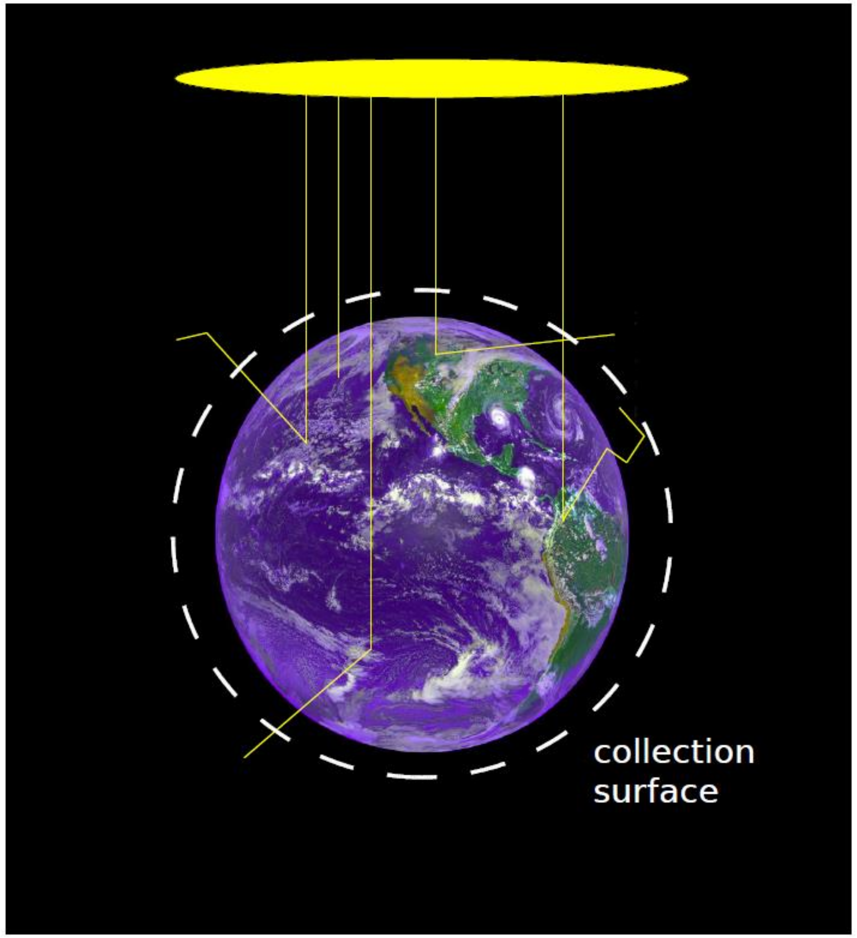

A full scale earth+atmosphere model was created using concentric spherical shells for the atmosphere layers

NRLMSISE-00 (year 2000 release) atmosphere data is used for temperature, pressure, mass density, and element number density in each layer (http://uap-www.nrl.navy.mil/models_web/msis/msis_home.htm)

Number and thickness of layers is arbitrary, easily changed

Capable of modeling 0-1000 km

A "plane wave" is incident upon the earth; the direction and energy of scattered photons is recorded when they cross a "collection surface" surrounding the model at the space-craft altitude.

Atmosphere Model (2)

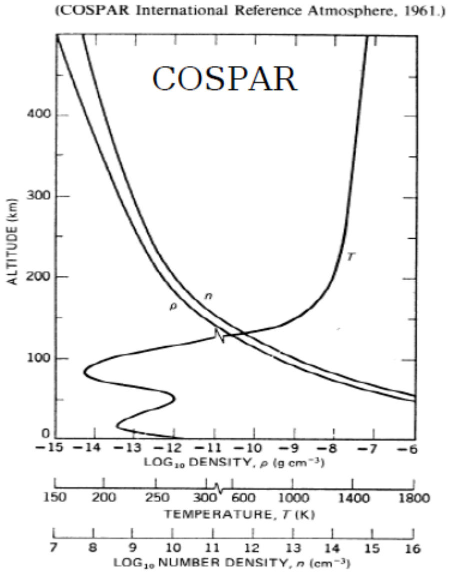

The G4 model temperature, pressure, and density compare well to COSPAR (1961) and US Standard Atmosphere (1976) (see Zombeck, *Handbook of Space Astronomy and Physics*)

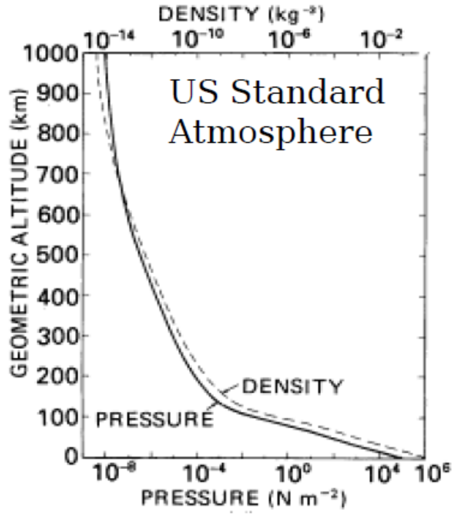

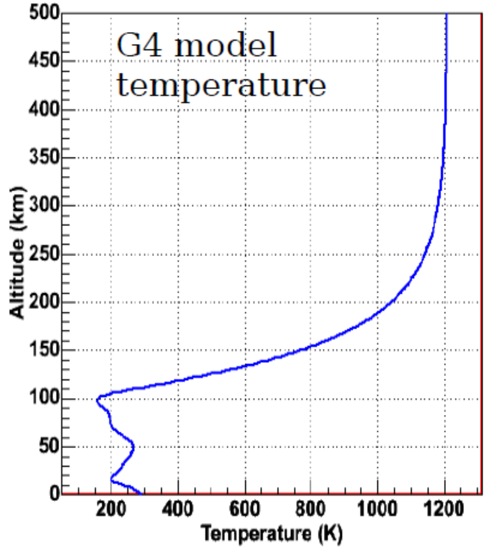

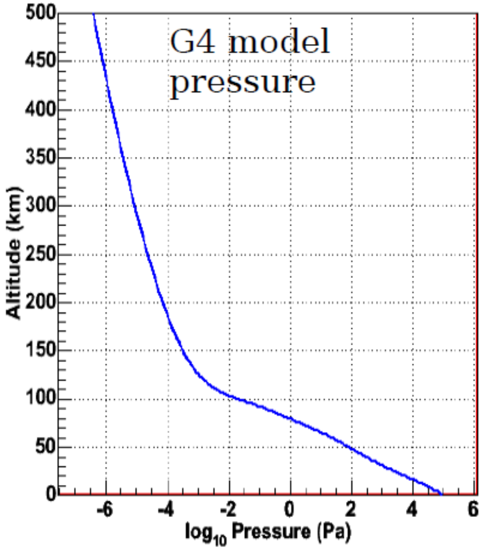

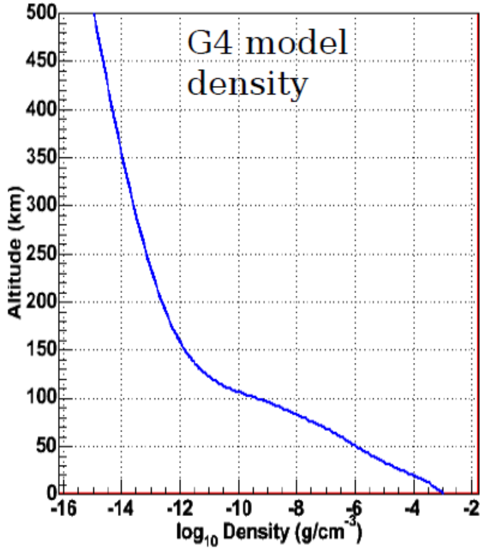

Hoover & Kippen 2004

Atmosphere Model (3)

The atmosphere is composed of 7 elements, with varying number density according to altitude

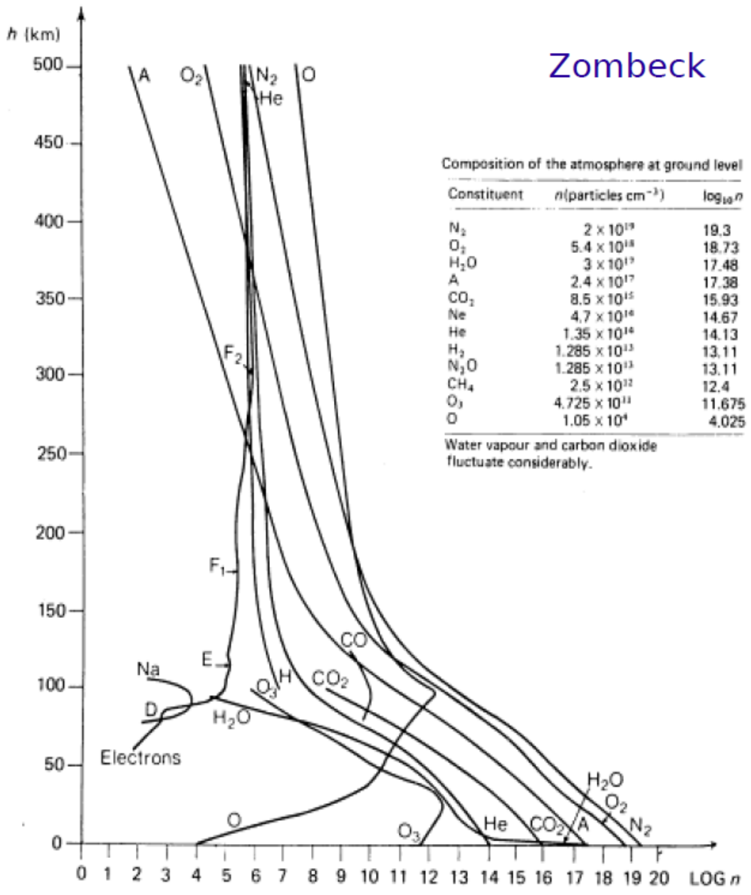

Composition of the atmosphere at ground level

Constituent	n(particles cm^{-3})	$\log_{10} n$
N_2	2×10^{19}	19.3
O_2	5.4×10^{18}	18.73
H_2O	3×10^{17}	17.48
A	2.4×10^{17}	17.38
CO_2	8.5×10^{15}	15.93
Ne	4.7×10^{14}	14.67
He	1.35×10^{14}	14.13
H_2	1.285×10^{13}	13.11
N_2O	1.285×10^{13}	13.11
CH_4	2.5×10^{12}	12.4
O_3	4.725×10^{11}	11.675
O	1.05×10^{4}	4.025

Water vapour and carbon dioxide fluctuate considerably.

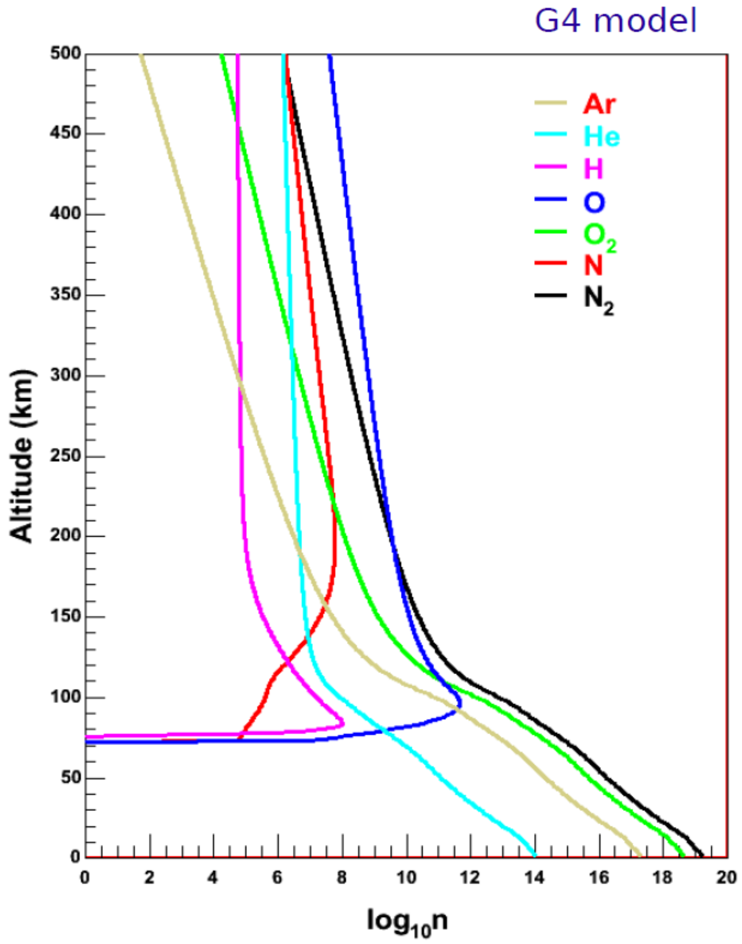

Hoover & Kippen 2004

Atmosphere Model (4)

Example (development version)

10k events per 158 energies

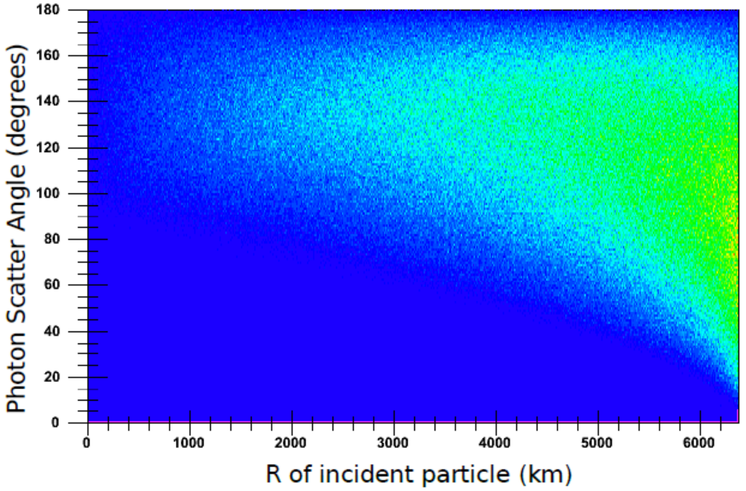

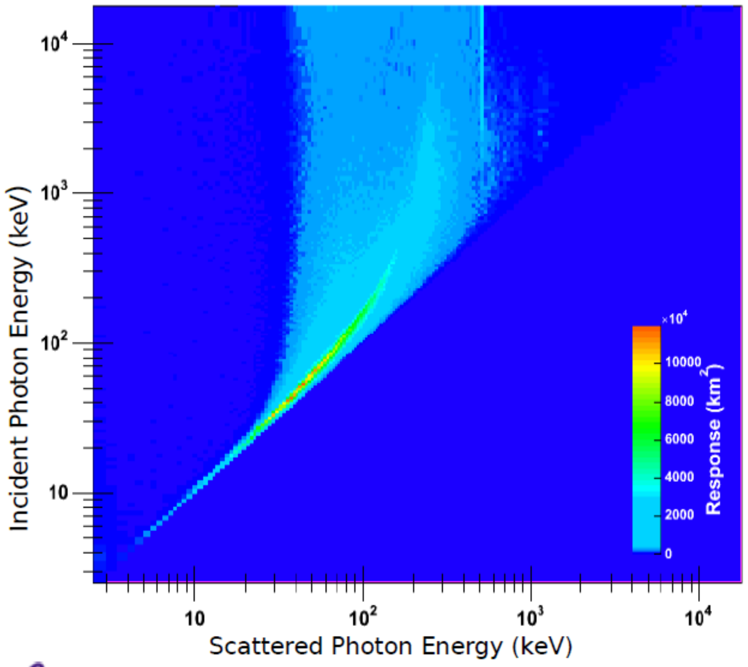

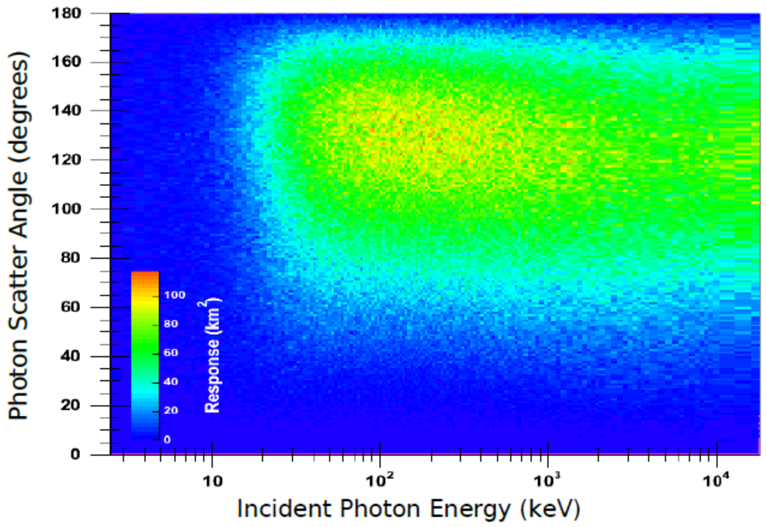

Hoover & Kippen 2004

Phased Software/Model Development

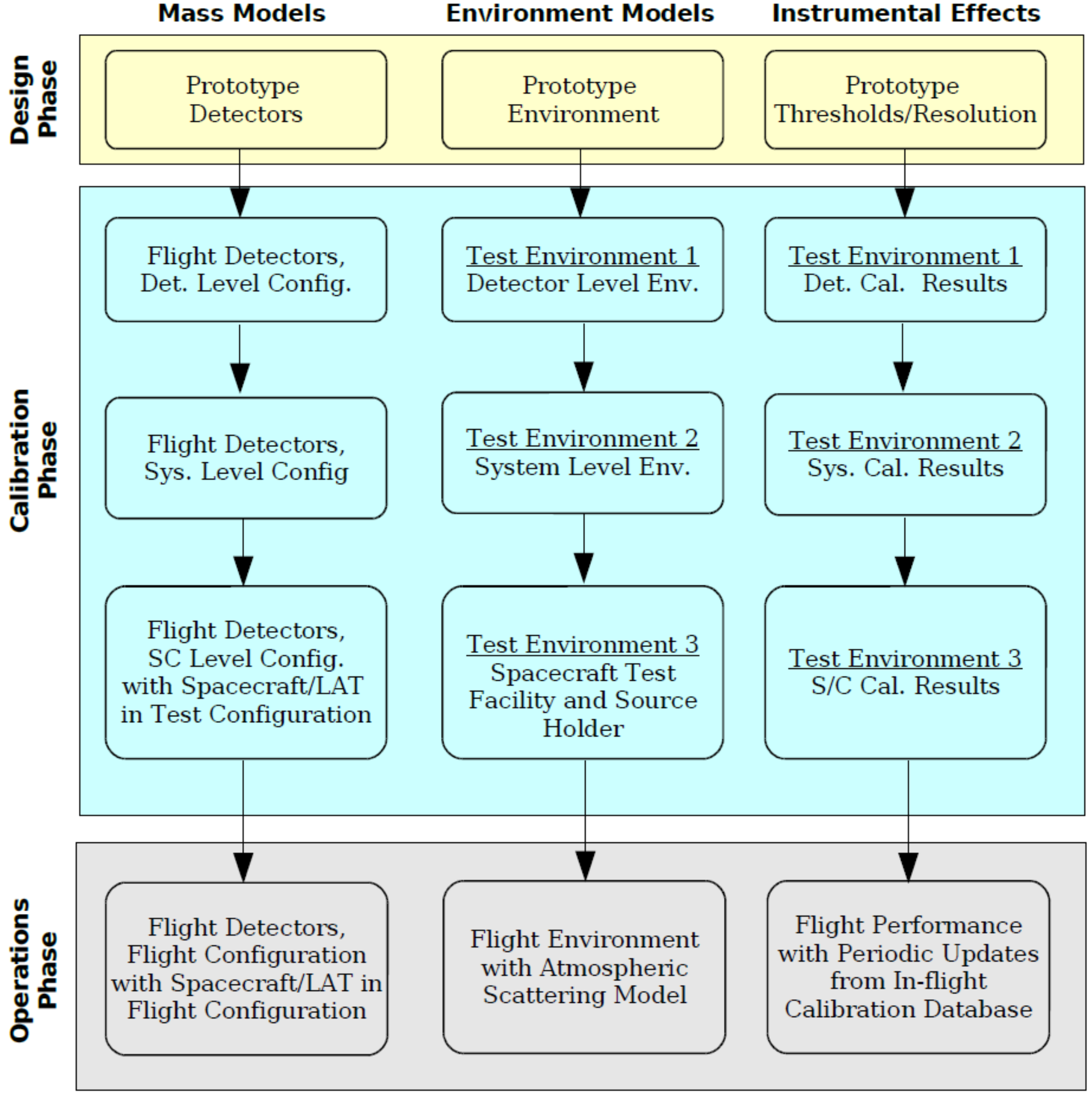

- Software and models require cross-validation with calibration data
- Three phases of SIM/DRM sw/model development
  - Design
    simulate prototype detectors
  - Calibration
    Simulate three levels of calibration/test
    - Detector level
    - GBM system level
    - On-spacecraft level
  - Operation
    - In-flight configuration appropriate for analysis of science data
    - DRM generation

Hoover & Kippen 2004

Some Remarks on GEANT

Strengths

- Flexibility of GEANT4 lets one tailor the application for their specific needs
- GEANT4 can simulate on the scale of nanometers (good for instrument models) or kilometers (good for planetary models)
- Data output format is entirely up to the user
- One can select only the physics processes that are needed, ignore the rest

Concerns

- Speed - we must simulate many energies for many source positions with low detection efficiency
- We have observed infinite loops for at least two geometries (volumes sharing a boundary, cylinder inside a sphere). We are worried about infinite loops appearing in the final geometry, which will be much more complex
- Low-energy Compton scattering – External packages? Penelope? Why not fix G4LowEnergyCompton?
- GDML: long term support? Compatibility with XERCES (currently it works with XERCES 2.4.0 but with error messages)
- Reluctance of G4 team to fix geometry/tracking errors

Hoover & Kippen 2004

Development Schedule

- Development version of simulation code is well underway, using simplified models for the NaI/BGO detectors
- Next few months... we expect detailed drawings and material composition information for NaI/BGO assemblies. This will be translated to G4 geometry models, followed by verification with calibration data
- 2005... we will receive drawings/material information for the spacecraft. Then we create G4 geometry for spacecraft + detectors, also verified with calibration data
- 2006... incorporate in-flight detector configuration into the simulation
- 2006... final DRM/CALDB databases
- 2007... GLAST launch

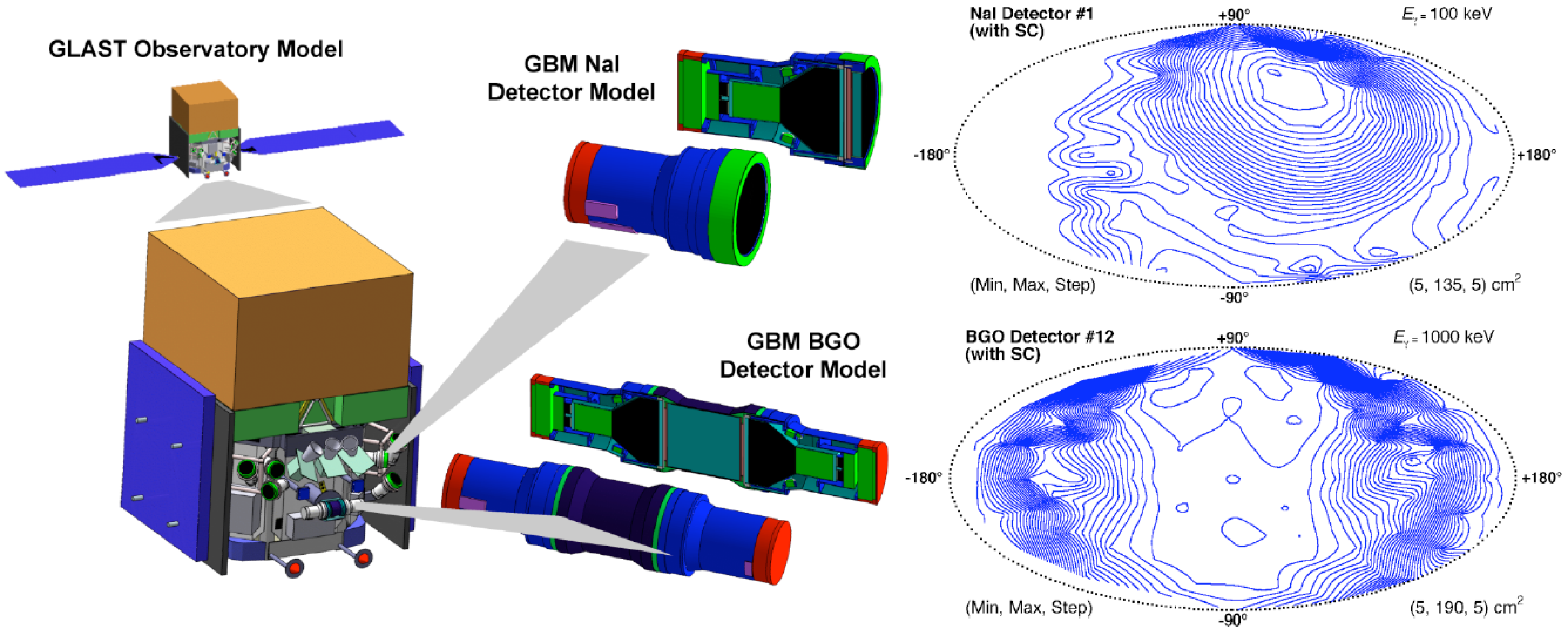

FIGURE 1. *Left:* Mass models of the GLAST observatory used for GBM instrument response simulations. *Right:* Preliminary GBM "direct" response as a function of sky direction for a single NaI (top) and a single BGO (bottom) detector at specific energies (LAT pointing axis is at latitude = 90°). The full DRM database will capture this information for all energies and angles.

Kippen+2007

MC-Code Validation – Detector-Level Calibration

- <u>Purpose of Calibration:</u>
  - Performance verification of
    - Energy calibration
    - Energy resolution
    - Effective area
  - Provide accurate data
    - Comparison with simulated detector response data
    - Scientific analysis

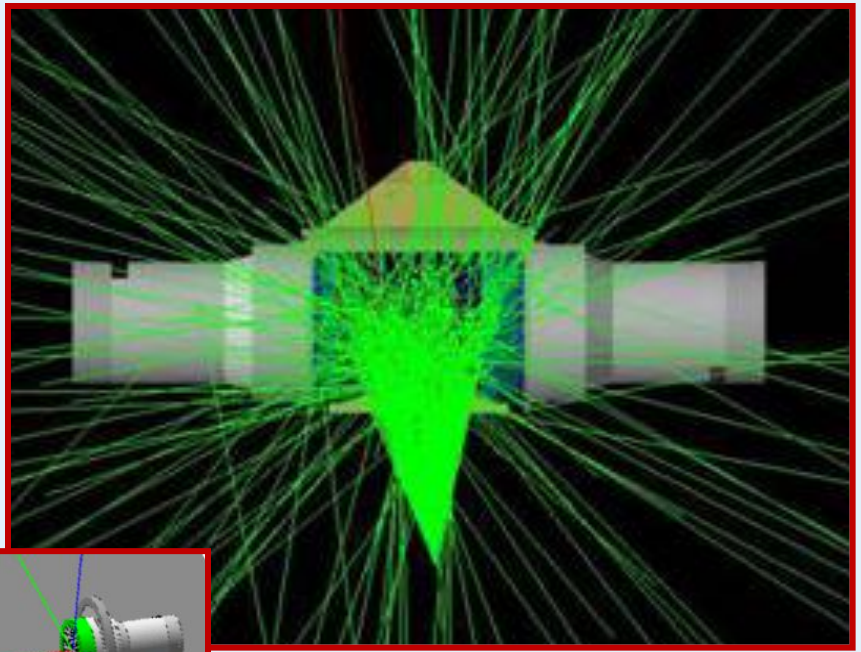

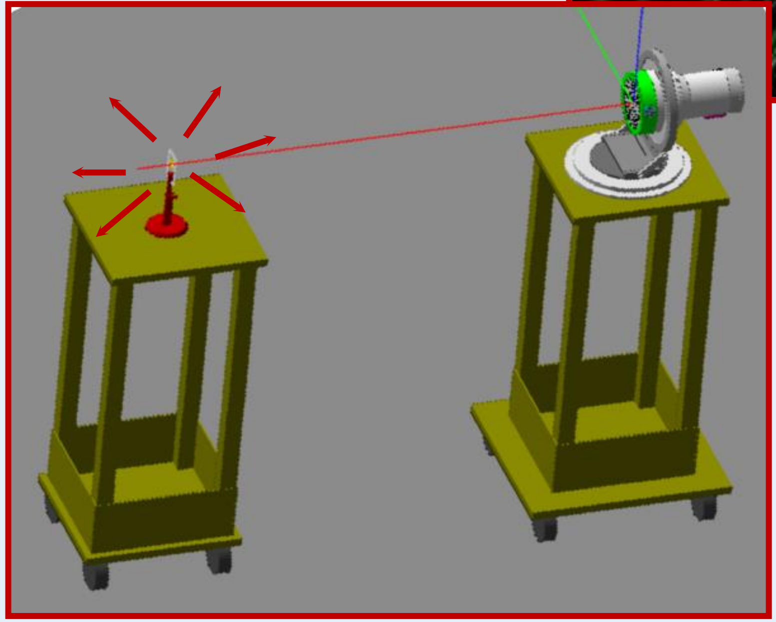

On-ground calibration measurements

1. **MPE (2005)**
   - Calibrated radioactive sources (14 keV - 4.43 MeV) in the laboratory

2. **BESSY synchrotron radiation** facility (Berlin, 2005)
   - Low-energy accelerator (10 – 60 keV)

3. **SLAC (USA, 2006)**
   - High-energy Van-de-Graaff accelerator (6 – 18 MeV)

1.

2.

3.

Model of MPE calibration setup full environment

- Including
  - Complete detailed models of NaI+BGO detectors with spacecraft mounting brackets
  - Complex holding structure, enabling rotation of detectors around all 3 axes during the calibration, included a wooden stand raising it about one meter above the laboratory floor,

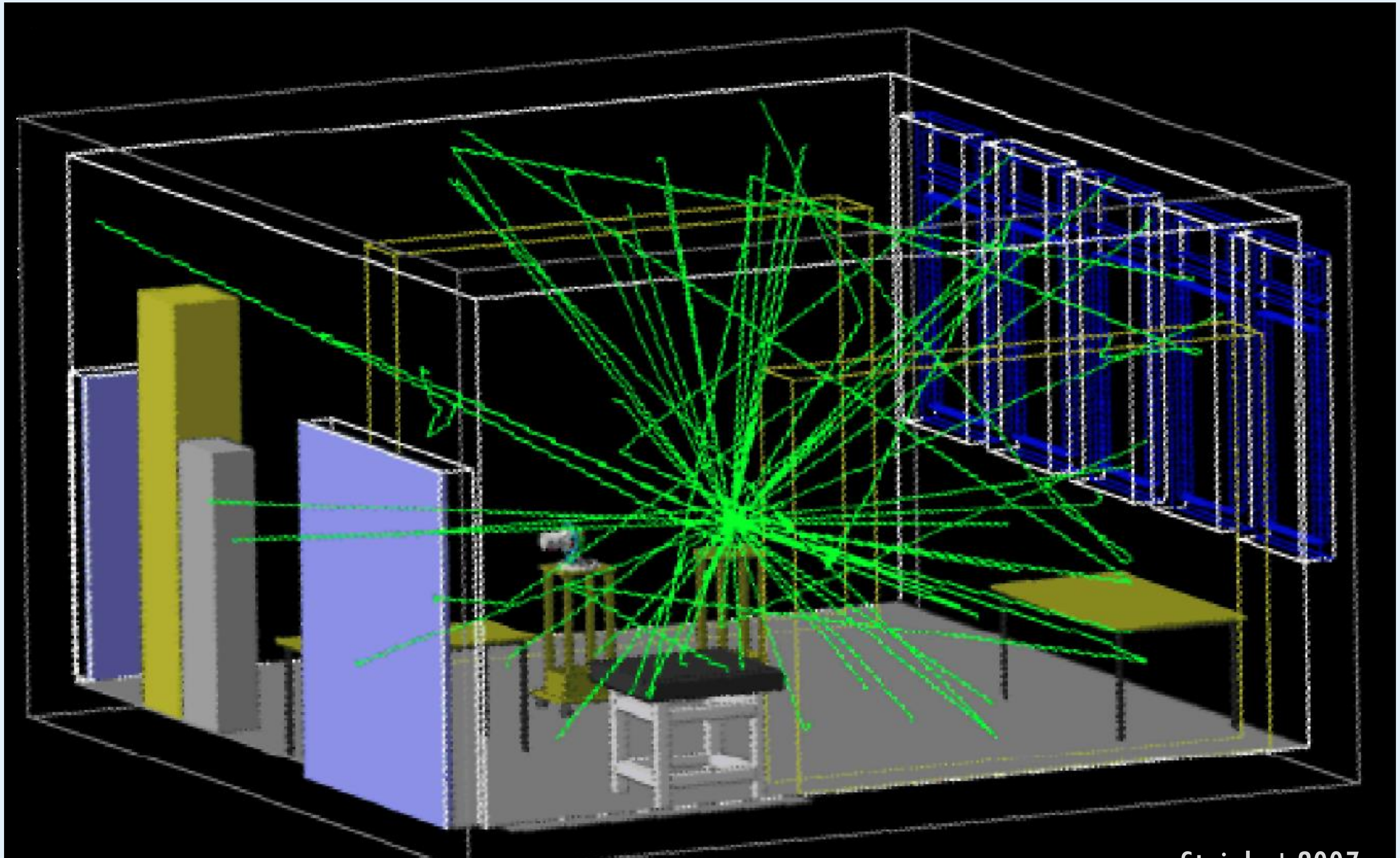

AIP Conference Proceedings 921, 572 (2007); http://dx.doi.org/10.1063/1.2757457

Steinle+2007

For simulations, the room is illuminated isotropically with the appropriate photon energy spectrum for each radioisotope. Tracks for 100 events are shown at left.

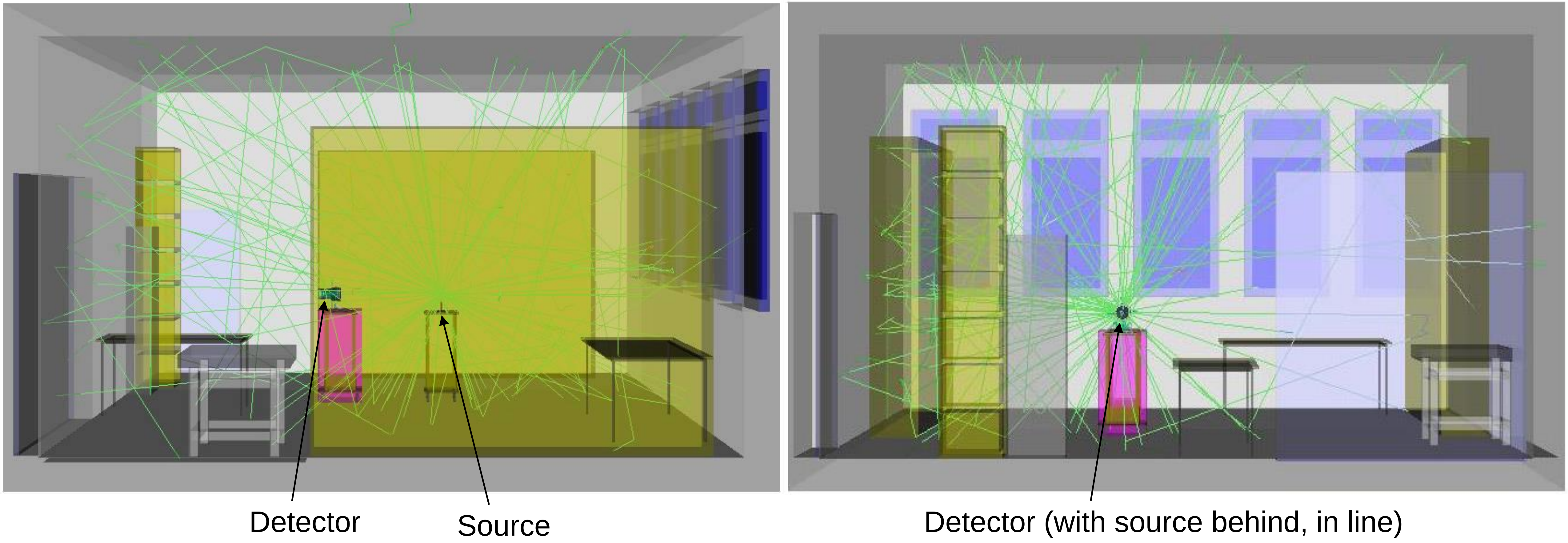

Hoover+2007

γ-ray lines for calibration

NaI:

Line # for Calib.	Line Energies [keV]	Nuclide
1	14.41	Co-57
2	22.1	Cd-109
3	25	Cd-109
4	32.06	Cs-137
5	36.6	Cs-137
6	59.4	Am-241
7	88.03	Cd-109
8	122.06	Co-57
9	136.47	Co-57
10	279.2	Hg-203
11	511	Na-22
12	661.66	Cs-137
13	834.84	Mn-54
14	898.04	Y-88

BGO:

Line # for Calib.	Line Energies [keV]	Nuclide
1	124.59	Co-57
2	279.2	Hg-203
3	511	Na-22
4	661.66	Cs-137
5	834.84	Mn-54
6	898.04	Y-88
7	1173.23	Co-60
8	1274.54	Na-22
9	1332.49	Co-60
10	1836.06	Y-88
11	4430	Am/Be

- **For NaI detectors: 14 lines from 8 radioactive nuclides**
- **For BGO detectors: 11 lines from 8 radioactive nuclides**

γ-ray lines for calibration of the NaI detector

Nuclide	Half-life	Decay	Line energies [keV]	Transition Probability	Weighted Mean [keV]	Prob.	Line for Calibration of
^{55}Fe	1001.0 (23) d / 2.741 (6) y	Mn-SumK	5.96	0.283 (10)			NaI(Tl)
^{241}Am	432.2 (7) y	Np-Lα1	13.95	0.1193 (11)			-
		Np-Lβ	17.54	0.1861 (15)			-
		Np-Lγ	21.01	0.0482 (4)			-
		γ	26.34	0.02400 (20)			-
		γ	59.4	0.359 (4)			NaI(Tl)
^{109}Cd	462.1 (14) d	Ag-SumKα	22.1	0.836 (6)	22.61	1.014	NaI(Tl)
		Ag-SumKβ	25	0.1777 (19)			NaI(Tl)
		γ	88.03	0.03626 (20)			NaI(Tl)
^{57}Co	271.83 (8) d	Fe-SumK	6.48	0.579 (8)			NaI(Tl)
		γ	14.41	0.0916 (15)			NaI(Tl)
		γ	122.06	0.8560 (17)	124.59	0.963	NaI(Tl)/BGO
		γ	136.47	0.1068 (8)			NaI(Tl)/BGO
^{203}Hg	46.604 (17) d	Tl-L	11.1	0.060 (12)			NaI(Tl)
		Tl-SumKα	72.11	0.102 (3)			NaI(Tl)
		γ	279.2	0.8146 (13)			NaI(Tl)/BGO
^{137}Cs	11000 (90) d / 30.13 (24) y	Ba-SumKα	32.06	0.0553 (10)	32.89	0.069	NaI(Tl)
		Ba-SumKβ	36.6	0.01321 (27)			NaI(Tl)
		Ba-137m	661.66	0.8500 (20)			NaI(Tl)/BGO
^{54}Mn	312.15 (8) d	Cr-SumK	5.47	0.258 (4)			NaI(Tl)
		γ	834.84	0.999750 (12)			NaI(Tl)/BGO
^{60}Co	1925.3 (4) d / 5.2712(11) y	γ	1173.23	0.9985 (3)			BGO
		γ	1332.49	0.999826 (6)			BGO
^{22}Na	950.5 (4) d	Annih.	511	1.798			NaI(Tl)/BGO
		γ	1274.54	0.9994			BGO
^{24}Na	0.62328 (23) d /14.959(6) h	γ	1368.63	0.999932 (7)			BGO
		γ	2754.01	0.99871 (8)			BGO
^{88}Y	106.630 (25) d	Sr-SumKα	14.14	0.522 (6)	14.39	0.616	NaI(Tl)
		Sr-SumKβ	15.8	0.094 (2)			
		γ	898.04	0.940 (3)			NaI(Tl)/BGO
		γ	1836.06	0.9933 (3)			BGO
^{241}Am/Be	432.2 (7) y	γ	4430	0.00004			BGO

γ-ray lines for calibration of the BGO detector

Nuclide	Half-life	Decay	Line energies [keV]	Transition Probability	Weighted Mean [keV]	Weighted Mean Prob.	Line for Calibration of
^{55}Fe	1001.0 (23) d / 2.741 (6) y	Mn-SumK	5.96	0.283 (10)			NaI(Tl)
^{241}Am	432.2 (7) y	Np-Lα1	13.95	0.1193 (11)			-
		Np-Lβ	17.54	0.1861 (15)			-
		Np-Lγ	21.01	0.0482 (4)			-
		γ	26.34	0.02400 (20)			-
		γ	59.4	0.359 (4)			NaI(Tl)
^{109}Cd	462.1 (14) d	Ag-SumKα	22.1	0.836 (6)	22.61	1.014	NaI(Tl)
		Ag-SumKβ	25	0.1777 (19)			NaI(Tl)
		γ	88.03	0.03626 (20)			NaI(Tl)
^{57}Co	271.83 (8) d	Fe-SumK	6.48	0.579 (8)			NaI(Tl)
		γ	14.41	0.0916 (15)			NaI(Tl)
		γ	122.06	0.8560 (17)	124.59	0.963	NaI(Tl)/BGO
		γ	136.47	0.1068 (8)			NaI(Tl)/BGO
^{203}Hg	46.604 (17) d	Tl-L	11.1	0.060 (12)			NaI(Tl)
		Tl-SumKα	72.11	0.102 (3)			NaI(Tl)
		γ	279.2	0.8146 (13)			NaI(Tl)/BGO
^{137}Cs	11000 (90) d / 30.13 (24) y	Ba-SumKα	32.06	0.0553 (10)	32.89	0.069	NaI(Tl)
		Ba-SumKβ	36.6	0.01321 (27)			NaI(Tl)
		Ba-137m	661.66	0.8500 (20)			NaI(Tl)/BGO
^{54}Mn	312.15 (8) d	Cr-SumK	5.47	0.258 (4)			NaI(Tl)
		γ	834.84	0.999750 (12)			NaI(Tl)/BGO
^{60}Co	1925.3 (4) d / 5.2712(11) y	γ	1173.23	0.9985 (3)			BGO
		γ	1332.49	0.999826 (6)			BGO
^{22}Na	950.5 (4) d	Annih.	511	1.798			NaI(Tl)/BGO
		γ	1274.54	0.9994			BGO
^{24}Na	0.62328 (23) d /14.959(6) h	γ	1368.63	0.999932 (7)			BGO
		γ	2754.01	0.99871 (8)			BGO
^{88}Y	106.630 (25) d	Sr-SumKα	14.14	0.522 (6)	14.39	0.616	NaI(Tl)
		Sr-SumKβ	15.8	0.094 (2)			
		γ	898.04	0.940 (3)			NaI(Tl)/BGO
		γ	1836.06	0.9933 (3)			BGO
^{241}Am/Be	432.2 (7) y	γ	4430	0.00004			BGO

Radioactive sources @ MPE

1. MPE Laboratory (2005):
Calibrated radioactive sources (14 keV - 4.43 MeV)

Nuclide	(1) Half-life	(2) Decay	(3) Line Energies (keV)		(4) Transition Probability (%)		(5) Calibration Line	
							NaI	BGO
^{55}Fe	2.741(6) y	Mn-SumK	5.96		0.283 (10)		–	–
^{241}Am	432.2(7) y	Np–Lα1	13.95		0.1193 (11)		–	–
		Np–Lβ	17.54		0.1861 (15)			
		Np–Lγ	21.01		0.0482 (4)			
		γ	26.34		0.02400 (20)			
		γ	59.4		0.359 (4)		6	
^{109}Cd	462.1(14) d	Ag–SumKα	22.1	22.61	0.836 (6)	1.014	2	–
		Ag–SumKβ	25		0.1777 (19)		3	
		γ	88.03		0.03626 (20)		7	
^{57}Co	271.83(8) d	Fe–SumK	6.48		0.579 (8)		–	–
		Fe–SumK	14.41		0.0916 (15)		1	
		γ	122.06	124.59	0.8560 (17)	0.963	8	1
		γ	136.47		0.1068 (8)		9	
^{203}Hg	46.604(17) d	Tl–L	11.1		0.060 (12)		–	–
		Tl–SumKα	72.11		0.102 (3)			
		γ	279.2		0.8146 (13)		10	2
^{137}Cs	30.13(24) y	Ba–SumKα	32.06	32.89	0.0553 (10)	0.069	4	–
		Ba–SumKβ	36.6		0.01321 (27)		5	
		Ba–137m	661.66		0.8500 (20)		12	4
^{54}Mn	312.15(8) d	Cr–SumK	5.47		0.258 (4)		–	–
		γ	834.84		0.999750 (12)		13	5
^{60}Co	5.2712(11) y	γ	1173.23		0.9985 (3)		–	7
		γ	1332.49		0.999826 (6)			9
^{22}Na	950.5(4) d	Annih.	511		1.798		11	3
		γ	1274.54		0.9994		–	8
^{40}K	1.277(8)E9 y	γ	1460.83		0.1067		–	S3
^{88}Y	106.630(25) d	Sr–SumKα	14.14	14.39	0.522 (6)	0.616	–	–
		Sr–SumKβ	15.8		0.094 (2)			
		γ	898.04		0.940 (3)		14	6
		γ	1836.06		0.9933 (3)		–	10
^{232}Th	1.405(6)E10 y	^{208}Tl (γ)	2614.53		0.3564		–	S5
^{241}Am/^{9}Be	432.2 (7) d	γ	4430		0.00004		–	11

BESSY and SLAC

2. **BESSY synchrotron radiation facility (Berlin, 2005)**
    - **Low-energy accelerator (10 – 60 keV)**

Beam Energy keV	Line Center Channel #	Beam Energy keV	Line Center Channel #
10	57.52 ± 0.23	33	173.95 ± 0.04
12	69.20 ± 0.07	34	172.69 ± 0.11
14	79.94 ± 0.06	35	179.93 ± 0.07
16	91.05 ± 0.05	36	185.60 ± 0.07
18	101.35 ± 0.05	37	191.41 ± 0.05
20	112.34 ± 0.04	38	196.95 ± 0.07
28.5	153.84 ± 0.08	40	208.00 ± 0.06
30	160.42 ± 0.04	50	259.56 ± 0.06
31	164.50 ± 0.04	60	307.83 ± 0.07
32	169.31 ± 0.04		

3. **SLAC (USA, 2006)**
    - **High-energy Van-de-Graaff accelerator (6 – 18 MeV)**

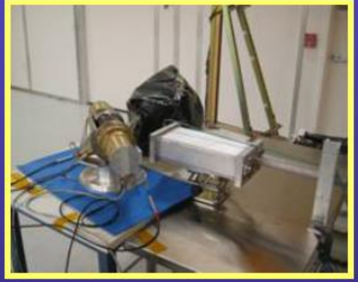

Nuclide	Line Energy (keV)	Line Number (EQM @ MPE)	Line Number (EQM @ SLAC)	FM01	FM02
^{57}Co	124.59	1	–		√
^{203}Hg	279.2	2	–	√	√
^{22}Na	511	3	S1	√	√
^{137}Cs	661.66	4	–	√	√
^{54}Mn	834.84	5	–	√	√
^{88}Y	898.04	6	–	√	√
^{60}Co	1173.23	7	–		
^{22}Na	1274.54	8	S2	√	√
^{40}K	1460	–	S3		
^{60}Co	1332.49	9	–		
^{88}Y	1836.06	10	–	√	√
^{208}Tl (SE)	2199	–	S4		
^{208}Tl	2600	–	S5		
AmBe (SE)	3929	–	S6		
AmBe	4430	11	S7		√
^{16}O (SE)	5619	–	S8		
^{16}O	6130	–	S9		
SE ^{8}Be (DE)	13564	–	S10		
^{8}Be (SE)	14075	–	S11		
^{8}Be	14586	–	S12		
^{8}Be (SE)	17108	–	S13		
^{8}Be	17619	–	S14		

NaI example spectrum

- **Radioactive Source: ^{57}Co**

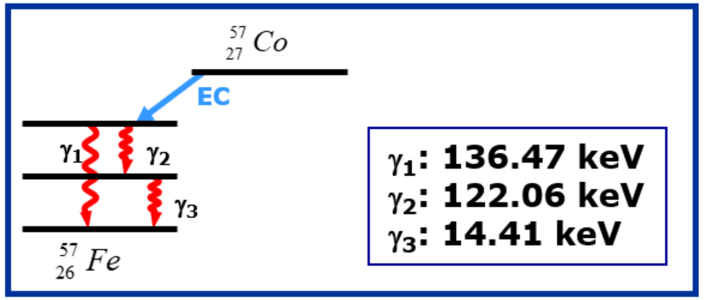

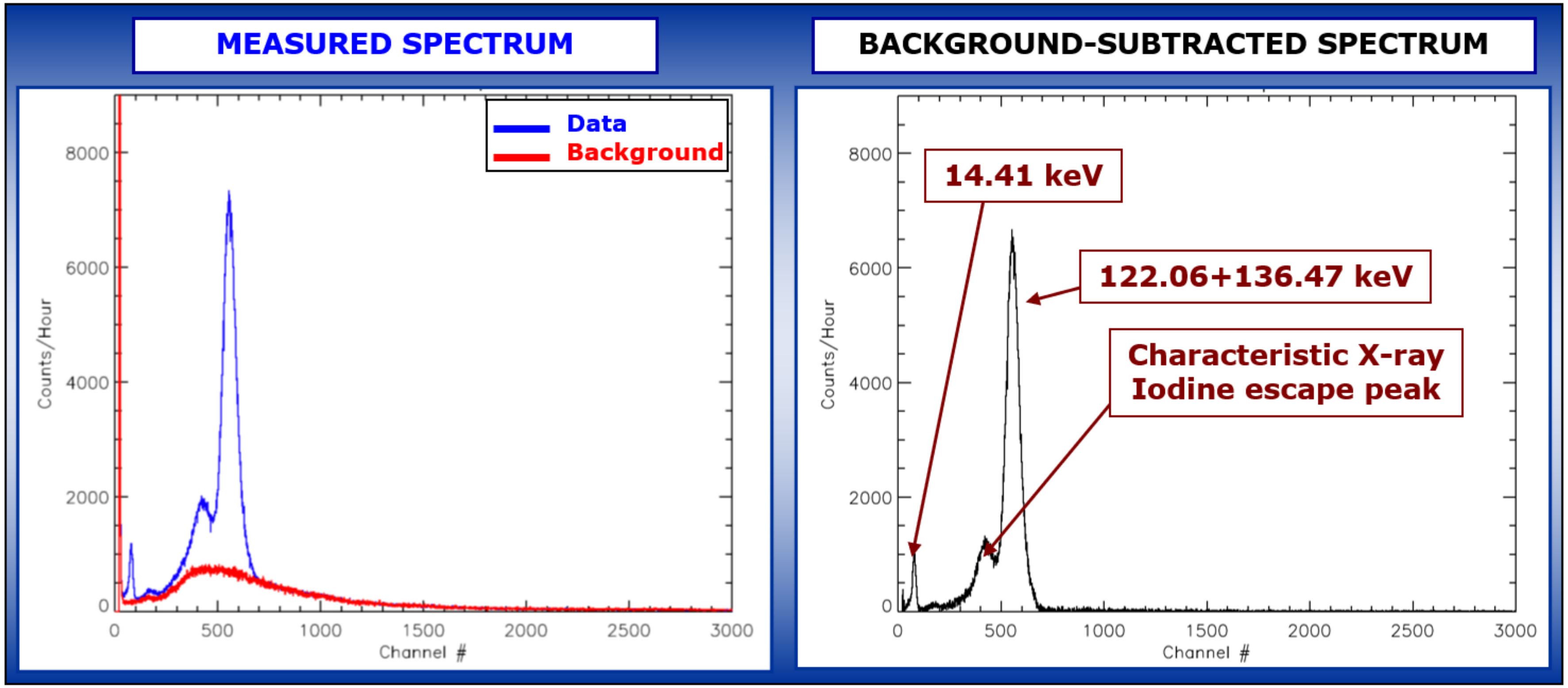

Example of detailed line analysis

^{57}Co • 122.06+136.47 keV

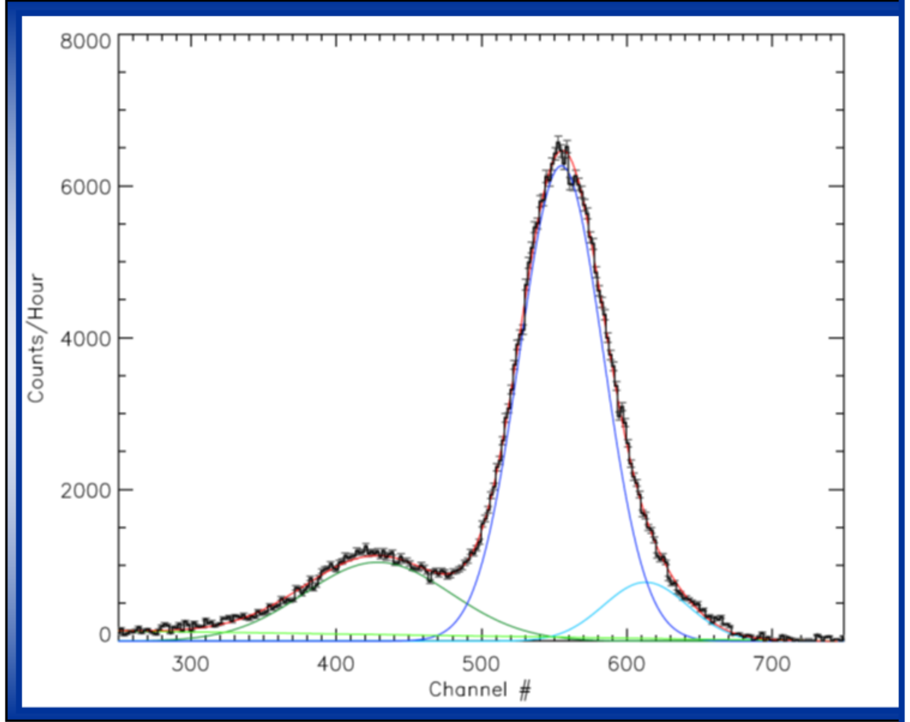

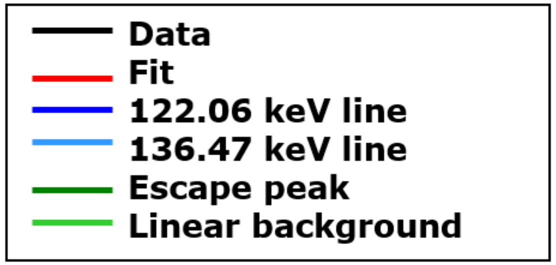

- **Example of triple gaussian fit**
  - **IDL routine *"mpfit"***
  - $$G(x) = \frac{A}{w} \cdot \sqrt{\frac{4 \ln 2}{\pi}}\, e^{-4 \ln 2 \frac{(x - x_c)^2}{w^2}}$$
  - **Free parameters:**
    - **Peak area (A)**
    - **Peak center (x_c)**
    - **FWHM (w)**
  - **Initial guessed parameters are crucial for good fit results**
    - **Area constraints**
      - $K_{area} = P_{122.06keV}/P_{136.47keV} = 8.015$
  - **For getting an estimate of the errors affecting the fit parameters, each line was fitted adopting different conditions:**
    - **Background**
    - **Range (ROI)**
    - **Rebinning**
  - **New errors larger then the statistical errors were added as systematic errors**

Response of NaI(Tl)

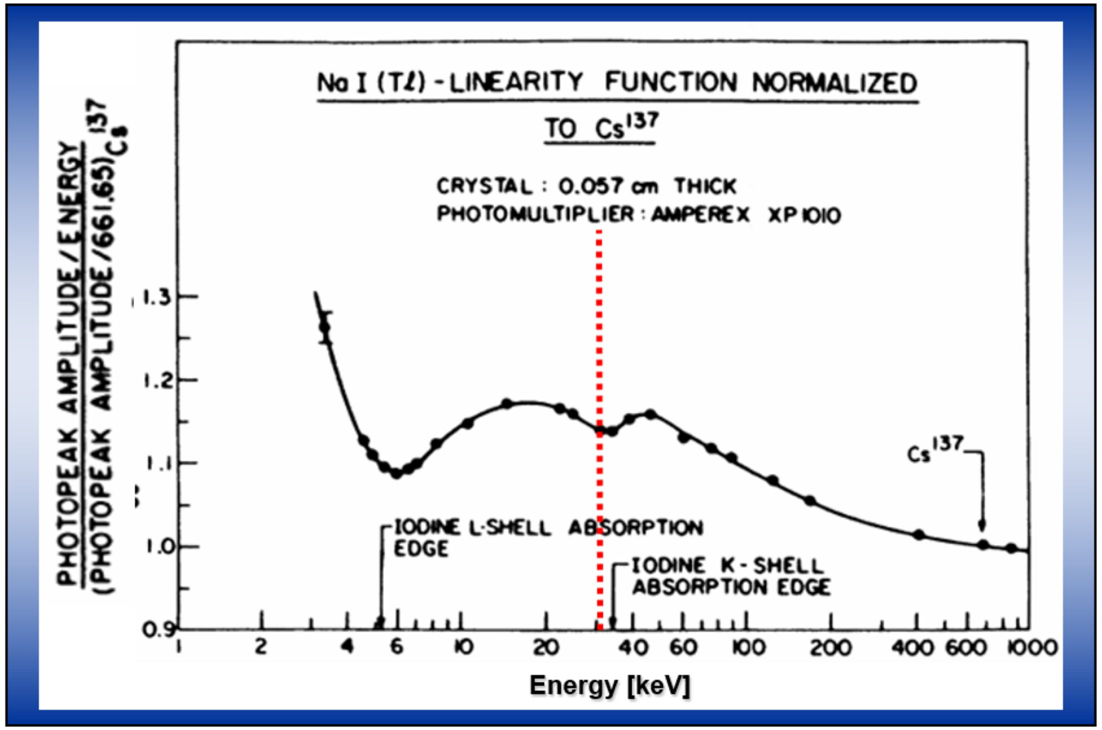

- **Nonlinearities appear at energies corresponding to the K- and L-edges in Iodine:**
  - **Photoelectrons ejected by incident gamma rays just above the K energy have very little kinetic energy so that the response drops. Just below this energy, however, K-shell ionization is not possible and L-shell ionization takes place. Since the binding energy is lower, the photoelectrons ejected at this point are more energetic which causes a rise in the response.**

Fermi-GBM detector characteristics

- **Fermi-GBM Response Functions**
  - NaI(Tl) spectra measured with monochromatic synchrotron radiation

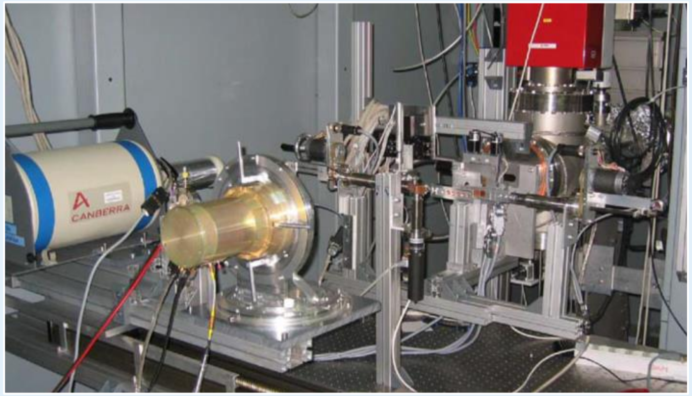

Calibration at Electron storage ring PTB/BESSY II in Berlin (2005)

Below K-edge energy

Above K-edge energy
➔characteristic Iodine escape peak

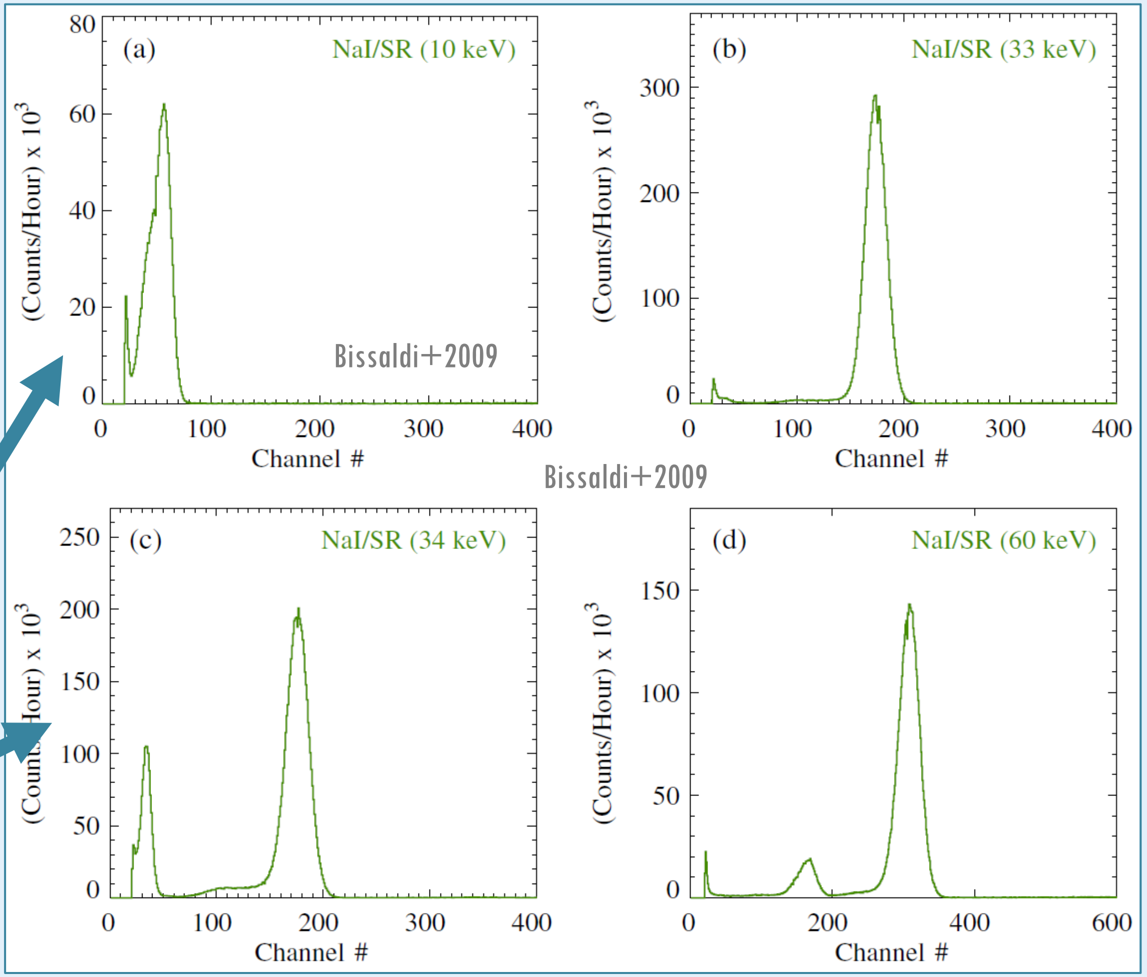

Fermi-GBM detector characteristics

- NaI(Tl) spectra measured with various radioactive sources

Nuclide	(1) Half-life	(2) Line origin	(3) Line Energies (keV)	(4) Transition Probability
^{22}Na	950.5(4) d	Annih.	511	1.798
		γ	1274.54	0.9994
^{40}K	1.277(8)E9 y	γ	1460.83	0.1067
^{54}Mn	312.15(8) d	γ	834.84	0.999750(12)
		γ	14.41	0.0916(15)
^{57}Co	271.83(8) d	γ	122.06	0.8560(17)
		γ	136.47	0.1068(8)
^{60}Co	5.2712(11) y	γ	1173.23	0.9985(3)
		γ	1332.49	0.999826(6)
^{88}Y	106.630(25) d	γ	898.04	0.940(3)
		γ	1836.06	0.9933(3)
		Ag−SumKα	22.1	0.836(6)
^{109}Cd	462.1(14) d	Ag−SumKβ	25	0.1777(19)
		γ	88.03	0.03626(20)
		Ba−SumKα	32.06	0.0553(10)
^{137}Cs	30.13(24) y	Ba−SumKβ	36.6	0.01321(27)
		Ba−137m	661.66	0.8500(20)
^{203}Hg	46.604(17) d	γ	279.2	0.8146(13)
^{232}Th	1.405(6)E10 y	^{208}Tl (γ)	2614.53	0.3564
^{241}Am	432.2(7) y	γ	59.4	0.359(4)
^{241}Am/^{9}Be	432.2 (7) y	γ	4430	0.00004

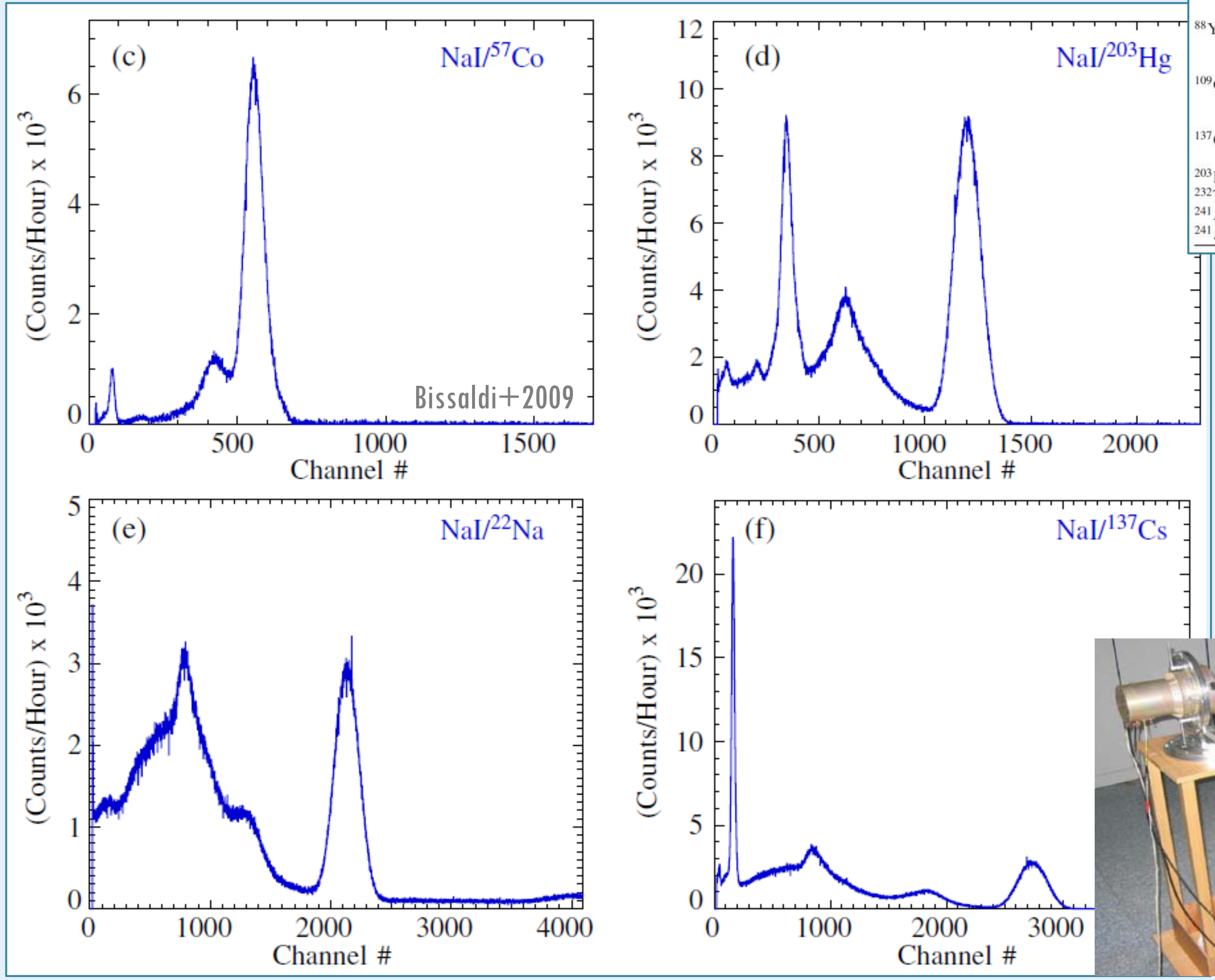

Fermi-GBM detector characteristics

- BGO spectra measured with various radioactive sources

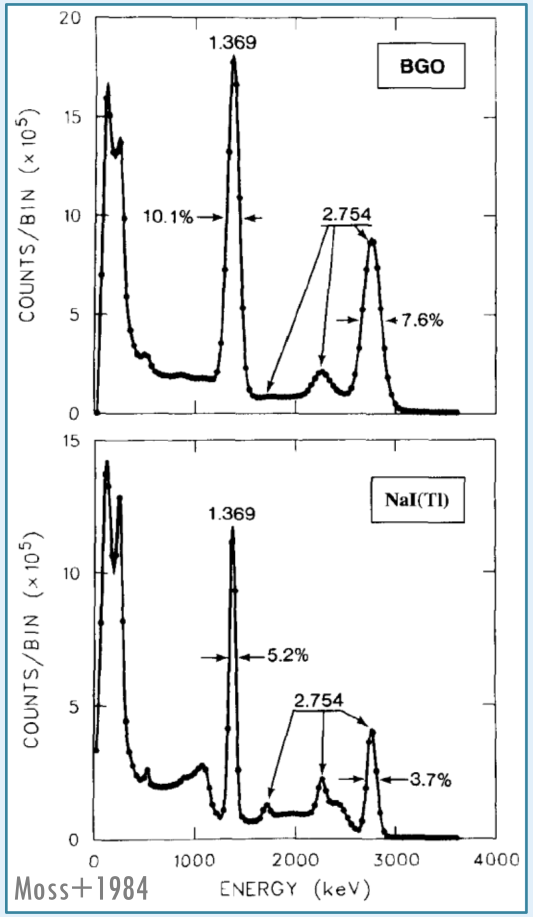

Comparative pulse height spectra measured for BGO and NaI(Tl) scintillators of equal size (7.6 x 7.6 cm) for gamma rays from ^{24}Na

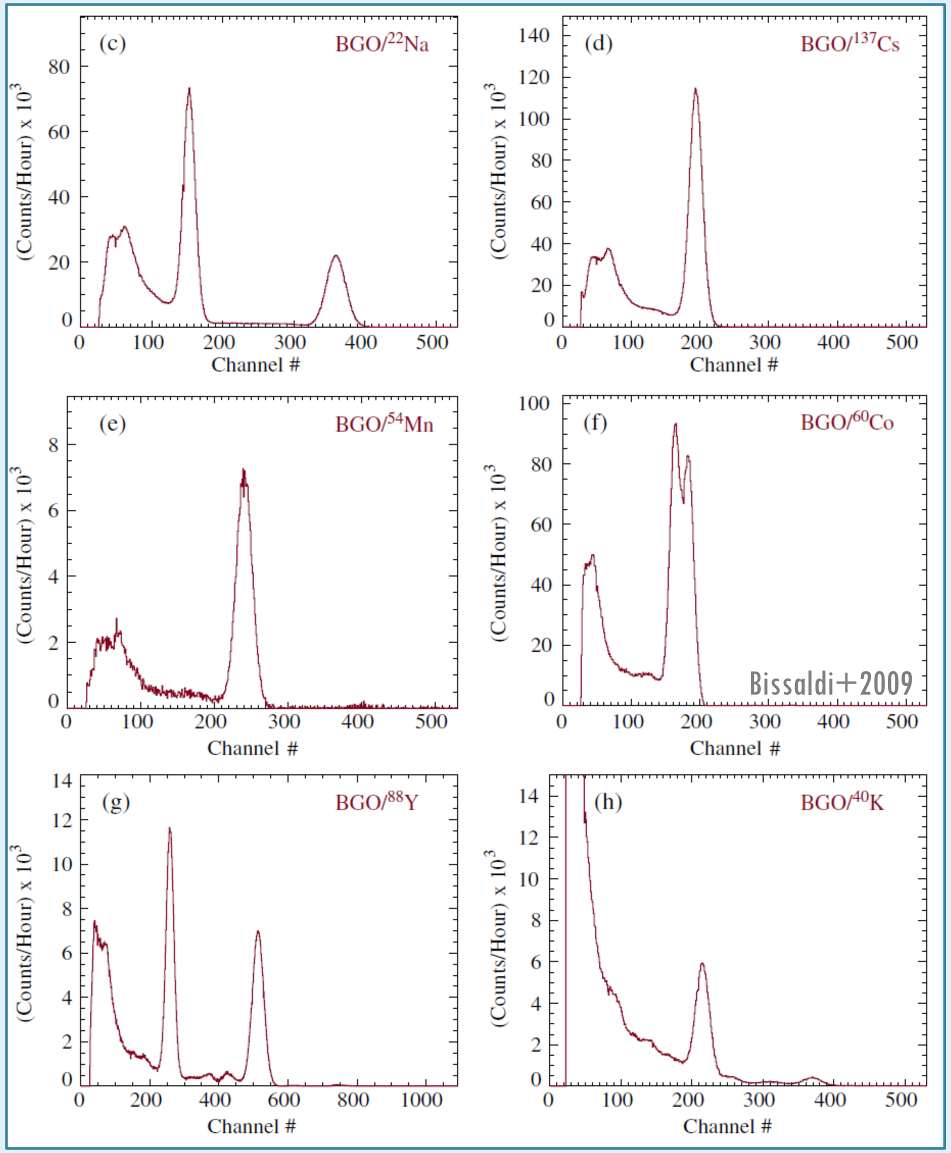

Fermi-GBM detector characteristics

Fermi-GBM Response Functions

- Full energy peak analysis
  - **Gaussian** fits with 3 parameters
    - Area
    - Center
    - FWHM
  - **Important**: background subtraction from the continuum

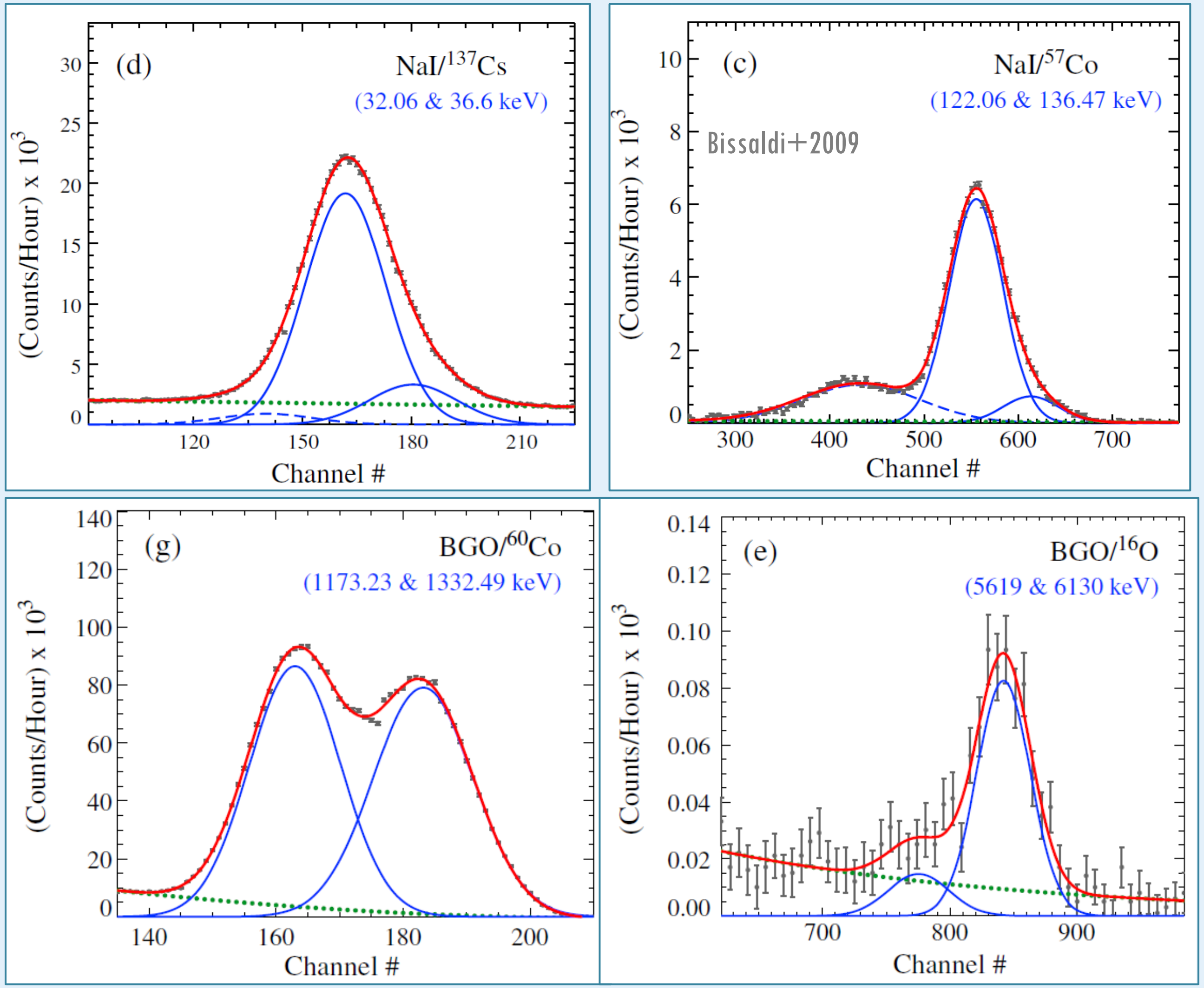

NaI validation results

Comparisons of measured and simulated data using the complete laboratory model are shown below for the NaI detector. Simulated data is normalized to the measurement livetime. The measured energy dependent resolution is applied to the simulated energy deposit in the NaI crystal to reproduce the detector resolution. In general, the simulation results reproduce the measured data quite well. Illuminating the room isotropically is critical for reproducing the backscatter peaks. **There are a few discrepancies to be understood, such as apparent missing low energy lines in the simulation for ^{241}Am and ^{109}Cd, and a slight offset in the profile of the Compton edge.**

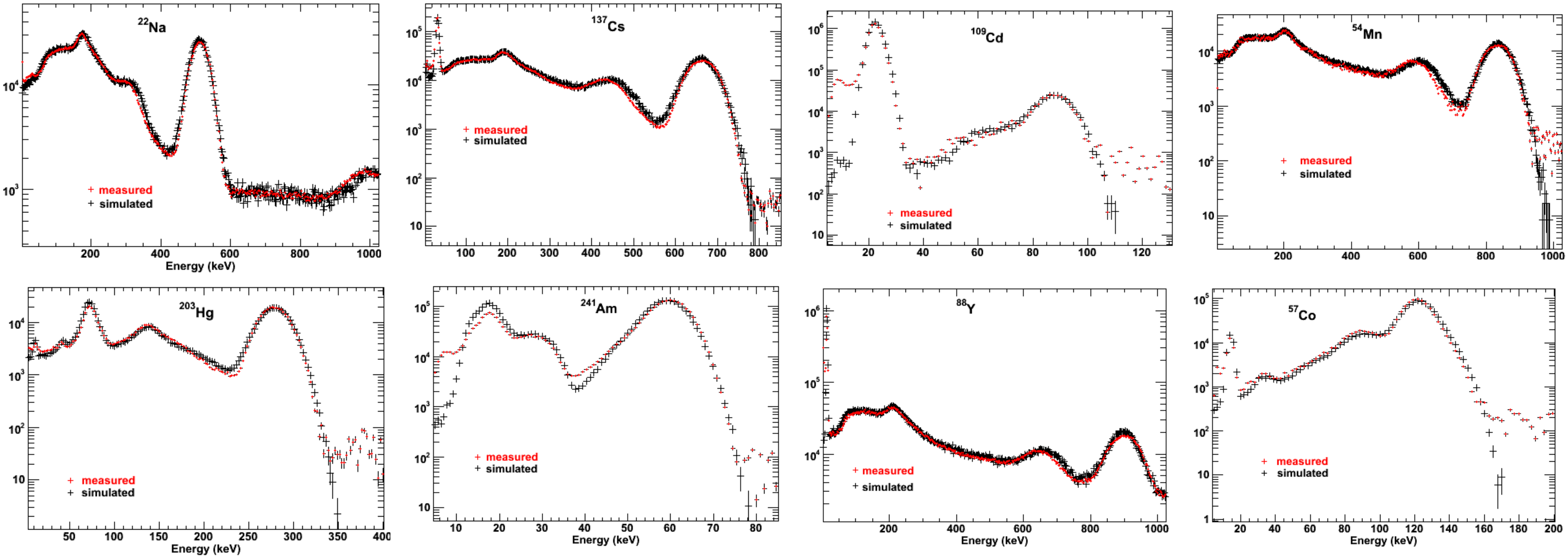

Hoover+2007

BGO validation results

BGO validation results are shown below. As with the NaI results, the measured detector resolution was applied to the simulated data. The BGO detectors are intended to operate in the ~150 keV to 30 MeV range. Shown here are low energy results from laboratory calibration sources. Higher energy calibrations are performed at an accelerator facility and do not lend themselves to straightforward validation simulations.

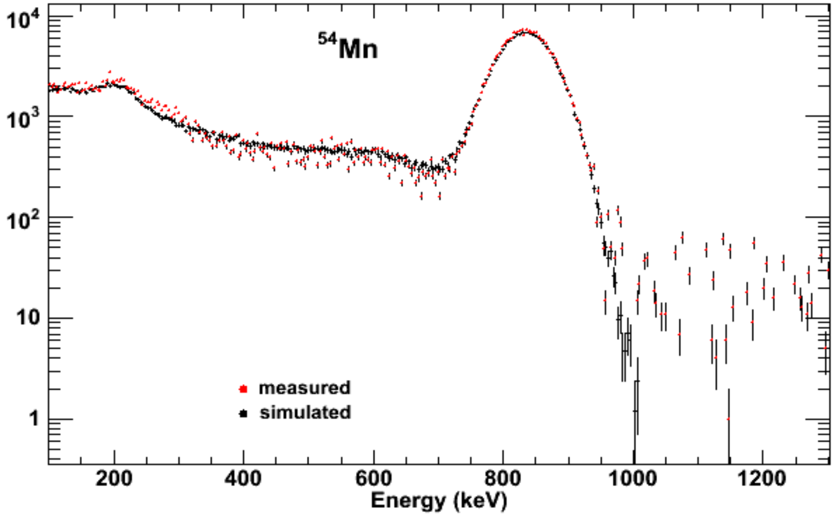

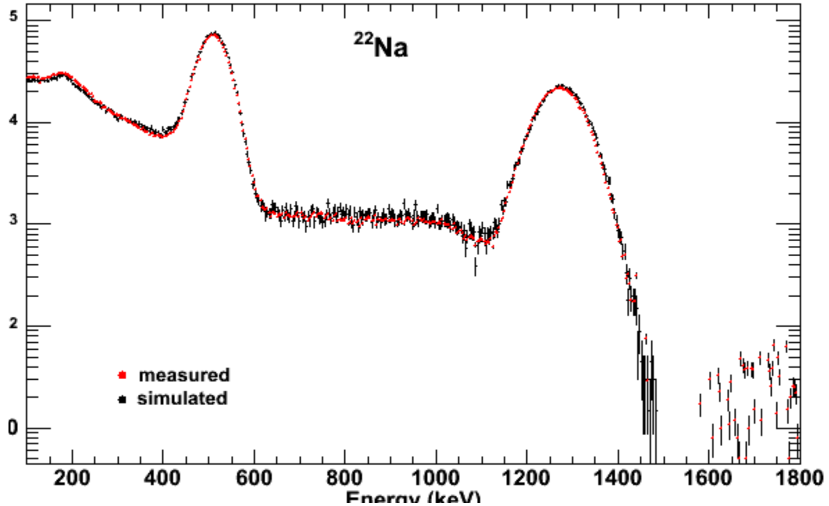

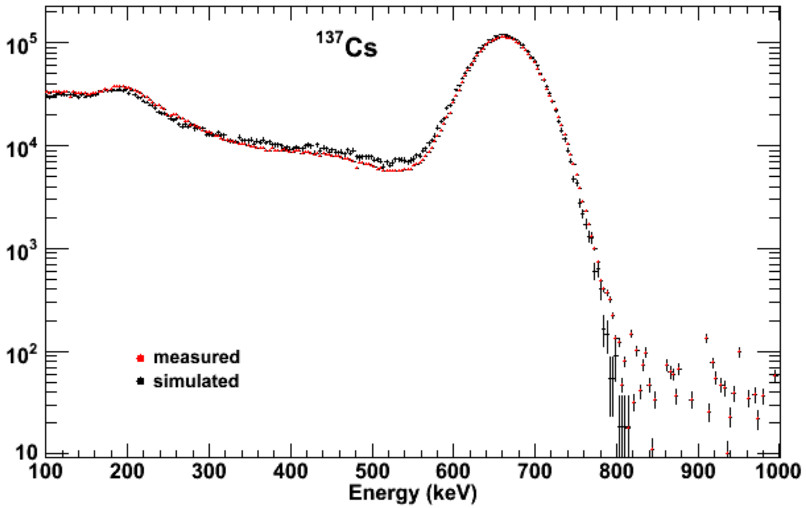

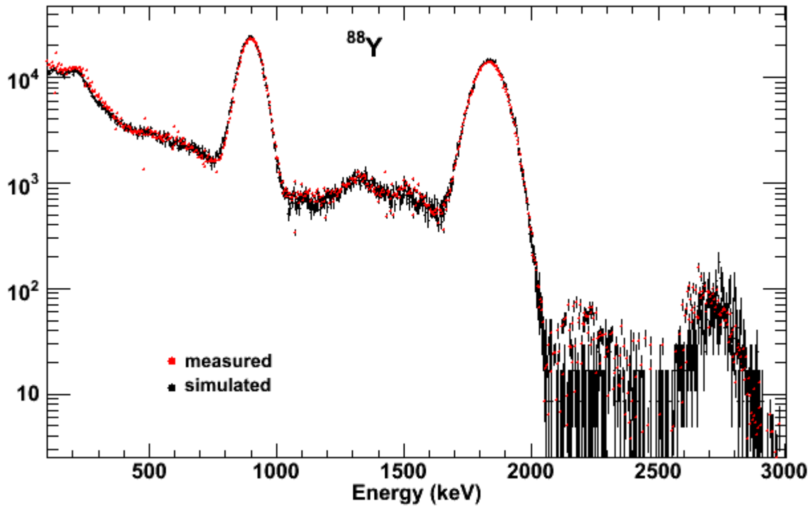

Hoover+2007

MC validation @ γ-lines

NaI FM04

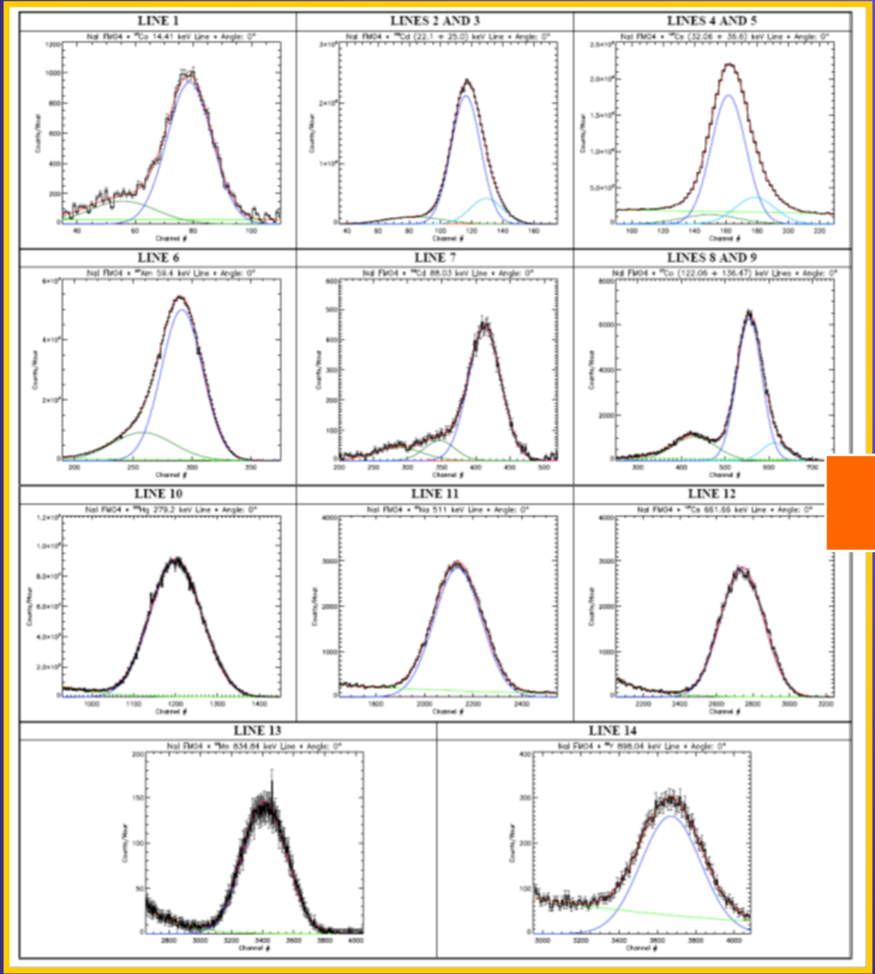

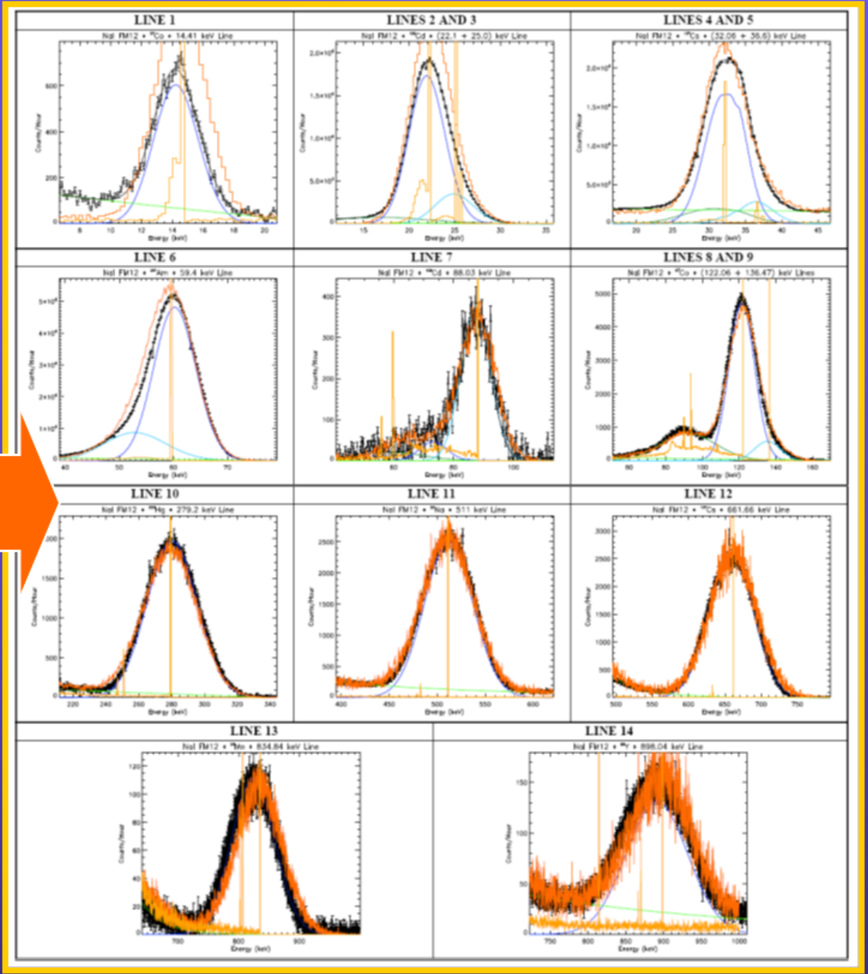

Simulation validation

Detector and laboratory simulations by H. Steinle

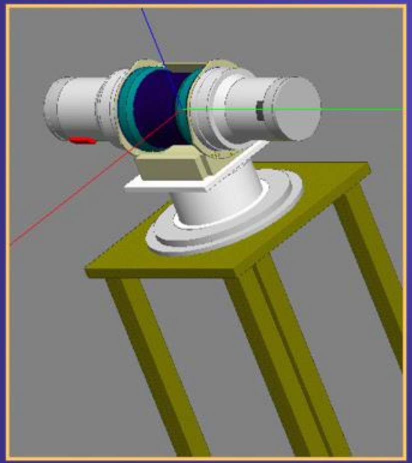

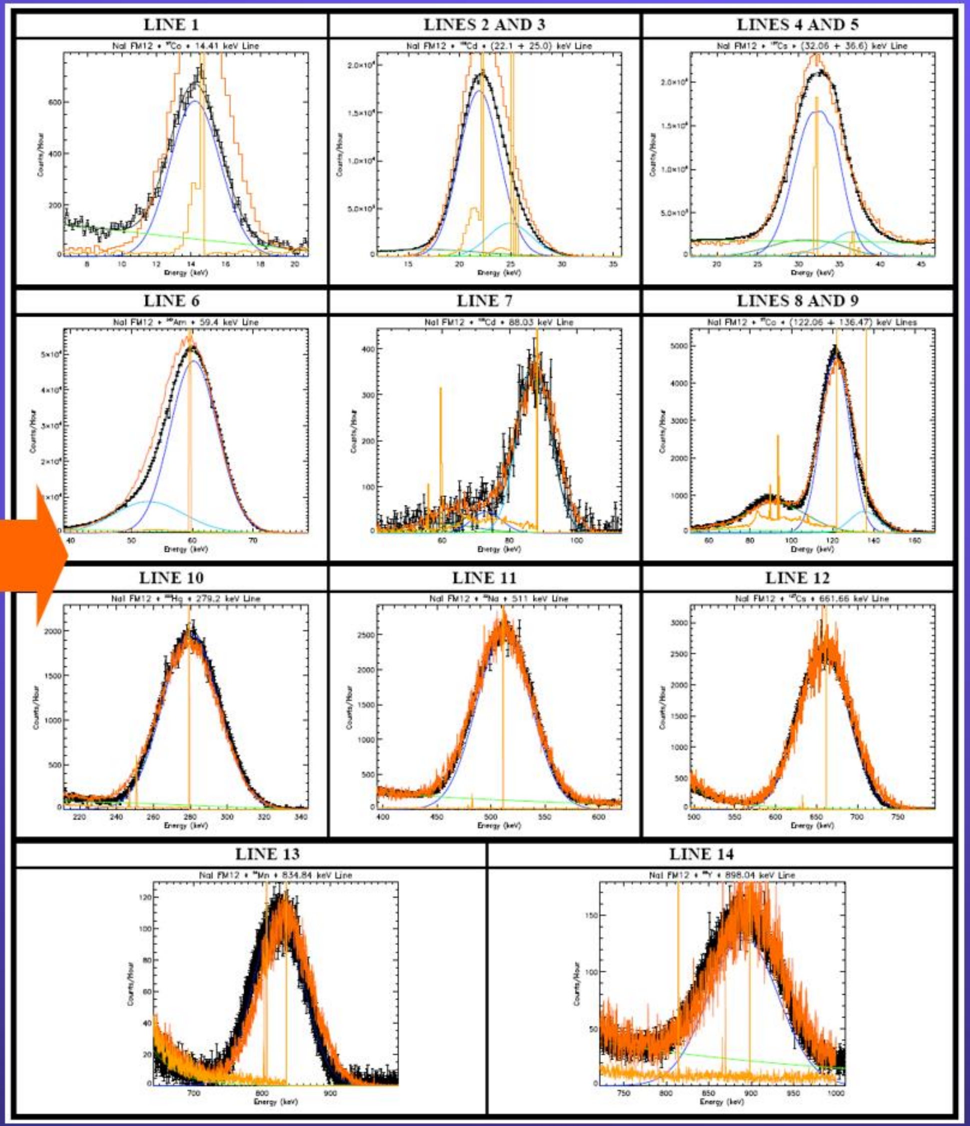

Simulation validation

^{57}Co • 122.06 & 136.47 keV

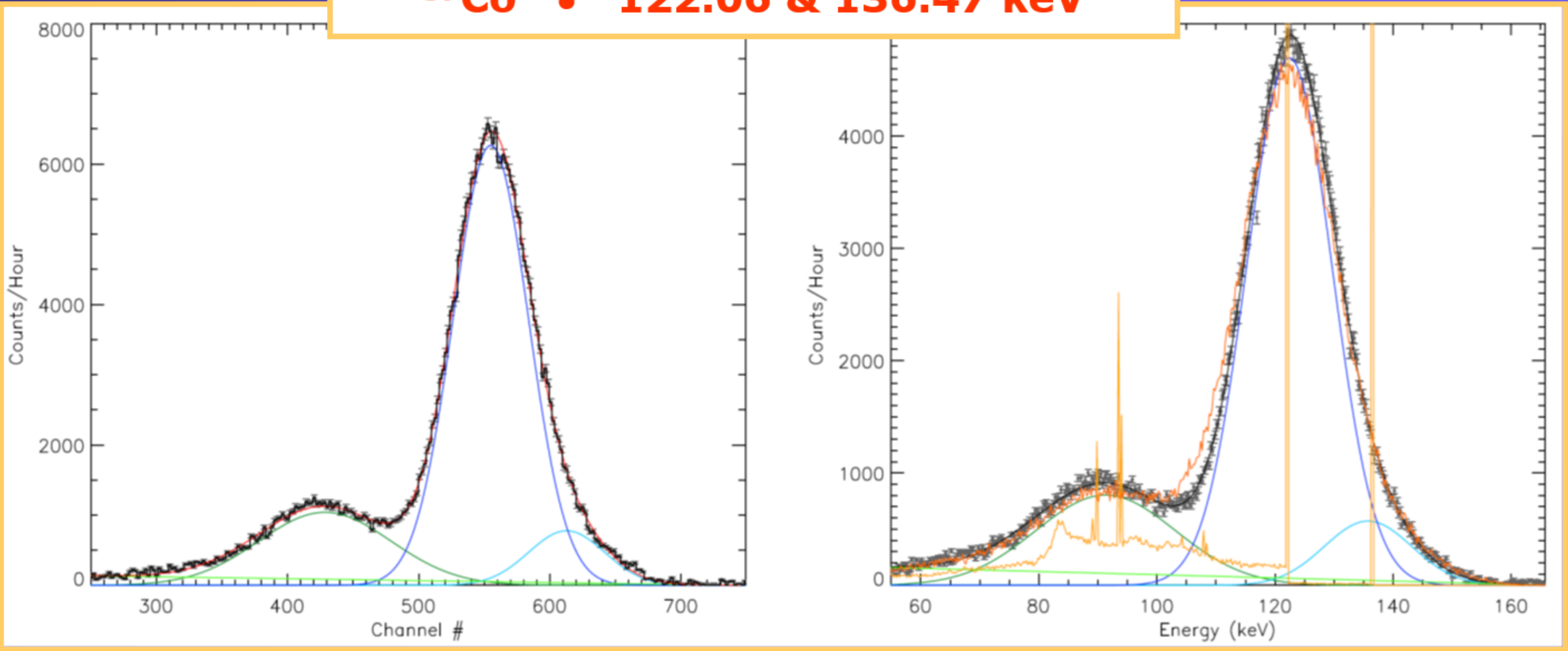

Data
Fit
122.06 keV line
136.47 keV line
Escape peak
Linear background

Data
Fit
122.06 keV line
136.47 keV line
Escape peak
Linear background
Unbroad sim lines
Broad sim lines

NaI Channel-Energy relation

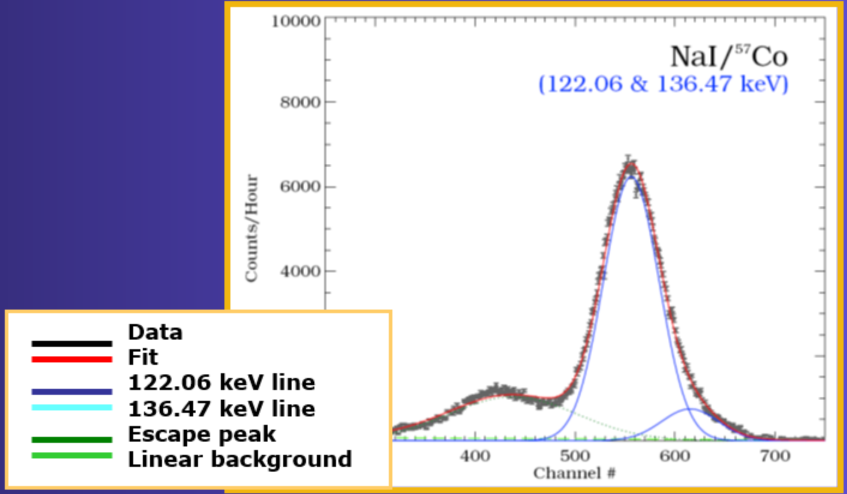

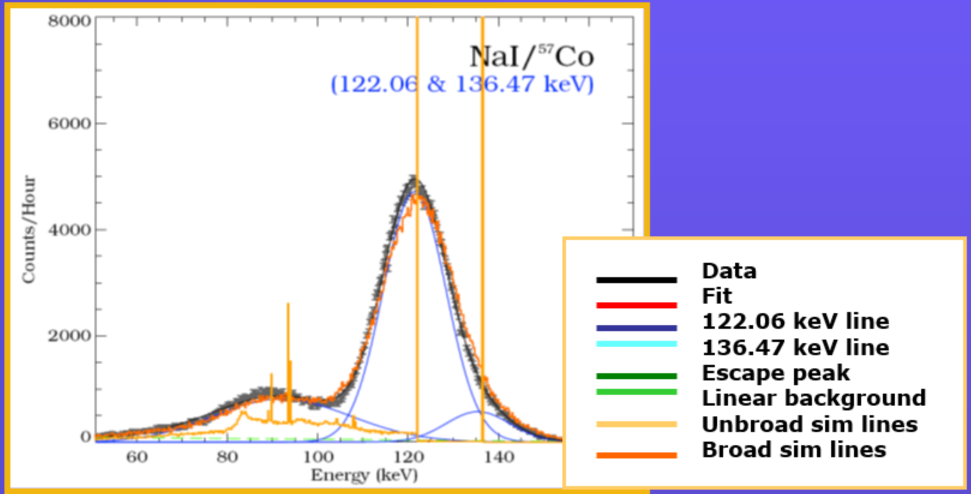

Bissaldi et al. 2008

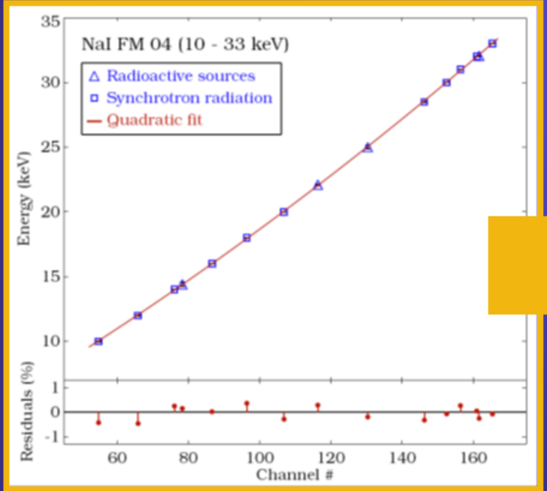

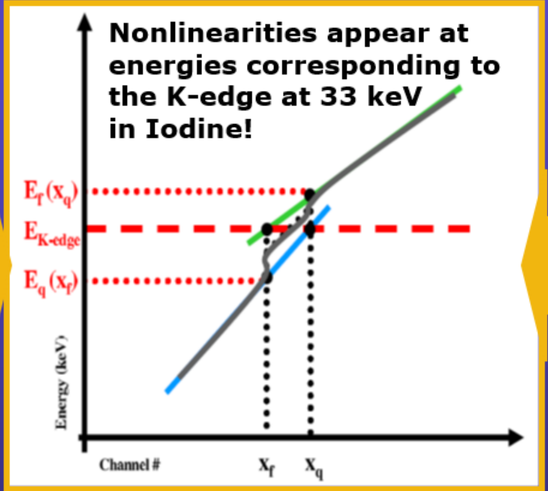

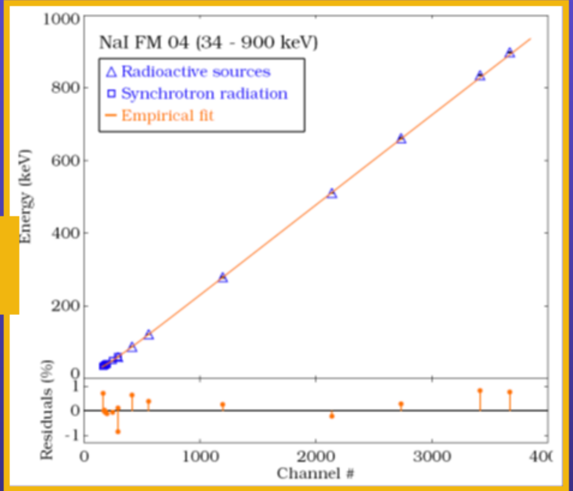

Code/Model Validation: SC Source Survey

Experiment

- Two sources, 12 orientations around SC
- ^{137}Cs (662 & 32 keV) & ^{60}Co (1.17 & 1.33 MeV)
- Custom lead source collimator
- Flight electronics (redundant DPU board)
- Calibration just completed

Simulations

- Separate collimator & spacecraft/room simulation
- Model being iterated

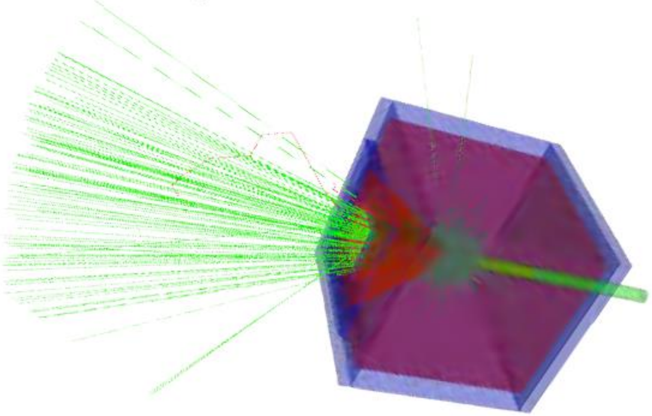

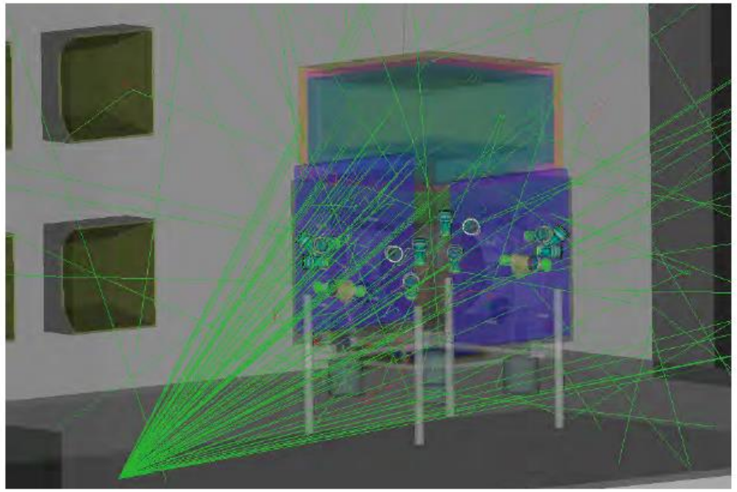

Source Collimator Model

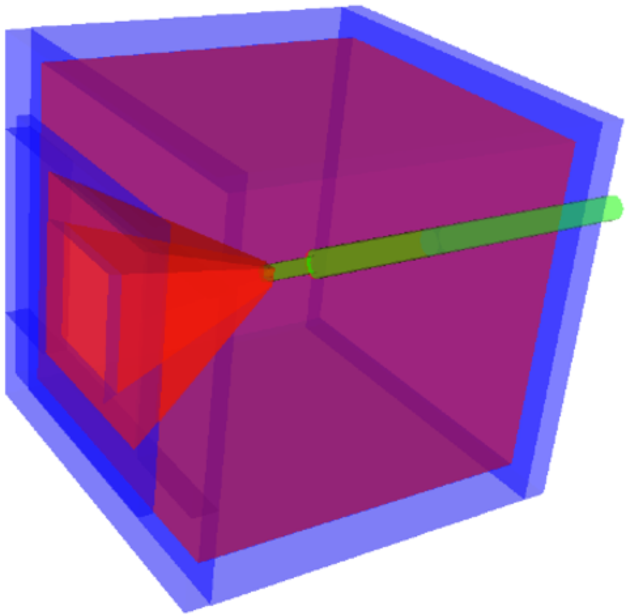

The source collimator is show above. The purple and red regions are made of lead. The blue is the aluminum outer shell. The green is a stainless steel source holder. The source is attached to the front of the stainless steel piece which is at the entrance of a 30 degree by 30 degree opening. The size is about 6” x 6” x 6” and weights about 60 lbs.

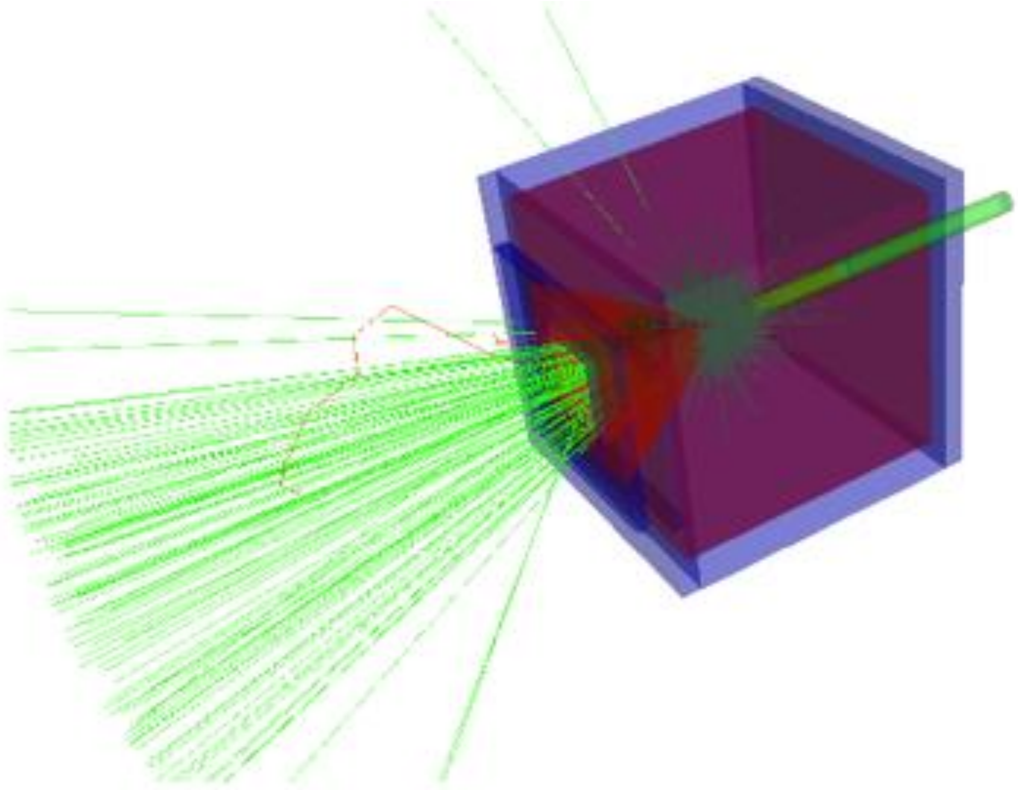

The image above shows 3000 simulated gamma-rays inside the collimator. As one can see it does a pretty good job but some gamma’s will get out through he collimator.

Wallace+2007

A simulations was done using about 250 million primary gamma-ray. The output energy and angles were recorded and used to model a source with similar energy and angular distribution but only throwing those gammas that escape.

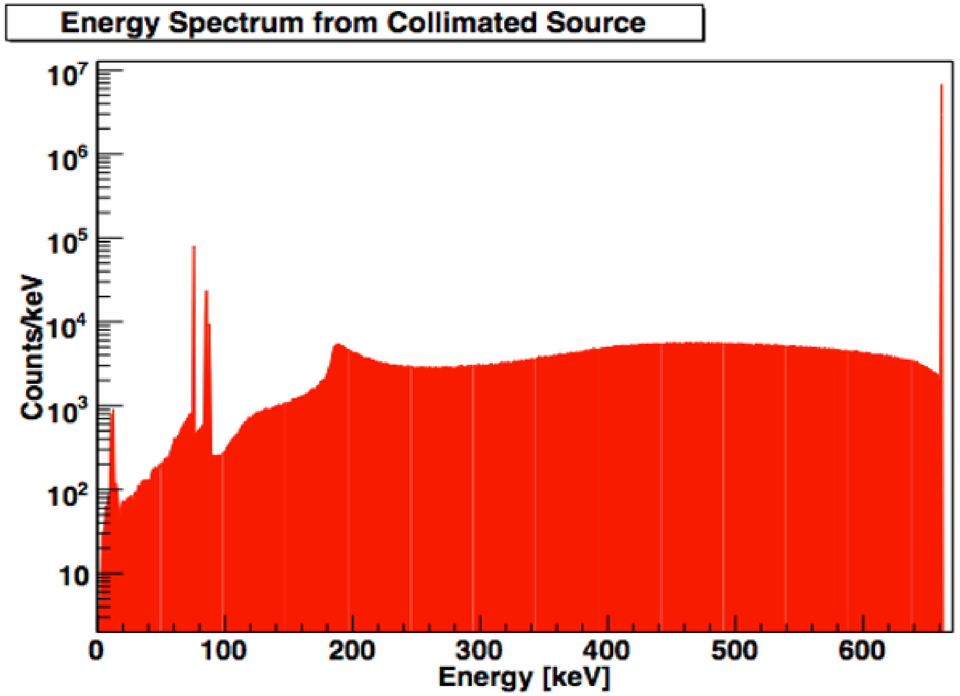

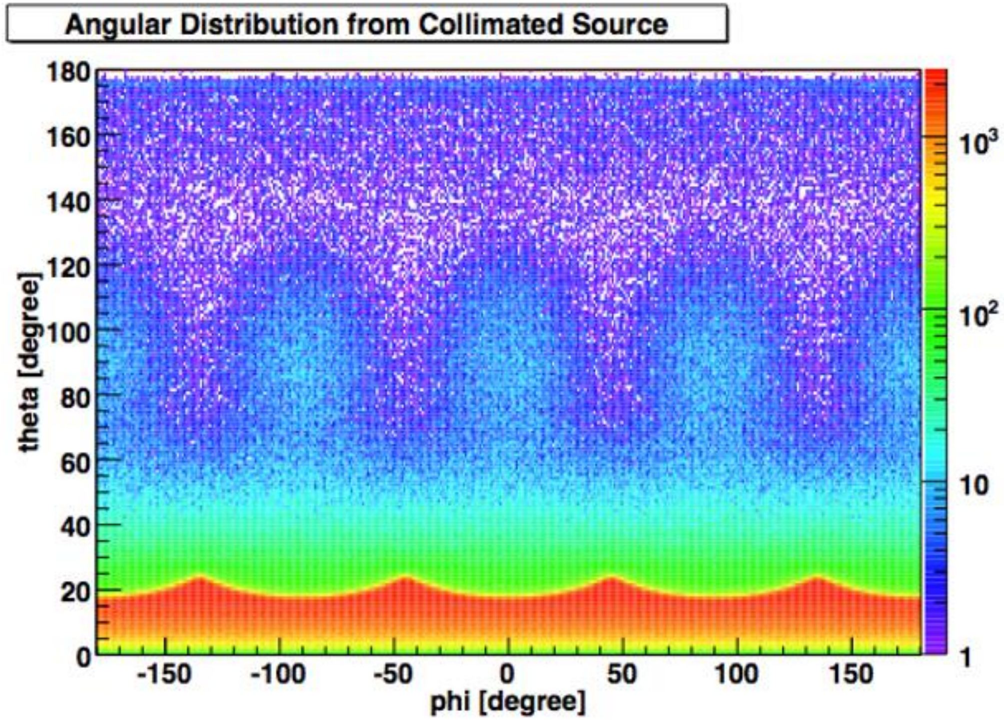

The output from the source model is shown above. Approximately 9 million gamma-ray per second are emitted. The modeled source is binned into 16 phi distributions based on theta and 64 different energy distribution based on the theta and phi.

Wallace+2007

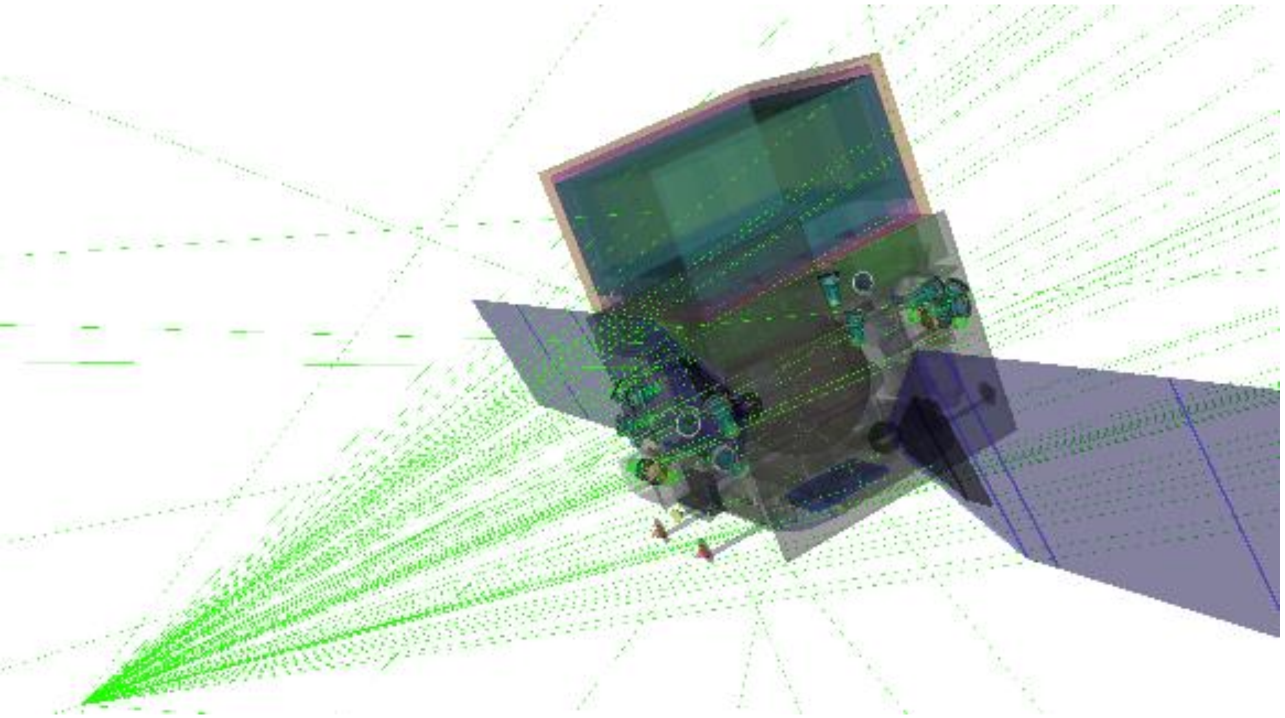

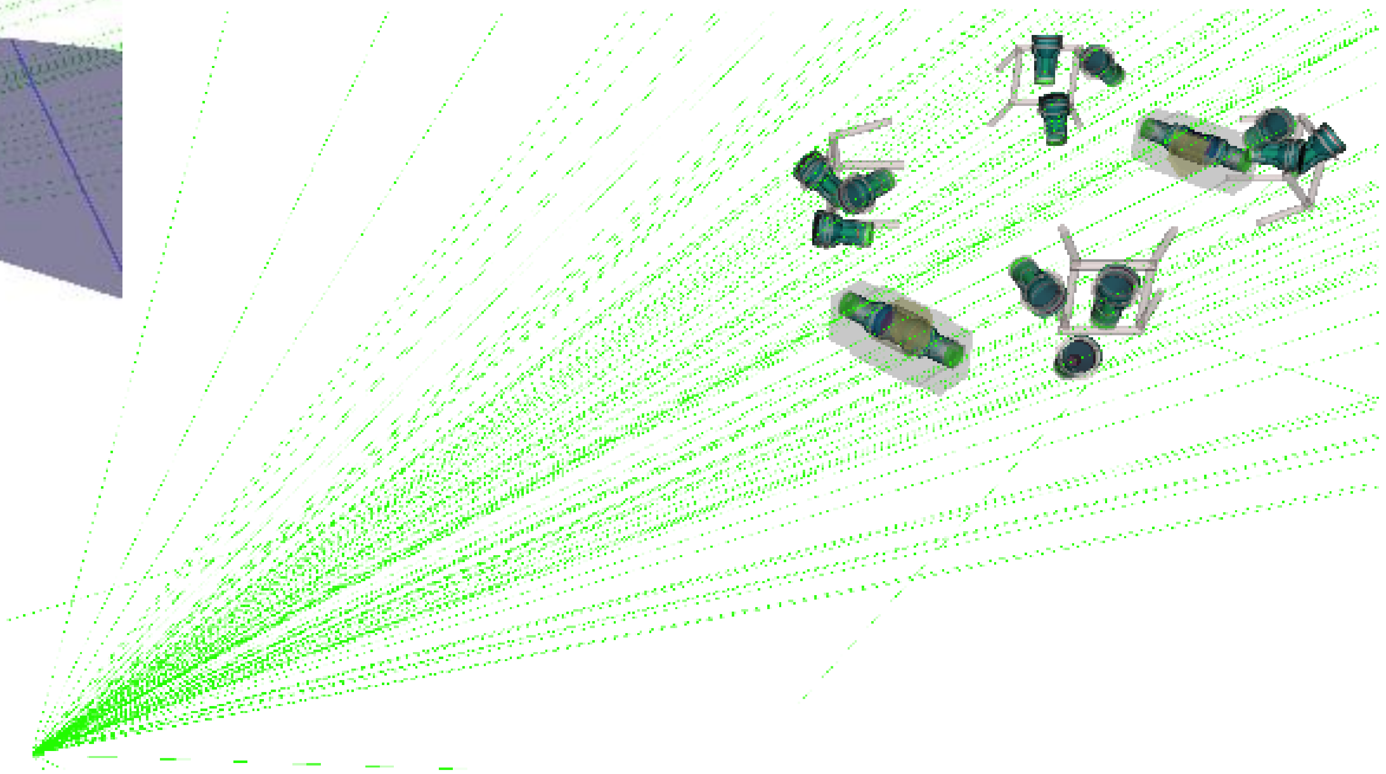

In order to understand to effect the spacecraft mass has on the detector response simulations using the source model were done with the full spacecraft as well as without but with detector in the proper location. Above shows the two configuration simulated. The left is the spacecraft in its flight configurations, the right image is only the GBM detectors.

Wallace+2007

Below is the energy spectrum for the BGO detectors with and without the spacecraft on both sides.

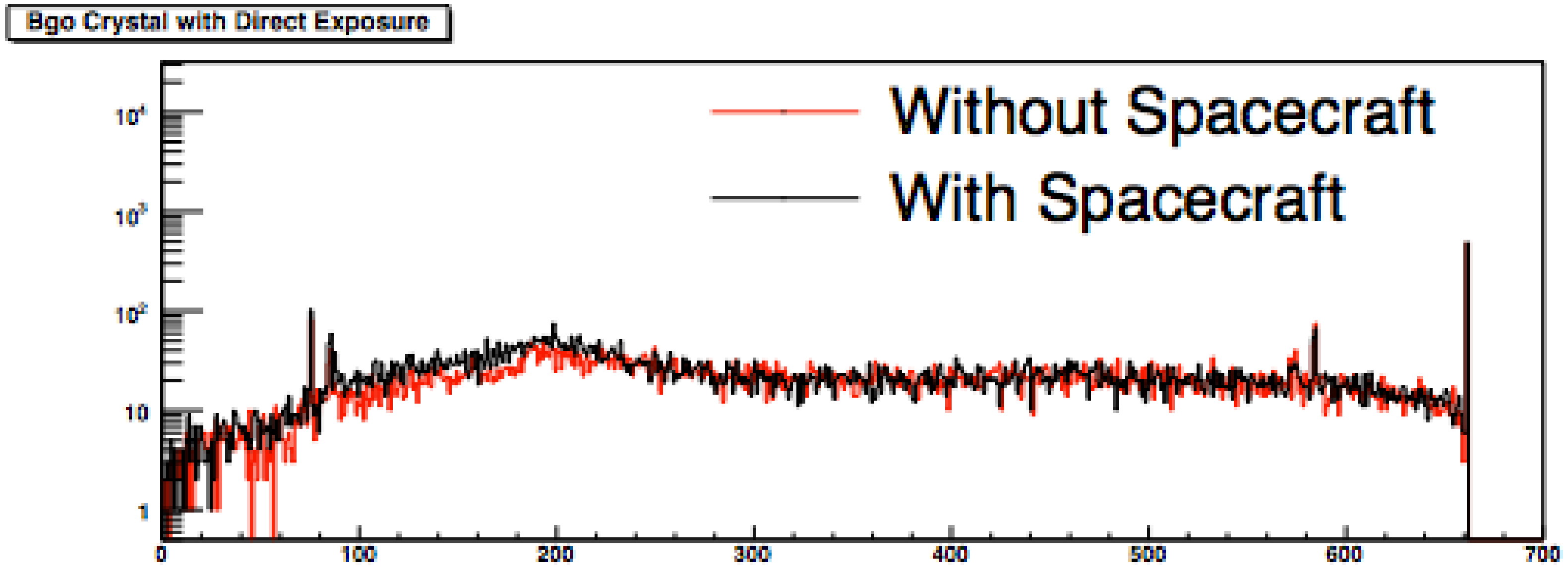

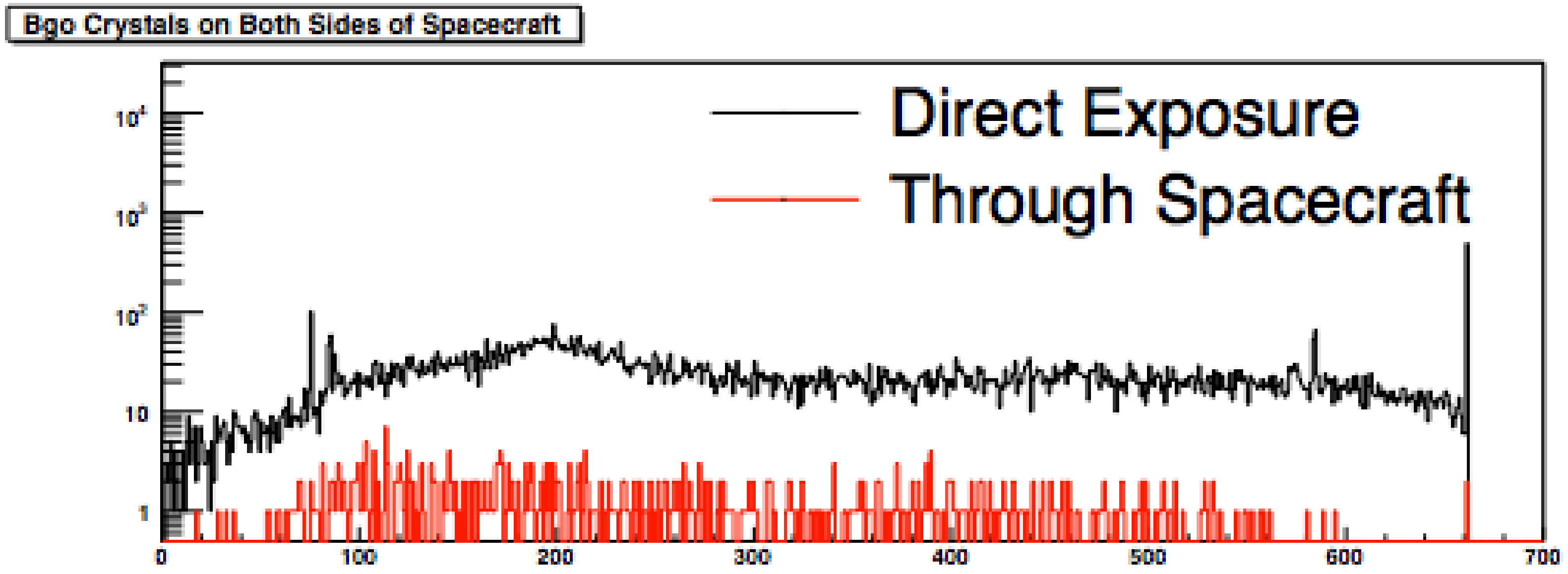

Wallace+2007

GBM Detector Response:

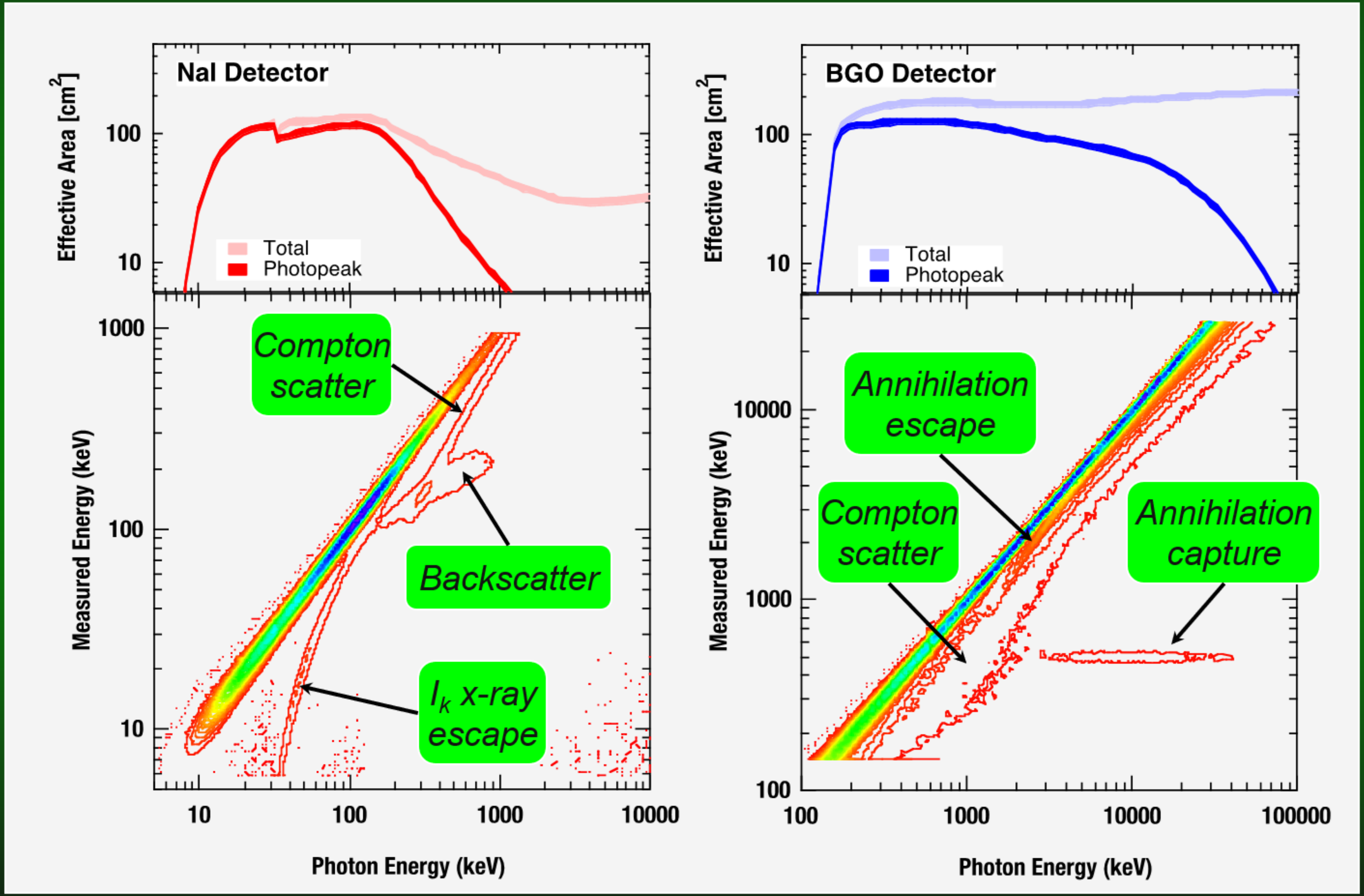

Kippen+2009

GBM Detector Response:

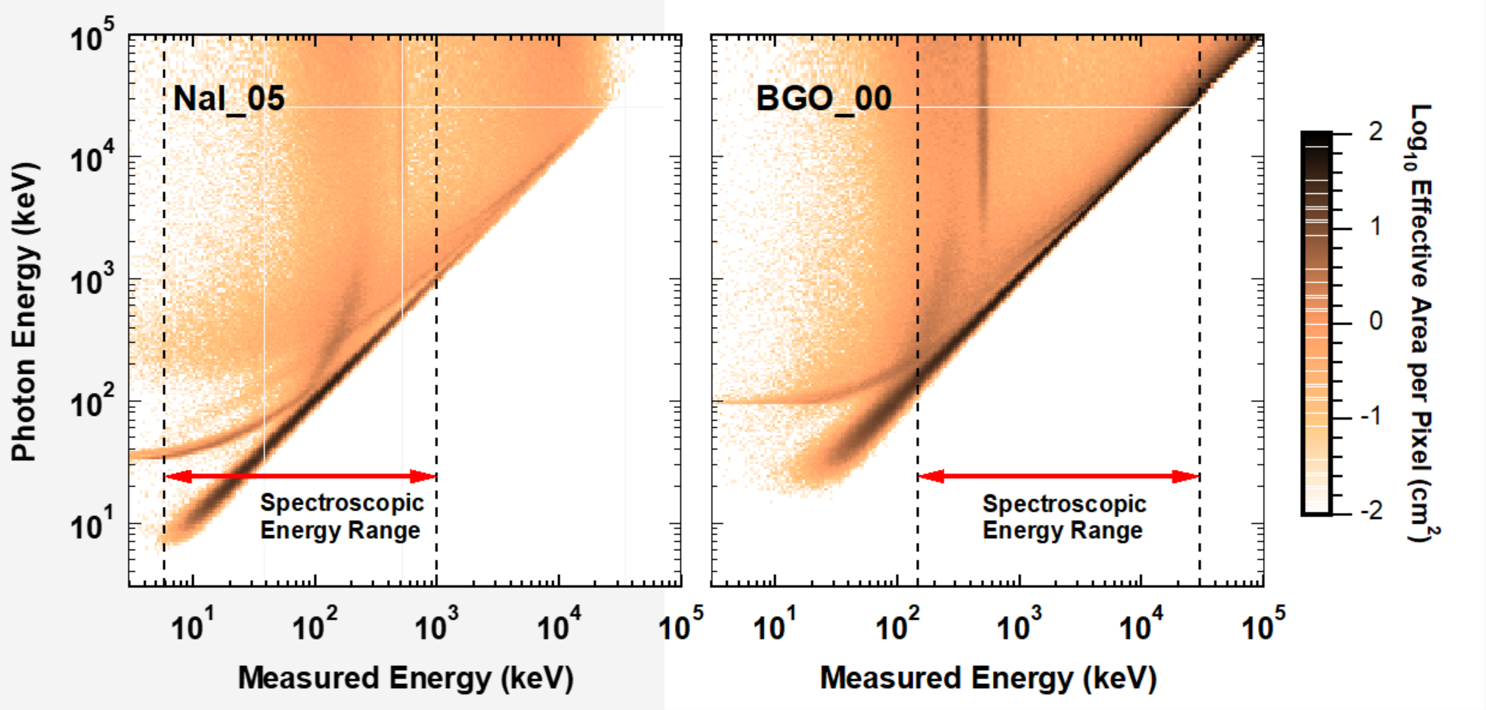

Kippen+2009

GBM performance: Energy calibration

Low-energy (NaI) range

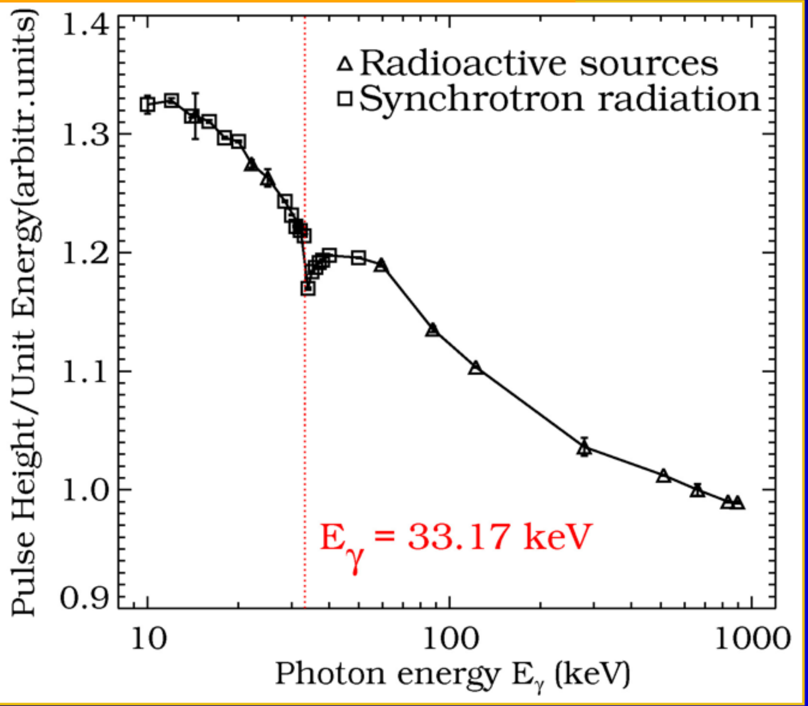

NaI(Tl) nonlinearities at the K-edge energy (33.17 keV) studied with radioactive sources + BESSY measurements

High-energy (BGO) range

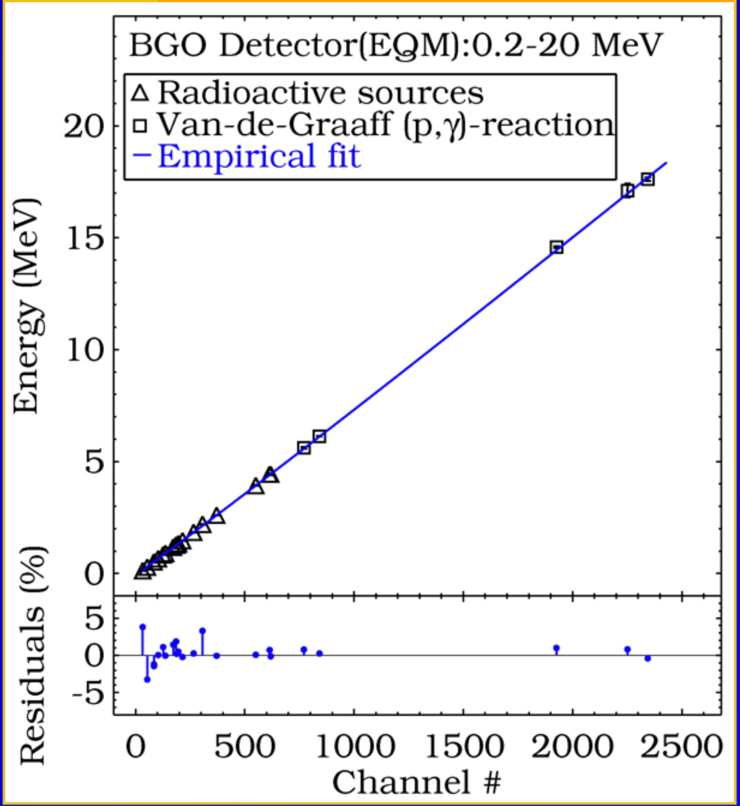

BGO high-energy calibration was performed up to 18 MeV

➔ Bissaldi et al. 2009, Exp. Astr. 24

Fermi-GBM detector Energy calibration

CHANNEL-ENERGY RELATION (CALIBRATION)

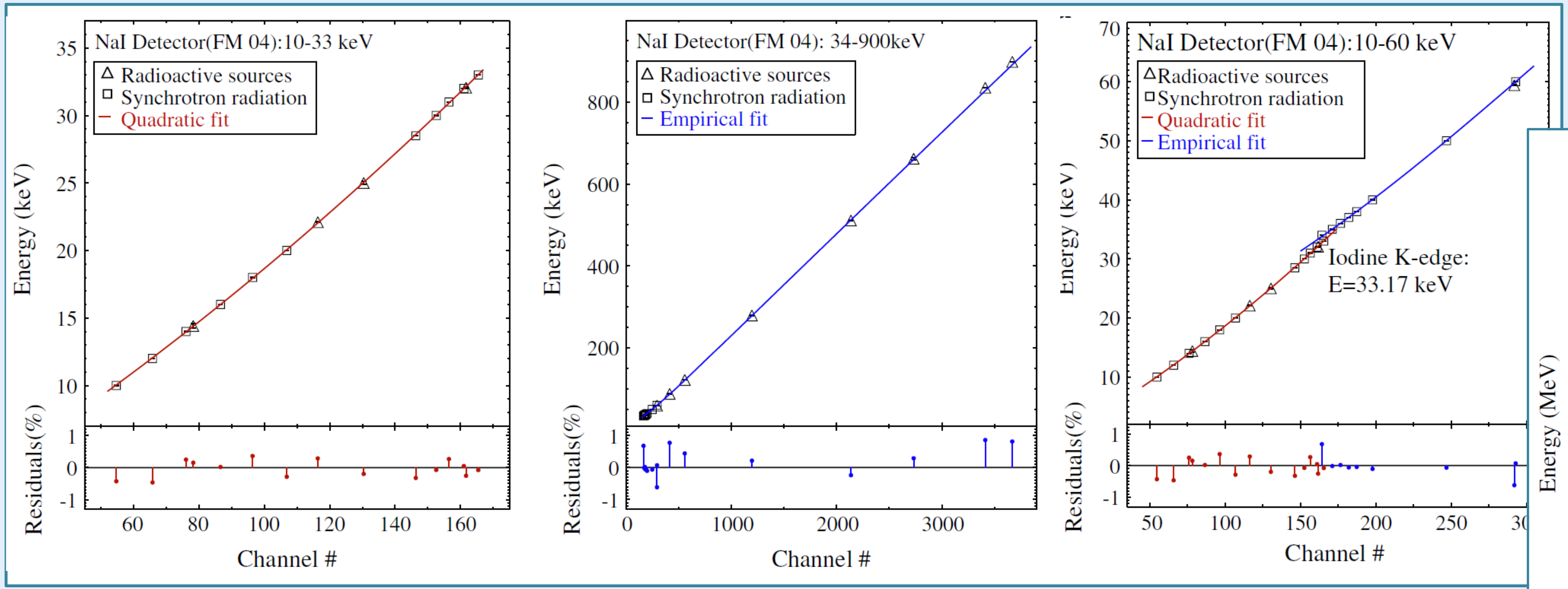

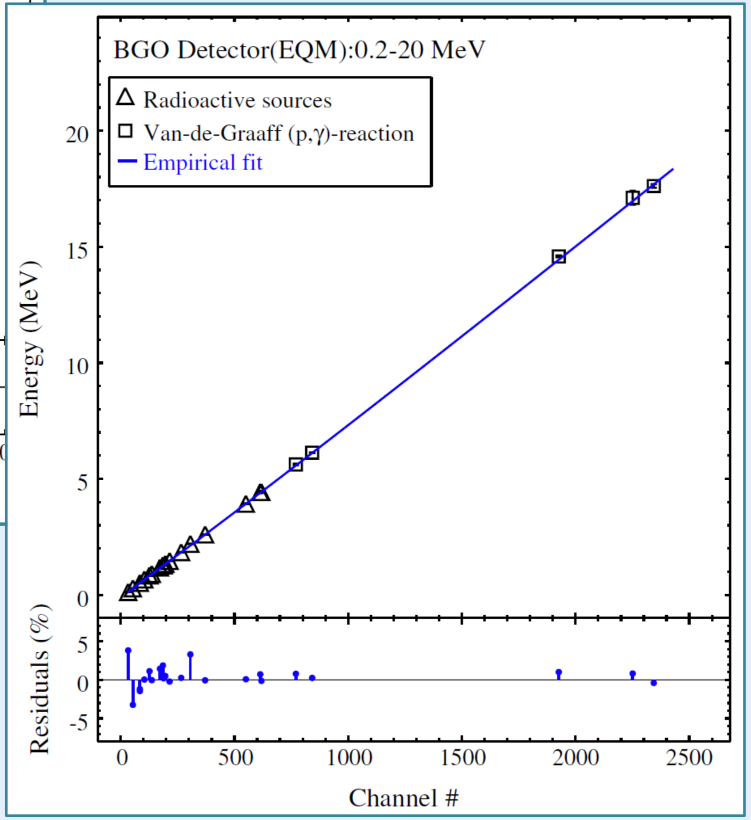

Bissaldi+2009

➔ Both Nai(Tl) and BGO scintillators show **good linearity** over the whole energy range

Fermi-GBM detector Energy Resolution

ENERGY RESOLUTION

NaI

BGO

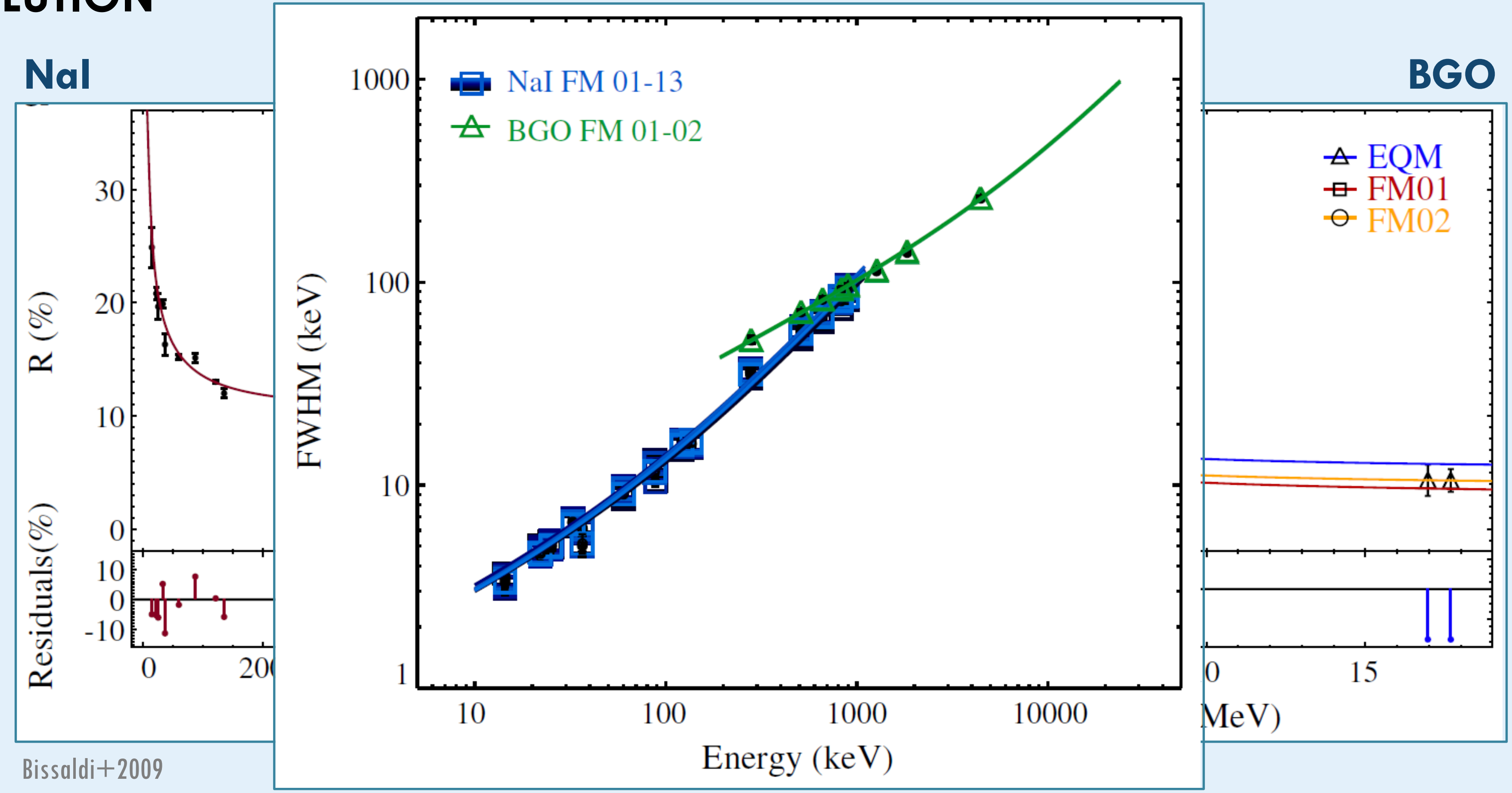

Bissaldi+2009

GBM performance: Effective area

On-axis effective area

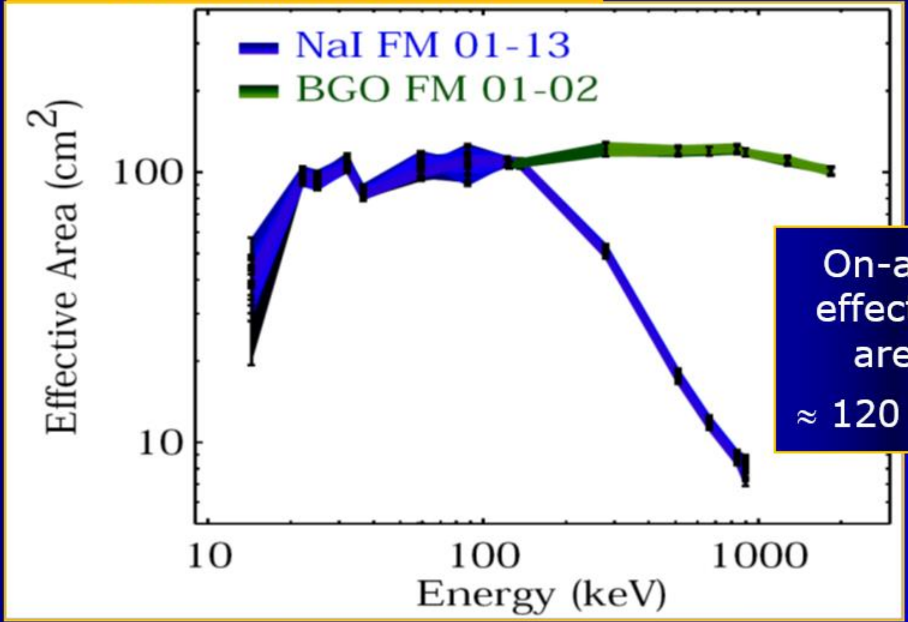

On-axis effective area
≈ 120 cm^2

Off-axis effective area

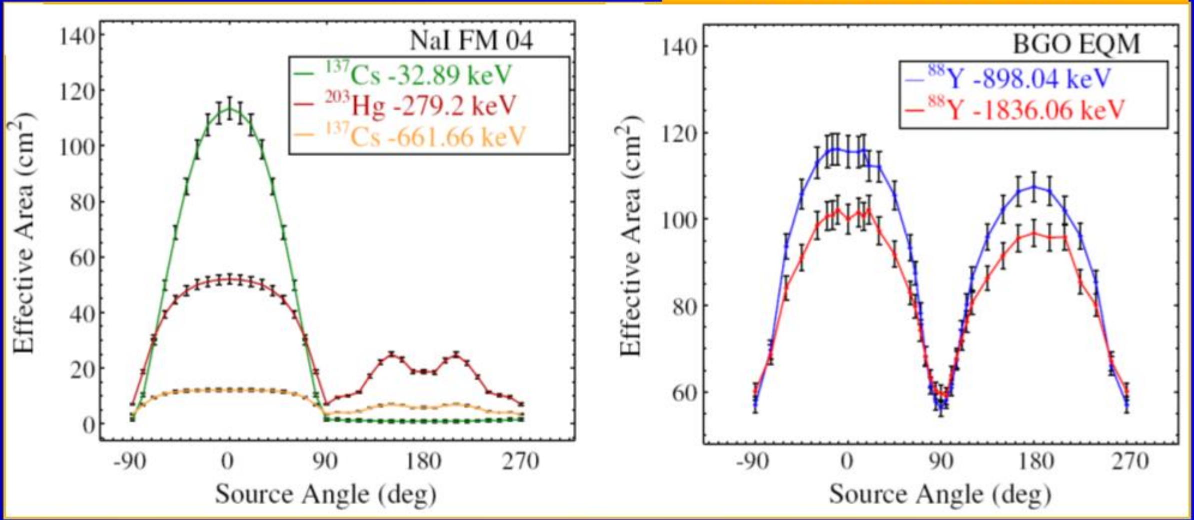

➔ Bissaldi et al. 2009, Exp. Astr. 24

NaI • Off axis effective area

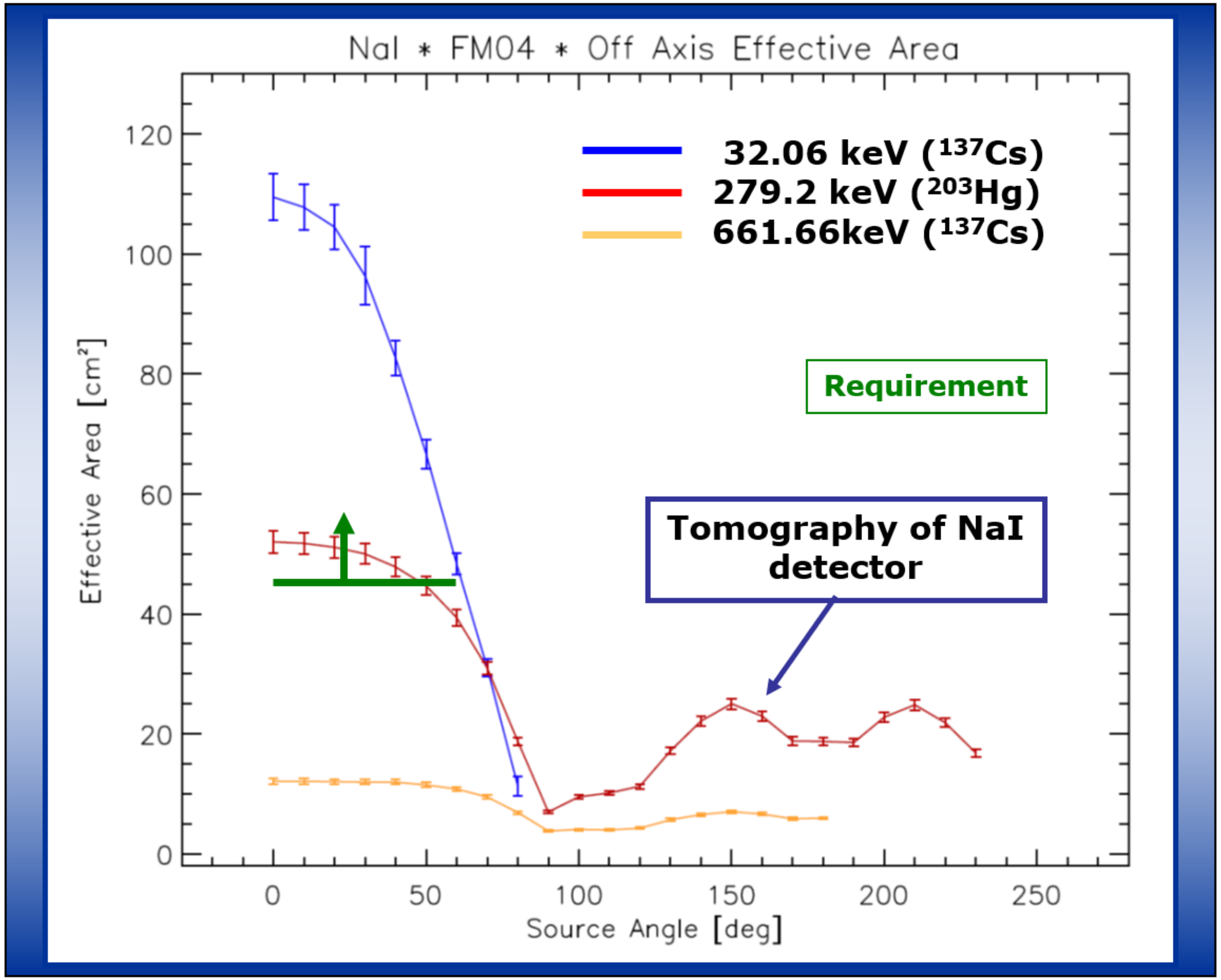

BGO • Off axis effective area

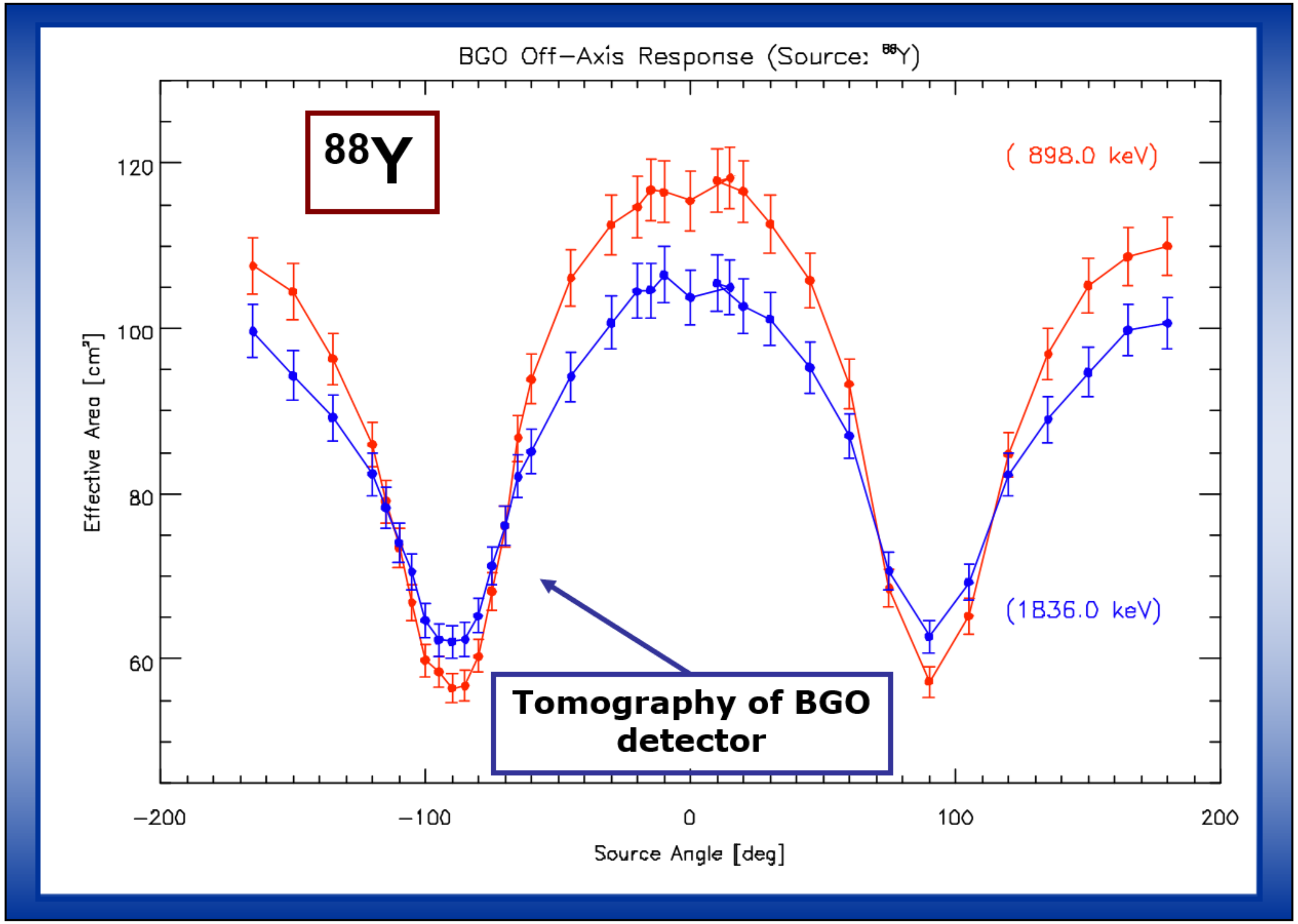

Fermi-GBM detector Uniformity

NAI(TL) SCINTILLATOR CRYSTAL UNIFORMITY

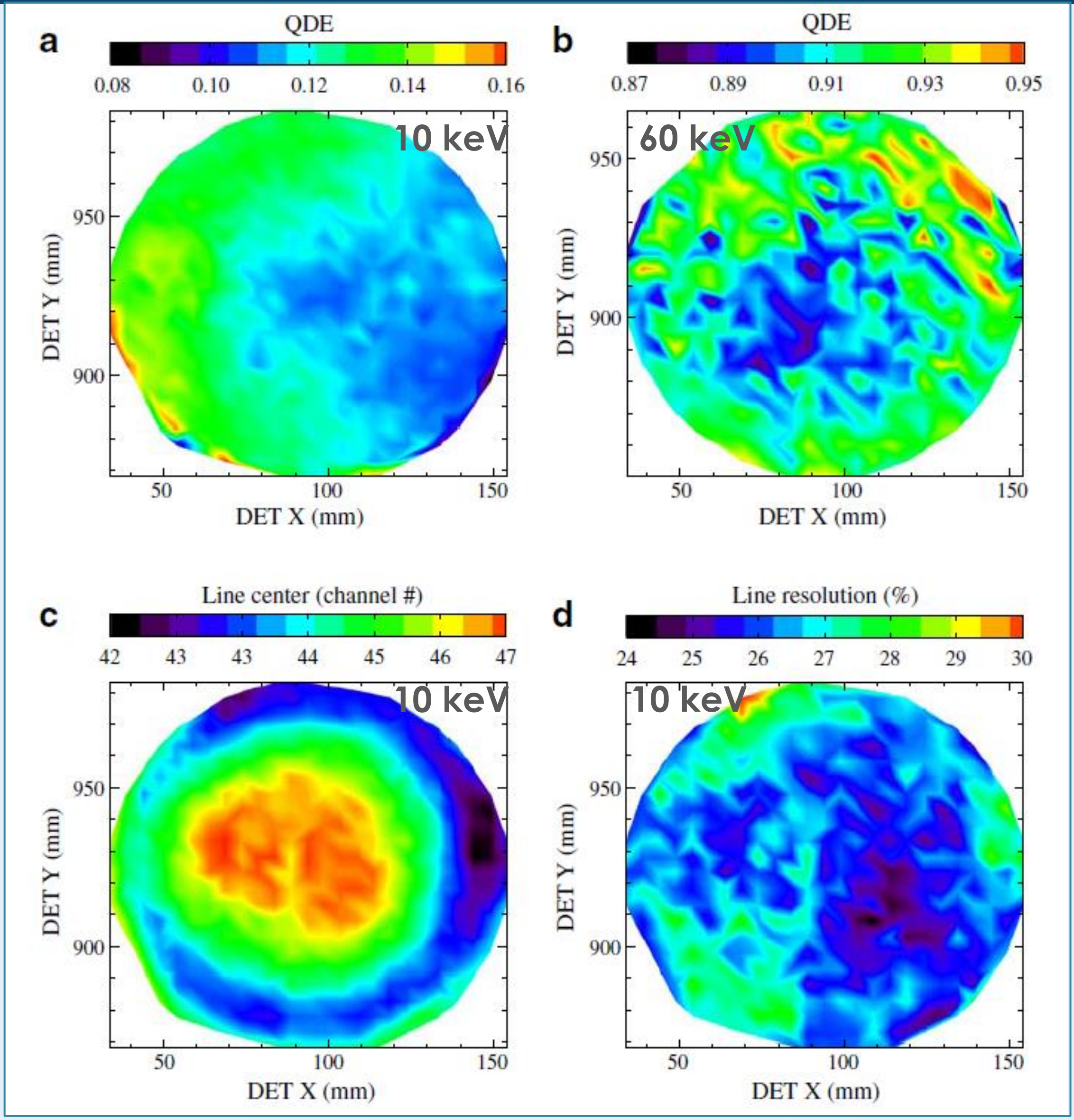

Bissaldi+2009

Fermi-GBM detector Background

NaI(Tl):

- **511 keV line** from positron annihilation in the atmosphere and nearby materials → **Used for AGC**
  - 2 lines from excited ^{127}I energy levels of (57.6 and 202.9 keV)
  - Passive materials in front the detectors limit the response of the detectors significantly at ~8-20 keV (low energy drop)

BGO:

- **2.2 MeV line** due to neutron capture in the large amount of H contained in the hydrazine tanks of the spacecraft → **Used for AGC**
  - 1.46 MeV line is due to ^{40}K from the potassium contained in the glass in the PMTs

Fermi-GBM 2.4 hr accumulations of background

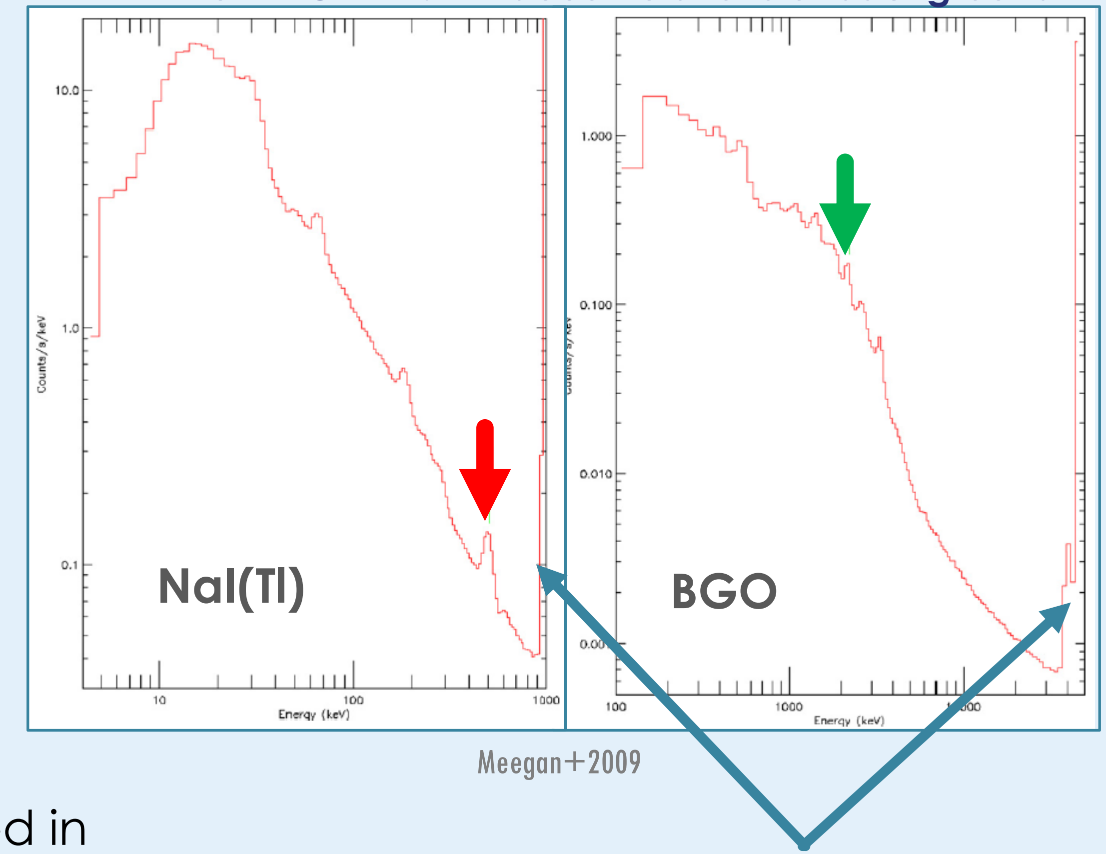

Meegan+2009

"Overflow channels"

NaI: ~1MeV
BGO: ~45 MeV

Fermi-GBM detector Background

Bacground rates: Temporal plots over 1 day (86400 s)

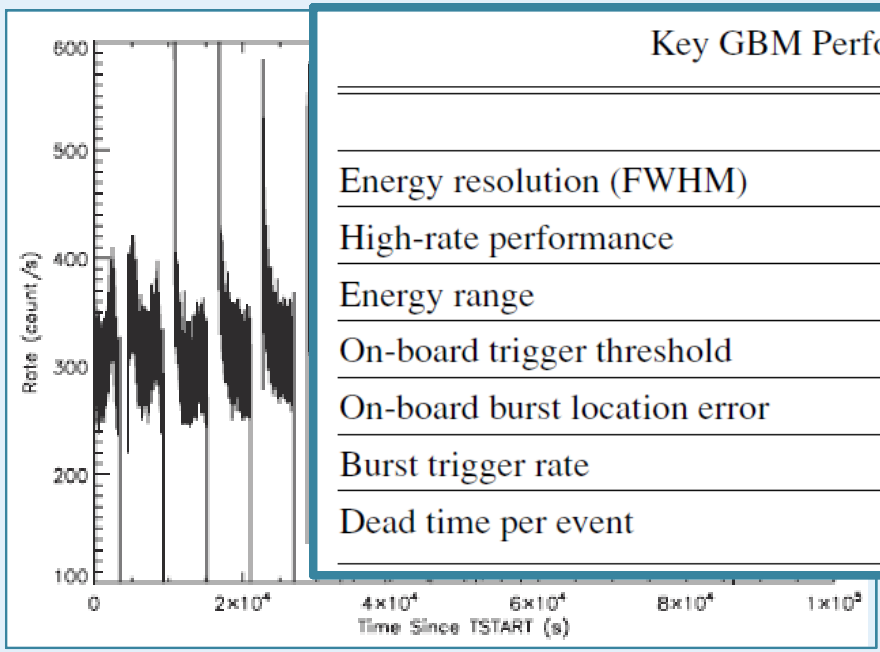

Key GBM Performance Capabilities

Energy resolution (FWHM)	∼15% at 100 keV; ∼10% at 1 MeV
High-rate performance	<2% distortion at 50,000 cps
Energy range	8 keV to 40 MeV
On-board trigger threshold	0.74 photons cm^{-2} s^{-1}
On-board burst location error	<15 deg
Burst trigger rate	∼260 per year
Dead time per event	2.6 μs

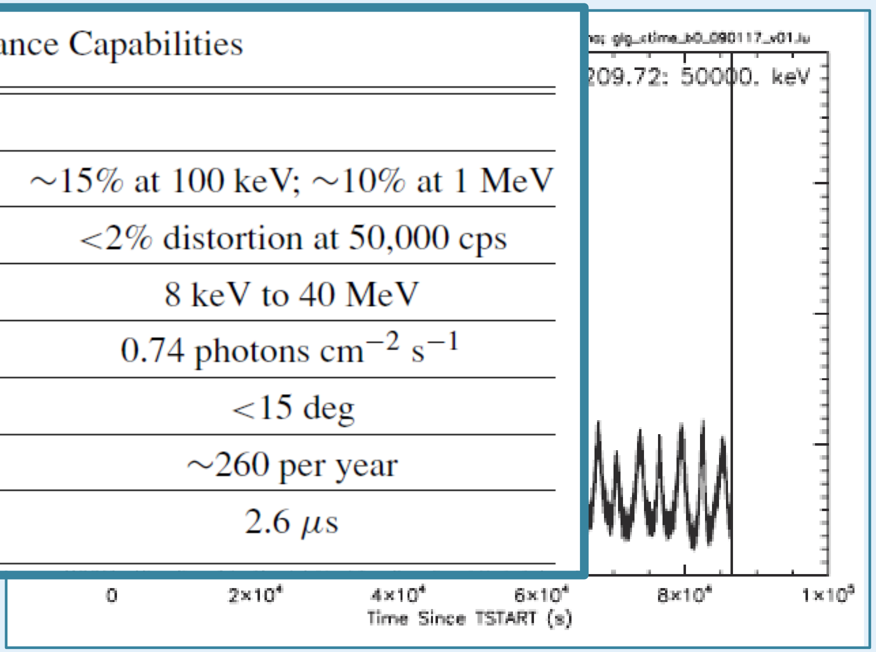

Meegan+2009

- Times of zero rate due to **turning off the PMTs** during **South Atlantic Anomaly (SAA) passages**
- High rates near the SAA boundaries
  - Effect of **activation** by the SAA **more pronounced in BGO** detectors
- NaI rates are shown for the **primary trigger energy range of 50–300 keV**
  - Average **~320 cps**, very little variation among the 12 detectors

9. The GBM catalogs!

2018

- GBM 10yr **GRB trigger** Catalog von Kienlin+2019 (in prep)
- GBM 10yr **GRB spectral** Catalog Poolakkil+2019 (in prep)
- GBM 10yr **GRB time-res. spectral** Catalog Bissaldi+2019 (in prep)
- GBM 10yr **Accreting Pulsar** Catalog Malacarian+2019 (in prep)

Coming soon!

- GBM 8yr **TGF** Catalog Roberts+2018 (submitted)

- GBM 6yr **GRB trigger** Catalog (3FGBM) Bhat+2016.ApJSS223
- GBM 5yr **Magnetar** Burst Catalog Collazzi+2015.ApJSS218
- GBM 4yr **GRB time-res. spectral** Catalog Yu+2016.A&A588
- GBM 4yr **GRB spectral** Catalog Gruber+2014.ApJSS211
- GBM 4yr **GRB trigger** Catalog (2FGBM) von Kienlin+2014.ApJSS211
- GBM 3yr **X-ray Burst** Catalog Jenke+2016.ApJ826
- GBM 3yr **EOM** catalog Wilson-Hodge et al. 2012
- GBM 2yr **GRB spectral** Catalog Goldstein+2012.ApJSS199
- GBM 2yr **GRB trigger** Catalog (1FGBM) Paciesas+2012.ApJSS199

2008

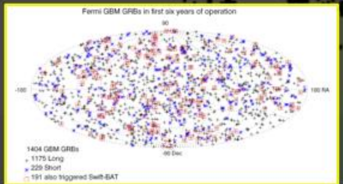

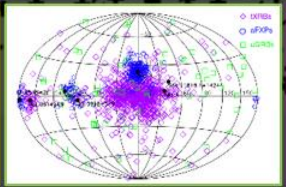
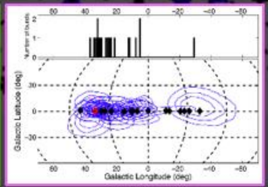

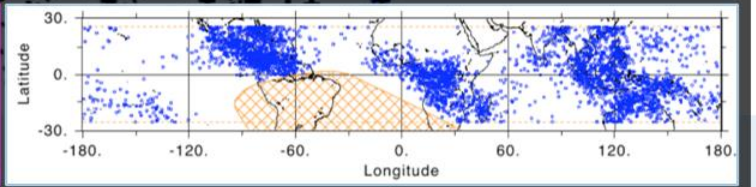

BREAKTHROUGH #1: GRB+GW DETECTION (2017)

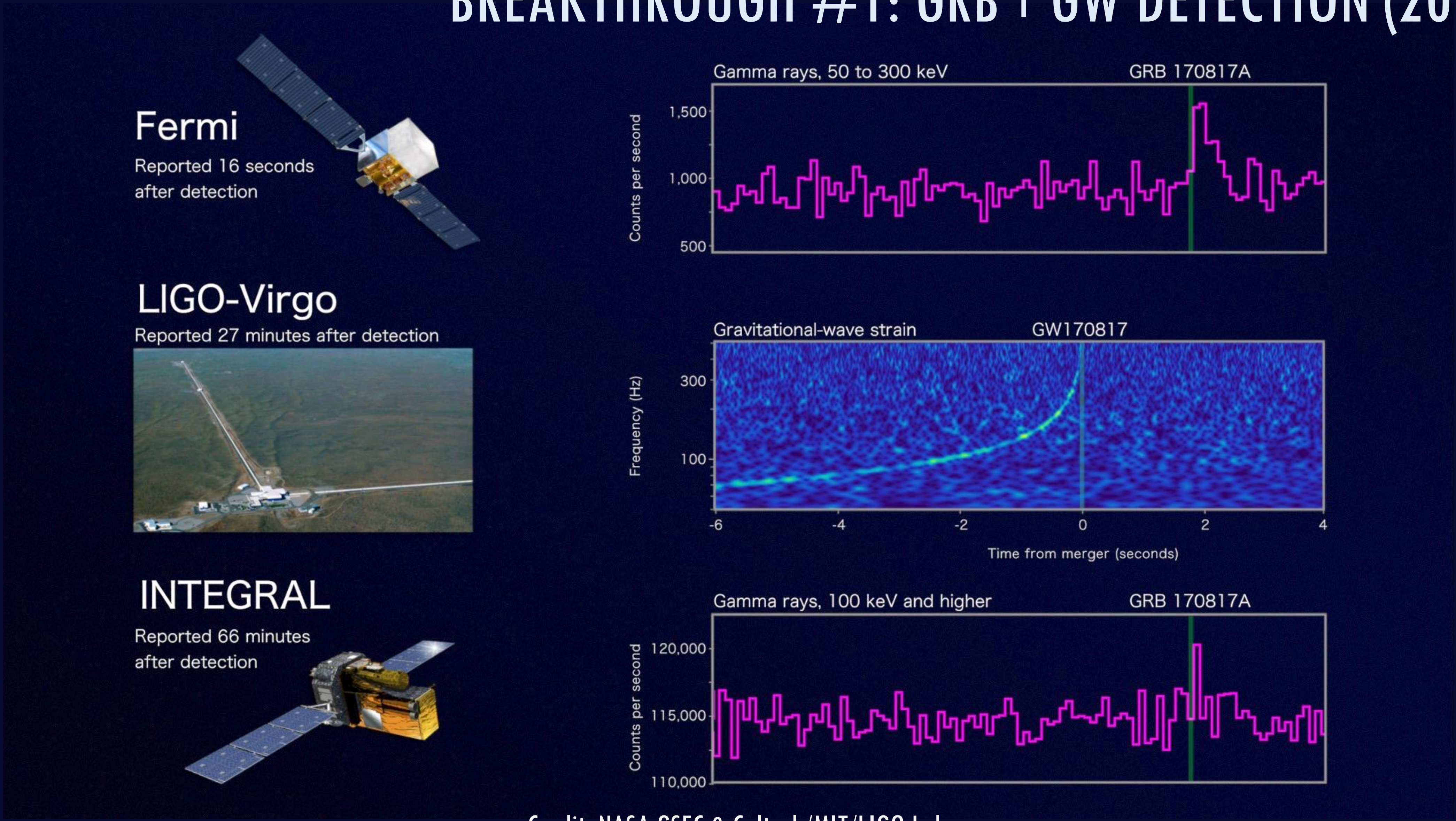

Credit: NASA GSFC & Caltech/MIT/LIGO Lab

https://www.youtube.com/watch?v=-Yt5EmEgz2w

BREAKTHROUGH #2: GRB DETECTIONS @VHE

- Announcements on 20 Nov. 2019
  1. H.E.S.S. observation of **GRB 180720B**
  2. MAGIC observation of **GRB 190114C**
- Announcement on 4 June 2021
  3. H.E.S.S. observation of **GRB 190829A**

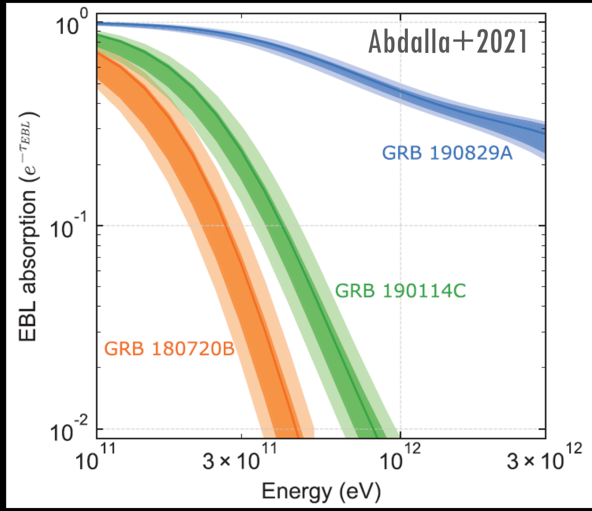

nature

Article | Published: 20 November 2019

A very-high-energy component deep in the γ-ray burst afterglow

H. Abdalla, R. Adam, [...] O. J. Roberts

Nature **575**, 464–467(2019) | Cite this article

z = 0.653

Abstract

Gamma-ray bursts (GRBs) are brief flashes of γ-rays and are considered to be the most energetic explosive phenomena in the Universe[1]. The emission from GRBs comprises a short (typically tens of seconds) and bright prompt emission, followed by a much longer afterglow phase. During the afterglow phase, the shocked outflow—produced by the interaction between the ejected matter and the circumburst medium—slows down, and a gradual decrease in brightness is observed[2]. GRBs typically emit most of their energy via γ-rays with energies in the kiloelectronvolt-to-megaelectronvolt range, but a few photons with

nature DOI: 10.1038/s41586-019-1750-x

Article | Published: 20 November 2019

Teraelectronvolt emission from the γ-ray burst GRB 190114C

MAGIC Collaboration

Nature **575**, 455–458(2019) | Cite this article

z = 0.4245

Abstract

Long-duration γ-ray bursts (GRBs) are the most luminous sources of electromagnetic radiation known in the Universe. They arise from outflows of plasma with velocities near the speed of light that are ejected by newly formed neutron stars or black holes (of stellar mass) at cosmological distances[1,2]. Prompt flashes of megaelectronvolt-energy γ-rays are followed by a longer-

Science Contents News Careers Journals

REPORT

Revealing x-ray and gamma ray temporal and spectral similarities in the GRB 190829A afterglow

H.E.S.S. Collaboration[*,†], H. Abdalla[1], F. Aharonian[2,3,4], F. Ait Benkhali[3], E. O. Angüner[5], C. Arcaro[6], C. Armand[7], T. Armstro...
+ See all authors and affiliations

Science 04 Jun 2021:
Vol. 372, Issue 6546, pp. 1081-1085
DOI: 10.1126/science.abe8560

z = 0.0785

Article | Figures & Data | Info & Metrics | eLetters | PDF

Abstract

Gamma-ray bursts (GRBs), which are bright flashes of gamma rays from extragalactic sou... followed by fading afterglow emission, are associated with stellar core collapse events. W... report the detection of very-high-energy (VHE) gamma rays from the afterglow of GRB 190829A, between 4 and 56 hours after the trigger, using the High Energy Stereoscopic System (H.E.S.S.). The low luminosity and redshift of GRB 190829A reduce both internal an... external absorption, allowing determination of its intrinsic energy spectrum. Between energi... of 0.18 and 3.3 tera–electron volts, this spectrum is described by a power law with photon index of 2.07 ± 0.09, similar to the x-ray spectrum. The x-ray and VHE gamma-ray light curves also show similar decay profiles. These similar characteristics in the x-ray and gamma-ray bands challenge GRB afterglow emission scenarios.

GRB 201216C MAGIC detection

https://heasarc.gsfc.nasa.gov/

National Aeronautics and Space Administration
Goddard Space Flight Center
Sciences and Exploration

GO Search HEASARC website
[Advanced Search]

HEASARC Quick Links
---Quick Links---

HEASARC Home | Observatories | Archive | Calibration | Software | Tools | Students/Teachers/Public

NASA's HEASARC
High Energy Astrophysics Science Archive Research Center

About the HEASARC | Resources for Scientists | Feedback, FAQ & Help Desk | Site Map | Other Archives

Active Guest Observer Facilities/Science Centers	
AGILE	*AstroSat*
Chandra	Fermi
HaloSat	INTEGRAL
MAXI	NICER
NuSTAR	*SRG/eROSITA*
Swift	TESS
XMM-Newton	XRISM

Historic Guest Observer Facilities/Science Centers	
ASCA	BeppoSAX
CGRO	COBE
EUVE	GALEX
Hitomi	HETE-2
LPF DRS	ROSAT
RXTE	Suzaku
WMAP	

NASA Archives	
ADS	EOSDIS
ExoArchive	HORIZONS

The High Energy Astrophysics Science Archive Research Center (HEASARC) is the primary archive for NASA's (and other space agencies') missions studying electromagnetic radiation from extremely energetic cosmic phenomena ranging from black holes to the Big Bang. Since its merger with the Legacy Archive for Microwave Background Data Analysis (LAMBDA) in 2008, the HEASARC archive contains data obtained by high-energy astronomy missions observing in the extreme-ultraviolet (EUV), X-ray, and gamma-ray bands, as well as data from space missions, balloons, and ground-based facilities that have studied the relic cosmic microwave background (CMB) radiation in the sub-mm, mm and cm bands.

The HEASARC is a member of the **NASA Astronomical Virtual Observatories (NAVO)** where we work with other NASA archives to ensure comprehensive and consistent VO access to NASA mission datasets. Users may now query the HEASARC's catalogs using VO-enabled services and specialized tools. **This page** describes how to get to the HEASARC VO-enabled services and provides information on other HEASARC VO activities.

HEASARC Picture of the Week

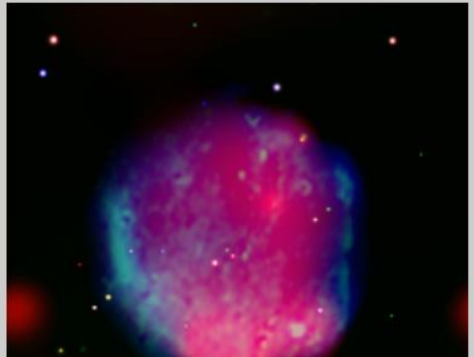

APOD: Astronomy Picture of the Day

Latest News

- **NICER follow up of the new X-ray transient IGR J17533-2928** (08 Mar 2021)
NICER observations of the new transient IGR J17533-2928 about a week after it was first detected by INTEGRAL showed that the spectrum was consistent with modified blackbody emission and did not detect any pulsed emission. The nature of the transient remains to be revealed.
- **XSPEC 12.11.1a-d Patch Released** (03 Mar 2021)
XSPEC patches 12.11.1a-d have been released. These patches improve the nsx model, fixes a crash in spectra in which all channels are ignored, fixes a bug in file checking, and fixes an error in the normalization of the gadem family of models.
- **NICER Spectroscopy of MAXI J1848-015 in the Stellar Cluster GLIMPSE-C01** (02 Mar 2021)
NICER observations of this new transient show complex iron line emission and a luminosity much less than the typical Eddington luminosity for a neutron star.
- **NICER detects pulsations from Swift J1749.4-2807** (02 Mar 2021)
NICER observations of the eclipsing, accreting millisecond pulsar Swift J1749.4-2807 finds a 1-

Topics | Missions | Galleries | NASA TV | Follow NASA | Downloads | About | NASA Audiences

Search

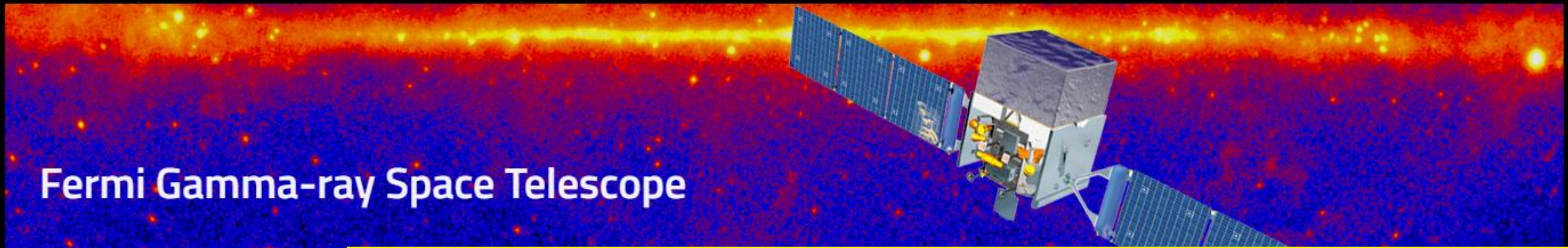

Fermi Gamma-ray Space Telescope

Fermi | Overview | Images | Videos

https://www.nasa.gov/content/fermi-gamma-ray-space-telescope

Follow

Follow

Learn More

- Spacecraft and Instruments
- Mission Team

Related Topics

- Active Galactic Nuclei
- Dark Energy/Matter
- Galaxies
- Gamma-Ray Bursts
- Pulsars
- All Topics A-Z

NASA Missions Unveil Magnetar Eruptions in Nearby Galaxies

Mission Overview

Launched on June 11, 2008, the Fermi Gamma-ray Space Telescope observes the cosmos using the highest-energy form of light. Mapping the entire sky every three hours, Fermi provides an important window into the most extreme phenomena of the universe, from gamma-ray bursts and black-hole jets to pulsars, supernova remnants and the origin of cosmic rays.

Gamma-Ray Bursts

NASA Missions Unmask Magnetar Flares in Nearb...

NASA Missions Team Up to Study Unique Magnetar Outburst

National Aeronautics and Space Administration
Goddard Space Flight Center

Fermi • FSSC • HEASARC
Sciences and Exploration

https://fermi.gsfc.nasa.gov/ssc/data/access/

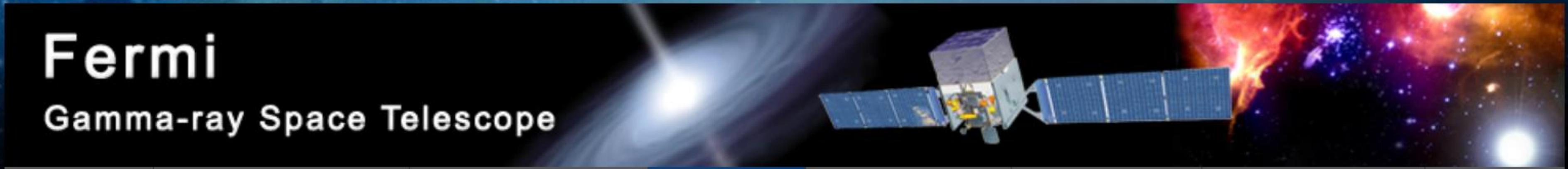

Home | Support Center | Observations | Data | Proposals | Library | HEASARC | Help

Data

- Data Policy
- **Data Access**
  - + LAT Data
  - + LAT Catalog
  - + LAT Data Queries
  - + LAT Query Results
  - + LAT Weekly Files
  - + GBM Data
- Data Analysis
- Caveats
- Newsletters
- FAQ

Currently Available Data Products

The Fermi data released to the scientific community is governed by the data policy. The released instrument data for the GBM, along with LAT source lists, can be accessed through the Browse interface specific to Fermi. LAT photon data can be accessed through the LAT data server.

The FITS files can also be downloaded from the Fermi FTP site. The file version number is the 'xx' in the characters before the extension in each filename; you should keep track of the version numbers of files you analyze since the instrument teams may update them.

Note that the LAT and GBM data are accompanied by caveats about their use.

- LAT Photon and Extended Data
  - LAT Data Server (updated with P8R3 data 26-Nov-2018)
  - LAT Low-Energy (LLE) Data (Browse table)
  - Products available on the FTP Site (current processing version of the data).
    - Weekly Photon Files
    - Weekly Spacecraft Files
    - Mission Long Spacecraft File
    - Weekly 1-second Spacecraft Files
    - Filtered Weekly Photon Files with Diffuse Response Columns
  - Previous processing versions available on the FTP site
    - Pass 8 (P8R2) Weekly Files
    - Pass 7 (V6d) Weekly Files
    - Pass 7 (V6) Weekly Files
    - Pass 6 (V11) Weekly Files
    - Pass 6 (V3) Weekly Files

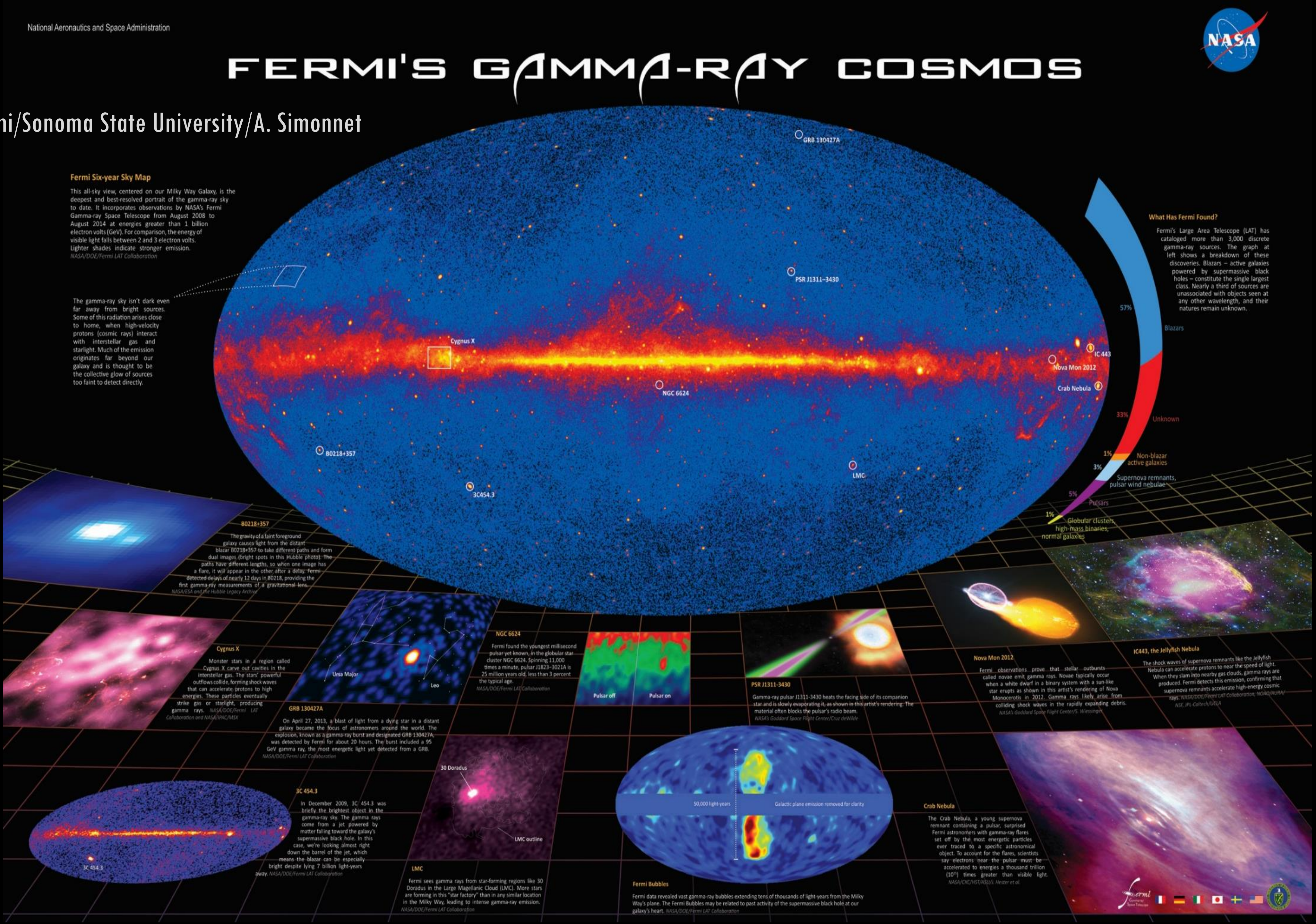
National Aeronautics and Space Administration
NASA
FERMI'S GAMMA-RAY COSMOS
Fermi Six-year Sky Map
This all-sky view, centered on our Milky Way Galaxy, is the deepest and best-resolved portrait of the gamma-ray sky to date. It incorporates observations by NASA's Fermi Gamma-ray Space Telescope from August 2008 to August 2014 at energies greater than 1 billion electron volts (GeV). For comparison, the energy of visible light falls between 2 and 3 electron volts. Lighter shades indicate stronger emission. NASA/DOE/Fermi LAT Collaboration
The gamma-ray sky isn't dark even far away from bright sources. Some of this radiation arises close to home, when high-velocity protons (cosmic rays) interact with interstellar gas and starlight. Much of the emission originates far beyond our galaxy and is thought to be the collective glow of sources too faint to detect directly.
GRB 130427A
PSR J1311–3430
Cygnus X
NGC 6624
IC 443
Nova Mon 2012
Crab Nebula
B0218+357
3C454.3
LMC
What Has Fermi Found?
Fermi's Large Area Telescope (LAT) has cataloged more than 3,000 discrete gamma-ray sources. The graph at left shows a breakdown of these discoveries. Blazars – active galaxies powered by supermassive black holes – constitute the single largest class. Nearly a third of sources are unassociated with objects seen at any other wavelength, and their natures remain unknown.
57%
Blazars
33%
Unknown
1%
Non-blazar active galaxies
3%
Supernova remnants, pulsar wind nebulae
5%
Pulsars
1%
Globular clusters, high-mass binaries, normal galaxies
B0218+357
The gravity of a faint foreground galaxy causes light from the distant blazar B0218+357 to take different paths and form dual images (bright spots in this Hubble photo). The paths have different lengths, so when one image has a flare, it will appear in the other after a delay. Fermi detected delays of nearly 12 days in B0218, providing the first gamma-ray measurements of a gravitational lens. NASA/ESA and the Hubble Legacy Archive
Cygnus X
Monster stars in a region called Cygnus X carve out cavities in the interstellar gas. The stars' powerful outflows collide, forming shock waves that can accelerate protons to high energies. These particles eventually strike gas or starlight, producing gamma rays. NASA/DOE/Fermi LAT Collaboration and NASA/IPAC/MSX
Ursa Major
Leo
GRB 130427A
On April 27, 2013, a blast of light from a dying star in a distant galaxy became the focus of astronomers around the world. The explosion, known as a gamma-ray burst and designated GRB 130427A, was detected by Fermi for about 20 hours. The burst included a 95 GeV gamma ray, the most energetic light yet detected from a GRB. NASA/DOE/Fermi LAT Collaboration
NGC 6624
Fermi found the youngest millisecond pulsar yet known, in the globular star cluster NGC 6624. Spinning 11,000 times a minute, pulsar J1823–3021A is 25 million years old, less than 3 percent the typical age. NASA/DOE/Fermi LAT Collaboration
Pulsar off
Pulsar on
PSR J1311-3430
Gamma-ray pulsar J1311-3430 heats the facing side of its companion star and is slowly evaporating it, as shown in this artist's rendering. The material often blocks the pulsar's radio beam. NASA's Goddard Space Flight Center/Cruz deWilde
Nova Mon 2012
Fermi observations prove that stellar outbursts called novae emit gamma rays. Novae typically occur when a white dwarf in a binary system with a sun-like star erupts as shown in this artist's rendering of Nova Monocerotis in 2012. Gamma rays likely arise from colliding shock waves in the rapidly expanding debris. NASA's Goddard Space Flight Center/S. Wiessinger
IC443, the Jellyfish Nebula
The shock waves of supernova remnants like the Jellyfish Nebula can accelerate protons to near the speed of light. When they slam into nearby gas clouds, gamma rays are produced. Fermi detects this emission, confirming that supernova remnants accelerate high-energy cosmic rays. NASA/DOE/Fermi LAT Collaboration, NOAO/AURA/NSF, JPL-Caltech/UCLA
3C 454.3
In December 2009, 3C 454.3 was briefly the brightest object in the gamma-ray sky. The gamma rays come from a jet powered by matter falling toward the galaxy's supermassive black hole. In this case, we're looking almost right down the barrel of the jet, which means the blazar can be especially bright despite lying 7 billion light-years away. NASA/DOE/Fermi LAT Collaboration
3C 454.3
30 Doradus
LMC outline
LMC
Fermi sees gamma rays from star-forming regions like 30 Doradus in the Large Magellanic Cloud (LMC). More stars are forming in this "star factory" than in any similar location in the Milky Way, leading to intense gamma-ray emission. NASA/DOE/Fermi LAT Collaboration
50,000 light-years
Galactic plane emission removed for clarity
Fermi Bubbles
Fermi data revealed vast gamma-ray bubbles extending tens of thousands of light-years from the Milky Way's plane. The Fermi Bubbles may be related to past activity of the supermassive black hole at our galaxy's heart. NASA/DOE/Fermi LAT Collaboration
Crab Nebula
The Crab Nebula, a young supernova remnant containing a pulsar, surprised Fermi astronomers with gamma-ray flares set off by the most energetic particles ever traced to a specific astronomical object. To account for the flares, scientists say electrons near the pulsar must be accelerated to energies a thousand trillion (10^{15}) times greater than visible light. NASA/CXC/HST/ASU/J. Hester et al.
Fermi

High-energy astroparticle physics group Bari @2022
(UniBA, PoliBA, INFN)

Thank you!

elisabetta.bissaldi@poliba.it